

Automatic Autism Spectrum Disorder Detection Using Artificial Intelligence Methods with MRI Neuroimaging: A Review

Parisa Moridian¹, Navid Ghassemi², Mahboubeh Jafari³, Salam Salloum-Asfar⁴, Delaram Sadeghi⁵,
Marjane Khodatars⁵, Afshin Shoeibi^{6*}, Abbas Khosravi⁷, Sai Ho Ling⁸, Abdulhamit Subasi^{9,10},
Roohallah Alizadehsani⁷, Juan M. Gorriz⁶, Sara A Abdulla^{4*}, U. Rajendra Acharya^{11,12,13}

¹ Faculty of Engineering, Science and Research Branch, Islamic Azad University, Tehran, Iran;

² Computer Engineering Department, Ferdowsi University of Mashhad, Mashhad, Iran.

³ Electrical and Computer Engineering Faculty, Semnan University, Semnan, Iran.

⁴ Neurological Disorders Research Center, Qatar Biomedical Research Institute, Hamad Bin Khalifa University, Qatar Foundation, Doha, Qatar.

⁵ Dept. of Medical Engineering, Mashhad Branch, Islamic Azad University, Mashhad, Iran.

⁶ Data Science and Computational Intelligence Institute, University of Granada, Spain.

⁷ Institute for Intelligent Systems Research and Innovations (IISRI), Deakin University, Geelong, Australia.

⁸ Faculty of Engineering and IT, University of Technology Sydney (UTS), Australia.

⁹ Institute of Biomedicine, Faculty of Medicine, University of Turku, 20520, Turku, Finland.

¹⁰ Dept. of Computer Science, College of Engineering, Effat University, Jeddah, 21478, Saudi Arabia.

¹¹ Ngee Ann Polytechnic, Singapore 599489, Singapore.

¹² Dept. of Biomedical Informatics and Medical Engineering, Asia University, Taichung, Taiwan.

¹³ Dept. of Biomedical Engineering, School of Science and Technology, Singapore University of Social Sciences, Singapore.

* Correspondence: Afshin Shoeibi (Afshin.shoeibi@gmail.com) and Sara A Abdulla (saabdulla@hbku.edu.qa)

Abstract: Autism spectrum disorder (ASD) is a brain condition characterized by diverse signs and symptoms that appear in early childhood. ASD is also associated with communication deficits and repetitive behavior in affected individuals. Various ASD detection methods have been developed, including neuroimaging modalities and psychological tests. Among these methods, magnetic resonance imaging (MRI) imaging modalities are of paramount importance to physicians. Clinicians rely on MRI modalities to diagnose ASD accurately. The MRI modalities are non-invasive methods that include functional (fMRI) and structural (sMRI) neuroimaging methods. However, the process of diagnosing ASD with fMRI and sMRI for specialists is often laborious and time-consuming; therefore, several computer-aided design systems (CADS) based on artificial intelligence (AI) have been developed to assist the specialist physicians. Conventional machine learning (ML) and deep learning (DL) are the most popular schemes of AI used for diagnosing ASD. This study aims to review the automated detection of ASD using AI. We review several CADS that have been developed using ML techniques for the automated diagnosis of ASD using MRI modalities. There has been very limited work on the use of DL techniques to develop automated diagnostic models for ASD. A summary of the studies developed using DL is provided in the appendix. Then, the challenges encountered during the automated diagnosis of ASD using MRI and AI techniques are described in detail. Additionally, a graphical comparison of studies using ML and DL to diagnose ASD automatically is discussed. We conclude by suggesting future approaches to detecting ASDs using AI techniques and MRI neuroimaging.

Keywords: ASD, Diagnosis, Neuroimaging, MRI Modalities, Machine Learning, Deep Learning

1. Introduction

A complex intricate network of millions of neurons is responsible for monitoring and controlling each part of the human body and brain [1-3]. These networks consist of many neurons that need to be directly interconnected and synchronized [4-5]. It has been suggested that certain disorders in the human body arise when brain networks are incorrectly connected to manage a specific activity [6-9]. Disorders of this type can be classified into three groups based on their psychological or neural characteristics and threaten the health of many individuals across the globe. Autism spectrum disorder (ASD) [10], schizophrenia [11], attention deficit hyperactivity disorder (ADHD) [12], epilepsy [13], Parkinson's disease [14], and bipolar disorder (BD) [15] are some of the most known neurodevelopmental disorders.

ASD is a neurodevelopmental disorder that manifests in childhood and causes a variety of challenges to individuals [1]. Those with ASD have difficulties with verbal and non-verbal communication, cognitive skills, social behavior, and entertaining activities. ASD begins in the early stages of embryonic development, according to research results. Autism is thought to be caused by specific signal patterns in the cortex, abnormalities in the immune system, growth hormone fluctuations, and abnormalities in the neural mirror system in the embryonic stage [16-17]. The overall ASD prevalence is one in 44 children aged 8 years, and ASD is around 4 times as prevalent among boys as among girls. [18-19]. In addition to lifelong social and adaptive disorders, one of the major consequences of autism is its negative impact on quality of life. Therefore, early diagnosis and treatment of ASD are of paramount importance for improving the quality of life of ASD children and their families [20].

According to the DSM-3, mental health professionals originally divided autism into five categories, including Asperger's syndrome, Rett syndrome, childhood disintegrative disorder (CDD), autistic disorder, and Pervasive developmental disorder-not otherwise specified (PDD-NOS) [21-22]. Using this method, physicians observed the symptoms of autistic individuals and compared their observations to those in the DSM-3 to diagnose the specific type of autism [21-23]. In 2013, the DSM-5 was published, making significant changes to the categorization of autism [24]. DSM-5 categorizes autism severity into three levels, and more information is given in [24]. According to DSM-5, the lower the severity level of autism, the less support the child requires. Autism individuals with the second and third severity levels show moderate to severe symptoms and therefore require more frequent support. Although the DSM-5 provides explanations of the autism spectrum, these explanations are incomplete and do not provide guidance on the specific support that may be required by autistic children. In addition, some individuals simply do not fall into any of these categories and ASD can change and intensify over time [24-25].

Neuroimaging techniques are one group of methods used for diagnosing neurological and mental disorders such as ASD. These methods comprise structural and functional neuroimaging modalities, which are of special interest to physicians, particularly in the diagnosis of various brain disorders [26-27]. The fMRI is one of the major functional neuroimaging methods that records data in a non-invasive manner. fMRI has a high spatial resolution, making it an excellent method for examining functional connectivity in the brain. fMRI data is classified into two categories: T-fMRI and rs-fMRI. Furthermore, fMRI data are composed of a 4-dimensional tensor, which permits the 3D volume of the brain to be segmented into smaller areas, and the activity of each area is recorded for a predetermined time period. Although fMRI has provided satisfactory results in the diagnosis of a variety of brain disorders, these techniques are costly and too sensitive to motion artifacts [29] [34].

sMRI and DTI have been used to examine brain anatomy and the interaction between brain regions, respectively. The structural neuroimaging modalities offer the advantage of cost-effectiveness and the availability of imaging protocols in most treatment facilities [34]. Physicians use sMRI modalities to diagnose autism in autistic individuals using i) geometric features and ii) volumetric features, which

physicians have used to demonstrate that autistic people demonstrate superior brain development in comparison to normal people [30-33]. Hazlett et al. [35] studied the brain structure of 51 autistic children and 25 normal children (1.5-3 years of age). Their findings indicated that the Cerebellum white matter volume of autistic children was 2-4 times greater than that of normal children.

Although MRIs offer many advantages, MRI artifacts reduce the accuracy with which clinicians are able to diagnose autism. Additionally, ASD individuals' MRI data is recorded with multiple slices and different protocols. Consequently, it takes a considerable amount of time to examine all MRI slices accurately, and clinicians should be highly precise. The fatigue of the physician may lead to an incorrect diagnosis of ASD in many cases. In addition, MRI data is problematic because most physicians are inexperienced in interpreting these images and may find it difficult to diagnose ASD in its early stages.

In order to improve the accuracy of ASD diagnosis, AI techniques can be used. The use of AI in diagnosing various diseases has been studied [36-38]. Several studies have demonstrated that AI techniques, along with MRI neuroimaging modalities, increase the accuracy of ASD diagnosis [36-37]. An increasing number of studies have been conducted on the detection of ASD using ML and DL methods. Researchers first demonstrated that ASD can be diagnosed from ML using MRI neuroimaging technologies [38]. Feature extraction, dimension reduction, and classification algorithms in CADs based on ML algorithms are selected through trial and error [39-40]. Choosing an appropriate algorithm for each CADs section can be challenging without adequate knowledge of AI [39-41]. Furthermore, ML techniques are not suitable for small data sets [42]. These methods therefore do not contribute to the development of software for the detection of ASDs using MRI neuroimaging modalities.

A variety of studies are being conducted in order to diagnose various diseases and disorders by using these methods in order to overcome the challenges inherent in ML techniques [43-46]. In contrast to ML methods, DL uses deep layers for feature extraction and classification and require fewer implementation steps in the diagnosis of ASD [47]. Furthermore, DL-based CADs can be more efficient and accurate with large input data.

An overview of studies relating to the detection of ASD using MRI neuroimaging methods is presented in this comprehensive systematic review. The first step was to review systematically all publications on ASD detection using MRI modalities and ML techniques. A recent review by the authors of this review discussed the use of different neuroimaging modalities and DL architectures to detect ASD [6]. Appendix A presents a review paper describing ASD detection in different neuroimaging modalities using DL techniques to make a comparison between ML and DL studies.

The following sections describe the following. Section 2 is search Strategy based on PRISMA guideline. In section 3, the review papers in AI techniques for ASD diagnosis are reviewed. Section 4 describes the CADs based on AI to detect ASD from MRI neuroimaging images. In section 5, a comparison between ML and DL studies to ASD detection using MRI modalities are presented. Section 6 examines the most critical challenges for detecting ASD using AI methods. Future directions and conclusion sections are presented in sections 7 and 8, respectively.

2. Search Strategy Based on PRISMA Guideline

The PRISMA protocol was used to select and review papers in this study [11]. Papers on the diagnosis of ASD by MRI modalities and AI models (ML and DL) published from 2016 to 2022 were included in this study. In this review paper, various citation databases, including IEEE, Wiley, Frontiers, ScienceDirect, SpringerLink, ACM, and ArXiv were used to search for papers in the field of ASD detection. Furthermore, Google Scholar has been used to search for the article entirety. Here are the keywords, including “ASD

classification,” “Feature extraction”, “fMRI”. “sMRI” and “Autism Spectrum Disorder,” which were used to search for articles relating to the diagnosis of ASD using ML algorithms. To search for articles related to DL, the keywords used were “Autism Spectrum Disorder”, “ASD”, fMRI”, “sMRI”, and "Deep Learning”.

As stated above, papers were selected and reviewed based on the PRISMA protocol at three different levels. In the first level, 34 out of 316 downloaded papers were eliminated as they were out of the scope of this study. Then, 28 papers were also excluded as they did not use MRI datasets in the ASD diagnosis, followed by excluding further 21 papers due to no use of AI techniques. Therefore, 233 papers were finally selected and used in this review paper. Figure (1) shows the selection procedure of papers based on the PRISMA protocol on three levels. The key criteria for the inclusion and exclusion of papers on the ASD diagnosis based on the PRISMA protocol are shown in Table (1).

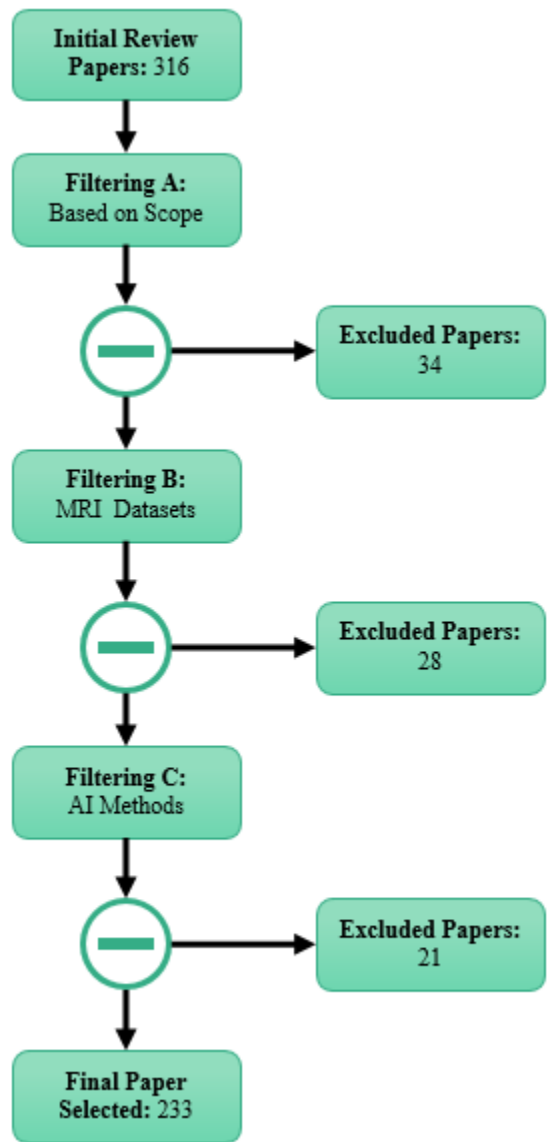


Fig 1. Papers selection process based on the PRISMA guidelines.

3. Artificial Intelligence Techniques for ASD diagnosis

For researchers in cognitive sciences, autism is a well-recognized neurodevelopmental disorder with a high prevalence in recent years. Challenges in the ASD diagnosis for physicians have resulted in extensive studies on this brain disorder. Scholars in AI, and cognitive sciences seek to develop a real diagnostic tool for ASD using various AI techniques. Accordingly, extensive studies have focused on ASD diagnosis using neuroimaging modalities and AI techniques, outlined in this section by reviewing articles in the field of ASD diagnosis using these techniques.

Table 1. The exclusion and inclusion criteria for diagnosis of ASD.

| Inclusion | Exclusion |
|--|---|
| 1. sMRI neuroimaging modalities 2. fMRI neuroimaging modalities 3. Different Types of Autism 4. DL models 5. Feature extraction methods 6. Dimension reduction methods 7. Classification methods | 1. Treatment of ASD 2. Clinical methods for ASD treatment 3. Rehabilitation systems for ASD detection (Without AI techniques) |

Pagnozzi et al. [344] reviewed 123 articles on ASD diagnosis using sMRI modalities and reported further developments in some brain areas of ASD individuals than those of HC. They also explained that ASD caused changes in the structure of patients' brains, including increased volume of frontal and temporal lobes, increased thickness of the frontal cortex, and increased volume of cerebrospinal fluid. This study assists scholars in applying AI techniques in ASD diagnosis from sMRI modalities in future studies.

Nogay et al. [345] published a review article on ASD diagnosis using brain imaging and ML techniques. They reviewed studies on ASD diagnosis for sMRI, fMRI and combined data using ML techniques and found a higher accuracy of ASD diagnosis at younger ages. They hope to develop a practical ASD diagnostic tool based on ML techniques from MRI modalities.

In another study, Xu et al. [38] reported methods and tools associated with ASD diagnosis from MRI data based on ML techniques. Initially, they introduced the most important ML-based algorithms, including feature extraction, feature selection and reduction, training and test models, and, finally, evaluation parameters.

Parlett-Pellerit et al. [37] reviewed studies on unsupervised ML techniques for ASD diagnosis. In this study, various clinical data and medical imaging data were discussed for ASD diagnosis using unsupervised ML techniques.

The most important feature selection and classification algorithms for ASD diagnosis were studied in Rahman et al. [346] paper. Their input data comprises various psychological tests such as ADOS and MRI modalities. They claimed that this study could assist scholars in developing future studies on ADS diagnosis.

A review article on the diagnosis of ASD and ADHD using AI techniques was published by Eslami et al. [347]. They discussed DL and ML-based studies on ASD and ADHD diagnosis from MRI modalities and the most important AI techniques (DL and ML). In the ML section, the authors presented the most important feature extraction techniques, such as dynamic effective connectivity, and outlined various popular DL techniques.

Khodatars et al. [6] presented a review paper on ASD diagnosis and rehabilitation using DL techniques. They initially introduced the public neuroimaging modalities datasets, such as MRI, pre-processing

techniques, and DL models, an ASD diagnosis. Then, they summarized the studies conducted in this field in a table. They also discussed studies in the field of autism rehabilitation using DL techniques.

In this section, the most important review papers on ASD diagnosis from various data and AI techniques were discussed. In our study, ASD diagnosis papers using MRI data and various AI techniques (ML and DL) were reviewed. This paper reports all ASD diagnosis articles from 2010 to 2022. Also, the most important challenges and future works for diagnosing ASD from MRI modalities are presented. To the best of our knowledge, no similar review article has been provided so far, and our review article has outstanding innovations.

4. CADS for ADS diagnosis by MRI Neuroimaging Modalities

The application of CADS based on AI techniques is presented in this section, and it is illustrated in Figure (2). The steps involved in CADS using ML for ASD detection are outlined in Figure (2). As shown in figure (2), CADS input consists of datasets containing MRI modalities. Standard preprocessing (low-level) methods for MRI neuroimaging modalities were demonstrated as a second step. Next, we will discuss these preprocessing methods for MRI neuroimaging modalities. The third step involves feature extraction. Feature reduction or selection techniques (dimension reduction) are considered to be the fourth step in the CADS based on ML. The final step involves the use of classification algorithms. The only difference between DL-based and ML-based CADS is the feature extraction to the classification step. This procedure is carried out in deep layers in CADS based on DL. This enables the extraction of features from MRI data without the user's intervention. Moreover, in CADS based on DL, diagnostics of ASD may be possible in case there are more input data, allowing the development of actual software for the detection of ASD. The details of ASD detection from MRI neuroimaging modalities using DL architectures are given in Appendix (A). Here we present the details of CADS based on ML, along with some of the most important algorithms in each section.

4.1. MRI Neuroimaging ASD Datasets

Various MRI modalities datasets for ASD diagnosis are available to researchers, including UCI [348], NDAR [349], AGRE [350], NRGR [351], GEO [352], SSC [353], Simons VIP [354], and autism brain imaging data exchange (ABIDE) [6]. Tables (2) and (3) summarize studies of ASD diagnosis using ML and DL techniques. As can be seen, the ABIDE database has a special place in research. ABIDE is recognized as the most complete and freely available database of MRI modalities for the automatic diagnosis of ASD [6]. This dataset has two parts, ABIDE I and ABIDE-II, containing sMRI data, rs-fMRI data, and phenotypic data. 1112 datasets are involved in ABIDE I, and 1114 datasets are included in ABIDE II [6]. ABIDE I also contains preprocessed data from MRI modalities for research, known as the preprocessed connectomes project (PCP) [6]. Additionally, other available datasets, such as NDAR, UCI, and NRGR, have been used in ASD diagnostic. The results show that these datasets have been able to achieve satisfactory results. The datasets used for each study are summarized in Tables (2) and (3).

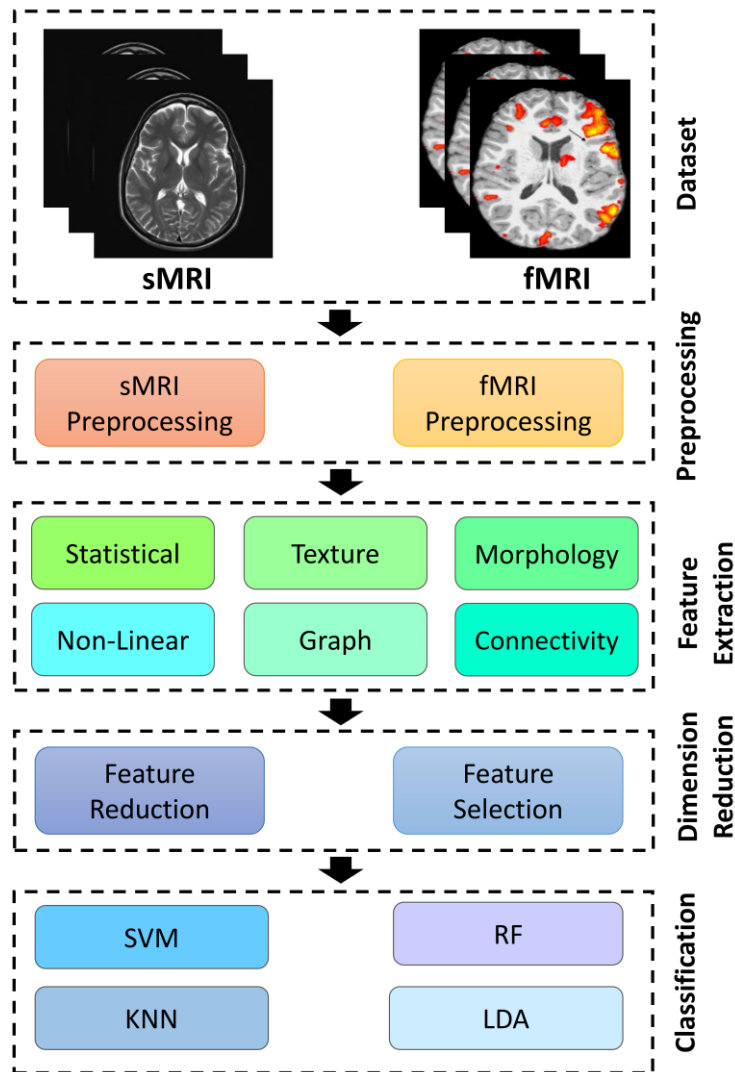


Fig. 2. Block diagram of CADs- based on ML techniques for automated ASD diagnosis.

4.2. Preprocessing Techniques for fMRI and sMRI Modalities

Preprocessing techniques are needed to help CADs to achieve promising results. The sMRI and fMRI neuroimaging modalities have implemented fixed preprocessing steps using different software packages. The most common software packages are brain extraction tools (BET) [48], FMRIB software libraries (FSL), statistical parametric mapping (SPM), and FreeSurfer [6]. The following is the standard preprocessing steps for fMRI and sMRI neuroimaging modalities. Some of them are common for both fMRI and sMRI modalities, so we will introduce them in the fMRI-related section. Figure (3) shows the standard fMRI and sMRI techniques. Also, the pipeline preprocessing techniques for ABIDE datasets will be introduced in another section.

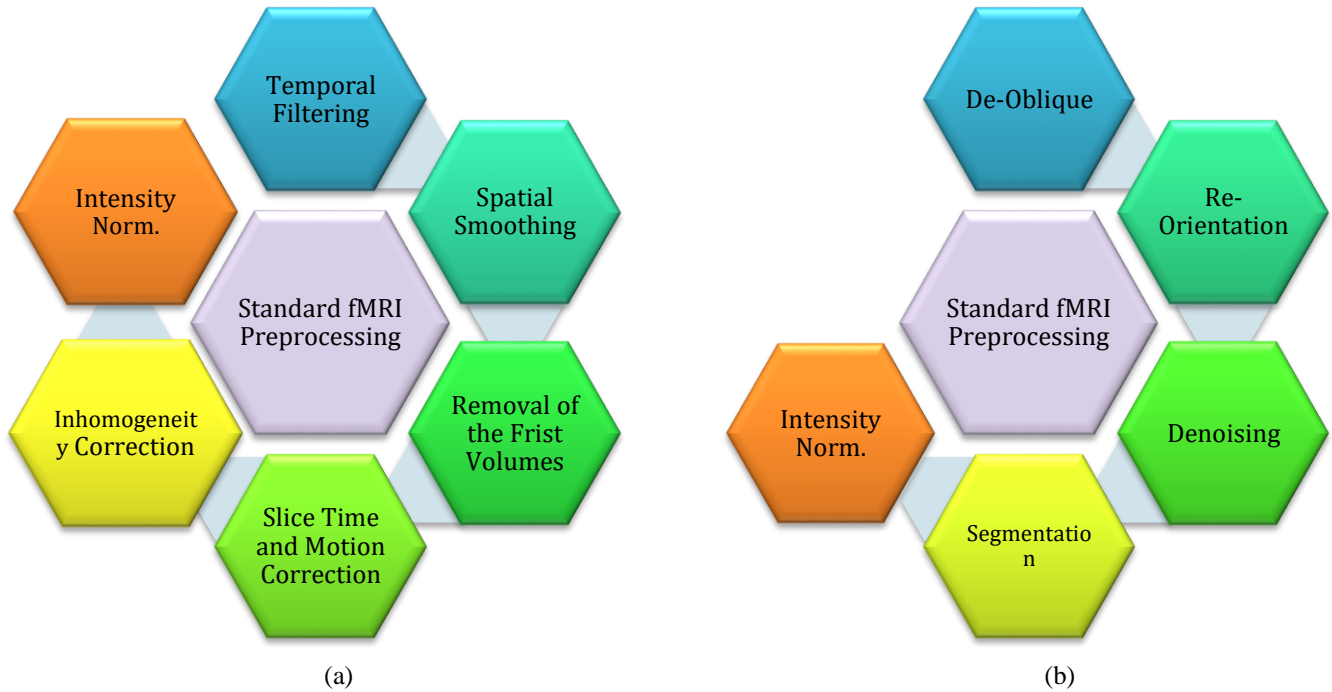


Fig. 3. Standard preprocessing methods for MRI neuroimaging modalities: a) Preprocessing for fMRI data, b) preprocessing for sMRI data.

The standard Preprocessing is a necessary step in fMRI, and if preprocessing is not carried out properly, it will lead to reduced performance of automated diagnosis of ASD. This step aims to extract regions suspected of having ASD and examine the function of brain neurons in those regions. The preprocessing steps of fMRI include delineation of the brain region, removal of the first few volumes, slice timing correction, inhomogeneity correction, motion correction, intensity normalization, temporal filtering, spatial smoothing, and ultimately registration standard atlas [6]. As mentioned earlier, this step is usually carried out by a toolbox, including BET [6], FSL [6], SPM [6][50], FreeSurfer [6][51], etc. In reference [6], the details for standard preprocessing steps of fMRI modalities are elaborately explained.

The preprocessing of sMRI data extracts helps physicians examine regions with suspected ASD more accurately. Besides, low-level sMRI preprocessing methods help AI-based CADs to process important information. This process increases the accuracy and efficiency of diagnosis of ASD CADs. The most important standard sMRI covers intensity standardization, de-oblique, re-orientation, Denoising, and segmentation [6]. In reference [6], each step of standard preprocessing for sMRI modalities is explained.

4.2.2. Pipeline Methods

The pipelines are a preprocessed version of ABIDE data using standard preprocessing procedures, which researchers can use to avoid the problems of variations in the output between different studies as a result of preprocessing. The most popular ABIDE pipelines include neuroimaging analysis kit (NIAK), data processing assistant for rs- fMRI (DPARSF), the configurable pipeline for the analysis of connectomes (CPAC), and connectome computation system (CCS) [6].

4.3. Feature Extraction

Representing data in a manner that allows ML algorithms to reason about them is the key to any related research. If this is not done, high performance cannot be achieved. Most commonly used feature extraction

schemes for fMRI and sMRI are statistical, texture, morphological, non-linear, graph, functional connectivity, and structural connectivity schemes.

- **Statistical Features**

ASD is typically detected with MRI modalities using statistical features, the most straightforward group of features. Despite their simplicity, these features are usually informative and can also serve as a benchmark for evaluating other methods of feature extraction as well. Additionally, the process of extracting these features is not time-consuming in comparison to other methods. However, these methods do not reveal non-linear or subtle patterns in data. Using statistical features for ASD diagnosis, Dekhil et al. [80] extracted various statistical features from MRI data and then applied KNN and SVM algorithms in the classification step. The authors reported 81% accuracy.

- **Texture Features**

As a group of features, spatial patterns form an indispensable group, possibly the most important group, since the cognitive system of the human is mostly dependent on them. Gray-level co-occurrence matrix (GLCM) [49] feature extraction is one of the most widely used methods in various research studies [94] among various textures-based features. Haweel et al. [67] presented an ASD diagnostic method based on MRI data. Texture features and the RFE technique were used in the feature extraction and feature selection steps. Then, the authors used the RF technique for classifying features and reached an accuracy of 72%. In another study, scholars used various methods, such as Haralick, in the feature extraction step from sMRI data. Then, the authors tested different feature selection methods and reached an accuracy of 72.5%.

- **Morphological Features**

Morphological operation is an important feature extraction technique frequently used in image processing [366]. In these methods, features are extracted from the appearance and shape of the image. Morphological operation is often used to process binary images, but they can also be used for gray and color-level images [367]. Morphological features are also commonly used for diagnosing brain diseases from sMRI modalities. Zheng et al. [75] proposed the idea of ASD diagnosis using morphological features. After feature extraction, RFE and SVM were tested for feature selection and classification, respectively. An accuracy of 78.63% was obtained

- **Non-Linear Features**

A non-linear characteristic of biological data is emphasized when considering non-linear features. The performance of CADs for ASD is significantly enhanced through the use of these features [50]. In reference [103], nonlinear-based features of likelihood are used to detect autism using MRI neuroimaging methods. Entropies are one of the most important nonlinear methods that are widely used to extract features from signals and brain images [368]. Functional imaging modalities are nonlinear and chaotic, which has led researchers to use entropy-based nonlinear features to diagnose brain disorders [330] [369]. Zhang et al. [133] introduced a novel ASD diagnostic method using fMRI data and a new entropy method. This study initially used fast entropy for feature extraction from preprocessed fMRI data. Then, they used the SVM algorithm for feature classification and obtained satisfactory results.

- **Graph Features**

This group of features is highly relevant to the analysis of MRI data. Graph-based features are derived first by shaping the data into a graph, and then, from the constructed graph, local and global features are extracted [51]. Researchers have explored graph features to diagnose ASD using fMRI data in many studies.

Bi et al. [70] employed rs-fMRI from the ABIDE database for ASD diagnosis using graph and genetic-evolutionary random SVM cluster (GERSVMC) for feature extraction and classification steps, respectively, and obtained an accuracy of 62%. Saad et al. [72] presented an ASD diagnostic method based on graph features in another study. After feature extraction via the graph method, PCA and SVM techniques were used for feature reduction and classification, which resulted in an accuracy of 75% for ASD diagnosis.

- **Connectivity Matrix**

In order to process sMRI and fMRI neuroimaging images, feature extraction methods based on connectivity matrix methods are typically employed [52-53]. Such features provide information about the brain's structure and function. The functional connectivity matrix (FCM) [56-57] and structural connectivity matrix (SCM) [58-59] are the measures employed for fMRI and sMRI modalities, respectively. Connectivity features are mostly used in diagnosing brain disorders. Tables (2) and (3) outlines studies on ASD diagnosis from MRI modalities using various AI techniques. Table (2) shows that connectivity methods are most frequently used for feature extraction from MRI modalities. Liu et al. [84] used dynamic functional connectivity (DFC) in the feature extraction step of rs-fMRI data. The feature selection step was also conducted by the MTFS-EM method. Finally, they used the SVM method for classification and obtained an accuracy of 76.84%. In another study, Mathur et al. [125] utilized DFC and static functional connectivity (SFC) in the feature extraction step. Then, the SVM was tested for connectivity-based classification of features. Authors could finally obtain satisfactory results for ASD diagnosis using connectivity features.

4.4. Feature Reduction / Selection Methods

It has been shown that increasing the number of extracted features can help algorithms to represent data in a more meaningful and robust way; however, the curse of dimensionality [54] may cause it to backfire and reduce performance. Several methods for reducing dimensionality and selecting features have been proposed in order to prevent this from occurring. In addition, these methods are widely used to increase the performance of CADs for the detection of autism spectrum disorders. A number of methods have previously been used in research papers, including principal component analysis (PCA) [55], recursive feature elimination (RFE) [56], T-test [57], autoencoder (AE) [58], conditional random forest (CRF) [59], Chi-squared [60], and least absolute shrinkage and selection operator (LASSO) [61]. The following is a brief description of these methods.

- **PCA**

PCA is arguably the most common dimensionality reduction method [55]. It works by finding and representing data by the principal components, i.e., the vectors that preserve the most data variance. One of the benefits of PCA is its ability to find a minimal number of features required to preserve a specified variance ratio [55]. Principal component analysis (PCA) is one of the most popular feature reduction techniques in medical applications and has also been used in ASD diagnosis research [72], [89], [110], [150].

- **RFE**

Recursive feature elimination is more of a wrapper-type algorithm, meaning that it is applied to a classification algorithm to find the best subset of features. As the name explains, this algorithm works by eliminating features one by one to reach the optimal number. First, a classification algorithm is trained on the dataset, ranking feature importances. The least important feature is then eliminated, and the process is repeated until the number of remaining features matches the desired number [56]. Haweel et al. [67] proposed a novel ASD diagnostic method using the GLM feature extraction technique. After feature

extraction from MRI data, the RFE technique was used for feature reduction. The RF method was also tested in the classification step with an accuracy of 72%.

- **T-Test**

To find the best set of features, T-Test calculates a score for each feature, then ranks them based on that score and picks the top features as selected ones. The score shows whether the values of a feature for a class are significantly different from those for another class by calculating the mean and standard deviation (STD) of each feature in each class [57]. A new ASD diagnostic method from MRI data was introduced by Sartipi et al. [71]. First, the graph technique was used for feature extraction from sMRI modalities. Then, they applied the t-test and SVM algorithms for the feature selection and classification steps and acquired an accuracy of 75%.

- **Chi-Squared**

Chi-Square is suitable when the features are categorical and the target variable is also categorical, such as classification. Chi-Squared measures the degree of association between two variables; thus, features that have a connection with the targets can be picked [60]. When the features are numerical, we can use a T-Test, or Chi-Square can be used for the numerical variable by discretizing them [60]. In reference [80]. The authors proposed a new ASD diagnostic method using various ML techniques from MRI data. Various methods were used for feature extraction. Then, the Chi-squared method was tested for the feature selection step. Next, the LR classification algorithm was applied, which resulted in a promising performance.

- **LASSO**

Lasso is mainly a regression method; however, this algorithm can also be used for feature selection [61]. Notably, linear regression with L1 regularization is called Lasso. After training, the lasso assigns a weight to each feature for the regression [61]. Using these weights, there are two methods to pick the best features, first, pick the K highest valued weights; second, pick all the weights which have a value higher than a specified threshold [61]. Fedro et al. [113] proposed a new ASD diagnostic method based on Hons and Lon features. Their paper used LASSO and SVM methods for feature selection and classification, respectively. They reported an accuracy of 81%.

4.5. Classification Methods

This section discusses the various classification algorithms used in CADs for ASD. As mentioned earlier, classification is the last step in a CADs based on ML methods. Support vector machine (SVM) [62-63], linear discriminant analysis (LDA) [65], k-nearest neighbor (KNN) [66], and random forest (RF) [64] are arguably among the most popular methods used in CADs created for ASD. Tables (2) and (3) shows the classification algorithms used for ASD detection. A brief summary of classification algorithms used for automated detection of ASD are presented below.

- **SVM**

Support vector machines (SVMs) are among the oldest classification which has been widely used in many applications [62-63]. SVM tries to find the best hyperplane to separate data points; however, it only needs the dot product between every two data points [62-63]. Consequently, to transform data into another space, only a function that gives the dot product of two points in that space would suffice; this is also named kernel trick and is used widely in other fields. Using an appropriate kernel, SVM is usually capable of yielding high classification performances [62-63].

- **RF**

Random forests (RFs) are an ensemble learning-based method proposed to make the decision trees robust to outliers [64]. The basic idea is to train many trees and determine the final output based on voting among their outputs. To make the final results robust, each tree is trained only on a fraction of the data, and also each tree sees a fraction of all features. The picked ratio for both of these is the square root of the available number.

- **LDA**

Used as a tool for dimension reduction, classification, and data visualization [65]. It is simple and robust and yields interpretable classification results [65]. It works by dividing the data space into K disjoint regions that represent all the classes; then, in the testing phase, the label is determined by finding the region in which the data belongs. LDA can be used as the first benchmarking baseline before other, more complicated ones are employed for real-world classification problems [65].

- **KNN**

This classifier is among the simplest yet efficient algorithms; its main idea is to assign the label of each data point based on the label of those closest [66]. Consequently, there is no training phase; however, for each test subject, the distance to all training points must be calculated, which scales with the size of the dataset; thus, this method is not applicable on enormous datasets. After finding the closest points, the final label is determined using a voting scheme [66].

Table 2: Automated diagnosis of ASD with MRI neuroimaging modalities using ML methods.

| Reference | Dataset | Number of cases | Modalities | Atlas + Pipeline | Feature Extraction | Feature Selection | Classification | The best Performance criteria (%) |
|-----------|----------|-----------------|----------------------|-----------------------------|---|--|---|--|
| [67] | NDAR | 39 ASD | rs-fMRI | Brainnetome (BNT) Atlas | GLM Features | RFE | RF | Acc=72 |
| | | | sMRI | MNI-152 Atlas | | | | |
| [68] | ABIDE | 505 ASD, 530 HC | rs-fMRI | CC400 Atlas + CPAC Pipeline | Different Features | Nilearn | Ridge | Acc=71.98 Pre=71.53 Rec=70.89 |
| [69] | NDAR | 30 ASD, 30 HC | sMRI | NA | Cortical Path Signature Features | -- | Siamese Verification Model | Acc=87 Sen=83 Spe=90 |
| [70] | ABIDE | 103 ASD, 106 HC | rs-fMRI | AAL Atlas + DPARSF Pipeline | Graph-Theoretic Indicators (Dimensional Features) | -- | GERSVMC | Acc=96.8 |
| [71] | ABIDE | 222 ASD, 246 HC | rs-fMRI | HO Atlas + CPAC Pipeline | GARCH Model | T-Test | SVM | Acc=75.3 |
| [72] | UMCD | 51 ASD, 41 HC | DTI | NA | Graph Theory-based Features | PCA | SVM | Acc=75 Sen=81.94 Spe=70 Pre=70.42 |
| [73] | ABIDE | 250 ASD, 218 HC | rs-fMRI | AAL Atlas + CPAC Pipeline | Dimensional Feature Vectors | -- | Elastic Net | Acc=83.33 |
| [74] | Clinical | 20 ASD | sMRI | NA | GLM | Different Feature Selection Methods | RF | NA |
| | | | rs-fMRI | | | | | |
| [75] | ABIDE | 66 ASD, 66 HC | sMRI | NA | Morphological and MFN Features | RFE | SVM | Acc=78.63 Sen=80 Spe=77.27 |
| [76] | NDAR | 122 ASD, 141 HC | DTI | MNI-152 Atlas | Global and Local Feature Extraction | Signal to Noise Ratio (s2n) Filter Based Feature Ranking | SVM | Acc=71 Sen=72 Spe=70 |
| [77] | NDAR | 57 ASD, 34 HC | sMRI | NA | Morphometrical Features | -- | K-Means Clustering | NA |
| [78] | NA | 2400 ASD | Different modalities | NA | Latent Clusters | + Bayesian Information Criterion | Linear Regression (LR) | Intensity=94.29 |
| [79] | ABIDE | 175 ASD, 234 HC | rs-fMRI | AAL Atlas | Patch-based Functional Correlation Tensor (PBFCT) Features, FC Features | MSLRDA, T-Test | Multi-View Sparse Representation Classifier (MVSRC) | NA |
| [80] | NDAR | 72 ASD, 113 HC | sMRI | Desikan-Killiany (DK) Atlas | Morphological, Volumetric, and Functional Connectivity Features | -- | KNN, RF | Acc=81 Sen=84 Spe=79.2 |
| | | | rs-fMRI | | | | | |
| [81] | NA | 189 ASD, 515 HC | AQ | NA | Different Fratures | Chi-Squared Test, LASSO | LR | Acc=97.54 Sen=100 Spe=96.59 |
| [82] | UCI | 104 ASD | ASD Scan Data | NA | Different Features | Grid Search Method | RF | Acc=100 Sen=100 Spe=100 |

| | | | | | | | | |
|------|----------|-------------------------------------|----------------------|---|---|-------------------------------------|---|--|
| [83] | ABIDE | 392 ASD, 407 HC | rs-fMRI | DPARSF Pipeline | ICA + Different Features (Reproducible REs, NMI Values, AC Maps) | gRAICAR | K-Means Clustering | Acc=82.4 Sen=77 Spe=87 |
| [84] | ABIDE 1 | 403ASD, 468 HC | rs-fMRI | AAL Atlas + CPAC Pipeline | Dynamic Functional Connectivity (DFC) and Mean Time Series Features | MTFS-EM | SVM | Acc=76.8 Sen=72.5 Spe=79.9 |
| [85] | ABIDE | 255 ASD, 276 HC | rs-fMRI | DPARSF Pipeline | Functional Connectivity Features | RFE | SVM | Acc=90.6 Sen=90.62 Spe=90.58 |
| [86] | Clinical | 46 ASD, 39 DD (Developmental Delay) | sMRI | DK Atlas | Neuroanatomical Features (Regional Cortical Thickness, Cortical Volume, Cortical Surface Area) | -- | RF | Acc=80.9 Sen=81.3 Spe=81 AUC=88 |
| [87] | CFMRI | 46 ASD, 47 HC | Different Modalities | Johns Hopkins (JH), HO Atlas | Anatomical Variables, Cortical, Mean Diffusivity Values, Conectivity Matrices, and DTI Features | -- | Conditional Random Forest (CRF) | Acc=92.5 Sen=97.8 Spe=87.2 |
| [88] | Clinical | 24 ASD, 21 HC | sMRI | NA | Morphological Features of Subcortical Volumes | -- | LR | Acc=73.2 |
| [89] | ABIDE | 54 ASD, 57 HC | sMRI t-fMRI | Different Atlase + DPARSF Pipeline | Regional Morphological Features | HSL-CCA, PCA | Linear SVM | Acc=81.6 F1-S =81.4 |
| [90] | NDAR | 123 ASD, 160 HC | sMRI rs-fMRI | All Atlases | PICA (Spatial Components, Correlation Values, Power Spestral Densities) | SAE | SVM | Acc=92 Sen=93 Spe=89 |
| [91] | ABIDE 1 | 260 ASD, 308 HC | rs-fMRI | AAL Pipeline | -- | -- | Attention Based Semi-Supervised Dictionary Learning (ASSDL) Model | Acc=98.2 |
| [92] | ABIDE 1 | 250 ASD, 218 HC | rs-fMRI | AAL Atlas + CPAC Pipeline | Multi Center Domain Adaptation (MCDA) Method | -- | KNN | Acc=73.45 Sen=69.23 Spe=79.17 |
| [93] | ABIDE 1 | 155 ASD, 186 HC | sMRI | DK Atlas | Low-Order Morphological Connectivity Network (LON), Single Cell Interpretation Via Multi-Kernel Learning (SIMLR), Similarity Matrix | -- | Hypergraph Neural Network (HGNN) | Acc=75.2 |
| [94] | ABIDE | NA | sMRI rs-fMRI | NA | GLCM | -- | ANN | NA |
| [95] | Clinical | 30 ASD, 30 HC | t-fMRI | BNT Atlas | GLM Feature Extraction | -- | Stacked Nonnegativity Constraint Auto-Encoder (SNCAE) | Acc=75.8 Sen=74.8 Spe=76.7 |
| [96] | ABIDE 1 | 109 ASD, 144 HC | rs-fMRI | AAL, Dosenbach 160, CC 200 Atlas + DPARSF Pipeline | Sparse Low-Rank Functional Connectivity Network | Different Feature Selection Methods | SVM | Acc=81.74 Sen=71.83 Spe=89.50 |
| [97] | ABIDE 1 | 870 Subjects | rs-fMRI | AAL, multi-subject dictionary learning (MSDL) Atlas + CPAC Pipeline | ROIs Extraction, Connectivity Graphs Construction + Minimum Spanning Trees Extraction | MSTs Elimination | SVM | Acc=74,89 Sen=24,19 Spe=93,59 |
| [98] | Clinical | 30 Subjects | t-fMRI | BNT Atlas | Multi-Level GLM + GLM3 Parameters, Z-Stats Maps for All Brain Areas | RFE | RF | Acc=78 |

| | | | | | | | | |
|-------|--------------------|-----------------|---------|------------------------------|---|---|--|--|
| [99] | ABIDE 1 | 250 ASD, 218 HC | rs-fMRI | AAL Atlas + CPAC Pipeline | Multi-Site Adaption Framework Via Low-Rank Representation Decomposition (maLRR) Method | -- | SVM, KNN | Acc=73:44 Sen=75:79 Spe=69:52 |
| [100] | NDAR | 22 ASD, 25 HC | t-fMRI | Proposed Atlas | GLM Analysis | -- | Stacked Autoencoder With Non-Negativity Constraint (SNCAE) | Acc=94.7 |
| | | | sMRI | | | | | |
| [101] | ABIDE 1 | 34 ASD, 34 HC | sMRI | HO Atlas | Curvelet Transform + Coefficient Distribution Per Curvelet Sub-Band | Generalized Gaussian Distribution (GGD) | SVM | Different Results |
| | ABIDE II | 42 ASD, 41 HC | | | | | | |
| [102] | ABIDE 1 | 432 ASD, 556 HC | rs-fMRI | CC200 Atlas+ DPARSF Pipeline | Graph-Theoretic Measures, Traditional FC Data | Recursive-Cluster-Elimination (RCE) | SVM | Acc= 70.1 |
| [103] | ABIDE 1 | 145 ASD, 157 HC | rs-fMRI | CC200 Atlas + CPAC Pipeline | Two-Group Cross-Localized Hidden Markov Model | Likelihood Values | SVM | Acc=74.9 |
| [104] | IMPAC | 418 ASD, 497 HC | rs-fMRI | All Atlases | Tangent-Space Embedding Metric | Permutation Feature Importance (PFI) | DenseFFwd | Acc=75.4-80.4 |
| [105] | Different Datasets | 72 ASD, 113 HC | sMRI | DK Atlas | Anatomical and Connectivity Matrix Features | -- | KNN, RF, and SVM | Acc=81 Sen=78 Spe=83.5 |
| | | | rs-fMRI | | | | | |
| [105] | Different Datasets | 97 ASD, 56 HC | DTI | JH Atlas | Global Features (FA, MD, AD) + Feature Mapping to Atlas + Local Feature Extraction (PDFs of Features for Each WM Area in the Atlas) | -- | KNN, RF, and SVM | Acc=81 Sen=78 Spe=83.5 |
| [106] | NAMIC | 2 ASD, 2 HC | sMRI | NA | Adaptive Independent Subspace Analysis (AISA) Method, Texture Analysis + Different Features | t-SNE | KNN | Acc=94.7 Sen=92.29 Spe=94.82 F1-S=93.56 |
| [107] | ABIDE 1 | 403 ASD, 468 HC | rs-fMRI | NA | Eigenvalues and Topology Centralities Features | Backward Sequential Feature Selection Algorithm | LDA | Acc=77.7 |
| | | | sMRI | | | | | |
| [108] | Clinical | 12 ASD, 12 HC | rs-fMRI | NA | Group Independent Component Analysis (gICA) + Wavelet Coherence Maps Extraction | -- | SVM | Acc=86.7 Sen=91.7 Spe=83.3 |
| | ABIDE | 12 ASD, 18 HC | | | | | | |
| [109] | ABIDE 1 | 561 ASD, 521 HC | sMRI | DK, AAL Atlas + CCS Pipeline | Anatomical Feature Extraction + Functional Connectivity Analysis | -- | KNN | Different Results |
| | | | rs-fMRI | | | | | |
| [110] | Clinical | 36 ASD, 106 HC | sMRI | NA | Cortical Thickness, Surface Area, and Subcortical Volume Features | PCA | SVM | Different Results |
| [111] | ABIDE 1 | 155 ASD, 186 HC | sMRI | DK Atlas | Low-Order Morphological Network Construction (LON), High-Order Morphological Network Construction (HON) Features | t-SNE, K-Means Clustering | SVM | Acc=61.7 |
| [112] | Clinical | 46 ASD, 39 DD | sMRI | Talairach, DK Atlas | Regional Cortical Thickness, Cortical Volume, And Cortical Surface Area | -- | RF | Acc= 80.9 Sen= 81.3 Spe= 81 |

| | | | | | | | | |
|-------|----------|---|----------|------------------------------------|---|---------------------------------------|---|--------------------------------------|
| [113] | ABIDE | 54 ASD, 46 HC | rs-fMRI | AAL Atlas + DPARSF Pipeline | LON and HONs Features | LASSO | Ensemble Classifier with Multiple Linear SVMs | Acc= 81 |
| [114] | ABIDE | 160 ASD, 160 HC | rs-fMRI | HO Atlas | Functional Connectivity Matrix | CRF | SVM | Acc=65 Sen=65 Spe=65 |
| [115] | ABIDE | 61 ASD, 46 HC | rs-fMRI | AAL Atlas | Graph Theory | -- | Random SVM Cluster | Acc=96.15 |
| [116] | ABIDE | 147 ASD, 146 HC | rs-fMRI | CC200 Atlas + DPARSF Pipeline | Two Different Features Sets | -- | SVM | Acc=61.1 Sen=61.8 Spe=60 |
| [117] | ABIDE | 42 ASD, 37 HC | rs-fMRI | NA | Functional Connectivity Matrix | -- | Different Classifiers | AUC= 97.75 |
| [118] | ABIDE | 306 ASD, 350 HC | rs- fMRI | NA | Functional Connectivity Matrix | CRF | RF | Acc= 73.75 |
| [119] | ABIDE 1 | 539 ASD, 573 HC | rs-fMRI | CPAC Pipeline | Feature Extaction (All Voxels Within Grey Matter Template Mask in MNI152 Space) | -- | SVM | Acc=62 |
| [120] | UMCD | 79 Functional and 94 Structural Connectomes | rs-fMRI | NA | Graph Theory + Global, Nodal Measurements and Gender Information | Relieff Algorithm | Ensemble Learning | Acc=67 pre=0.67 Recall=70 |
| | | | DTI | | | | | Acc=68 Pre=0.73 Rec=70 |
| [121] | NDAR | 124 ASD, 139 HC | DTI | JH Atlas | Global and Local Features | Signal to Noise Ratio (S2n) Filter | SVM | Acc= 73 Sen= 70 Spe= 76 |
| [122] | ABIDE II | 31 ASD, 23 HC | rs-fMRI | AAL Atlas | Connectivity Matrix | -- | SVM | Acc= 72.34 |
| | | | DTI | | | | | |
| | | | sMRI | | | | | |
| [123] | ABIDE | 126 ASD, 126 HC | rs- fMRI | NA | Functional Connectivity Matrix | CRF | SVM | Acc > 90 |
| | Clinical | 42 ASD, 30 HC | | | | | | |
| [124] | ABIDE | 167 ASD, 205 HC | rs-fMRI | CCS Pipeline | Functional Connectivity Matrix | -- | SVM | Different Results |
| [125] | ABIDE 1 | 403 ASD, 465 HC | rs-fMRI | HO Atlas + CPAC Pipeline | sFC, dFC, and Haralick Texture Features | -- | SVM | -- |
| [126] | ABIDE | Whole Dataset | rs-fMRI | AAL Atlas + DPARSF Pipeline | Pearson Correlation Coefficient, Graph Measures, and Mean Intensities Features | -- | Adaboost | Acc=66.08 |
| [127] | Clinical | 46 ASD, 47 HC | sMRI | JH Atlas | Functional Connectivity Matrix Features | -- | CRF | Acc=92.5 Sen=97.8 Spe=87.2 |
| | | | DWI | HO Atlas | | | | |
| | | | rs-fMRI | | | | | |
| [128] | Clinical | 19 ASD | t-fMRI | NA | Elastic Net Regression | -- | RF | NA |
| | ABIDE | 64 ASD | rs-fMRI | | | | | |
| [129] | ABIDE 1 | 816 Subjects | rs-fMRI | AAL Atlas + CPAC Pipeline | Graph Theoretical Metrics | Sequential Forward Floating Algorithm | SVM | Acc=95 Sen=97 Spe=91 |
| [130] | ABIDE 1 | 119 ASD, 116 HC | rs-fMRI | AAL, CC200 Atlas + DPARSF Pipeline | Community Pattern Quality Metrics Features | -- | LDA, KNN | Acc= 75 Prec= 76.07 Rec= 71.67 |
| | ABIDE II | 97 ASD, 117 HC | | | | | | |
| [131] | Clinical | 64 ASD, 66 ADHD, 28 HC | rs-fMRI | NA | 43 Executive Functions (EF) | -- | Functional Random Forest (FRF) | Different Results |

| | | | | | | | | |
|-------|----------|---------------------------------|----------------|-------------------------------|---|---|-------------------------------|---|
| [132] | Clinical | 29 ASD, 31 HC 20 ASD, 20 HC | sMRI t-fMRI | Different Atlas | Graph Theory + Different Features | Statistical Analysis | SVM | Acc= 92 |
| [133] | ABIDE 1 | 21 ASD, 26 HC | rs-fMRI | AAL Atlas + DPARSF Pipeline | Fast Entropy Algorithm + Important Entropy | -- | SVM | AUC= 62 |
| [134] | ABIDE 1 | 59 ASD, 46 HC | rs-fMRI | AAL Atlas + DPARSF Pipeline | Function Connectivity + Minimum Spanning Tree (MST) | -- | SVM | Acc=86.7 Sen=87.5 Spec=85.7 |
| [135] | ABIDE 1 | 437 ASD, 511 HC | sMRI | -- | Computing the Brain Asymmetry with The BrainPrint + Asymmetry Values | -- | LR Models | NA |
| [136] | Clinical | 14 ASD, 33 HC | MRI, DTI | DK Atlas | Different Features | -- | Naïve Bayes, RF, SVM, NN | Acc= 75.3 Sen= 51.4 Spec= 97.0 |
| [137] | ABIDE | 45 ASD, 47 HC | rs-fMRI | AAL Atlas | Modified Weighted Clustering Coefficients | t-Test and SVM-RFE | Multi-Kernel Fusion SVM | Acc=79.35 Sen=82.22 Spec=76.60 |
| [138] | ABIDE I | 505 ASD, 530 HC | rs-fMRI | CC200 Atlas + CPAC Pipeline | Functional Connectivity | Graph-Based Feature Selection | MMoE Model | Acc=68.7 Sen= 68.9 Spec= 68.6 |
| [139] | ABIDE, | 86 ASD, 83 ADHD, 125 HC | sMRI, rs-fMRI | DK Atlas | Functional Connectivity | Univariate t-Test and Multivariate SVM-RFE | SVM | Acc=76.3 Sen= 79.2 Spec= 63.9 |
| [140] | ABIDE | 24 ASD, 35 HC | rs-fMRI | AAL Atlas | Mutual Connectivity Analysis with Local Models (MCA-LM) | Kendall's τ Coefficient | RF and AdaBoost | Acc= 81 |
| [141] | ABIDE II | 23 ASD, 15 HC | rs-fMRI | AAL Atlas + AFNI Pipeline | Functional Connectivity | ANOVA F-Score | SVM | Acc=80.76 |
| [142] | ABIDE 1 | 74 ASD, 74 HC | fMRI | DPARSF, CCS Pipeline | Bag-of-Feature (BoF) Extraction | -- | SVM | Acc=81 Sen=81 Spec=86 |
| [143] | ABIDE | 70 ASD, 74 HC | fMRI | NA | Functional Connectivity | Elastic SCAD SVM | SVM | Acc=90.85 Sen=90.86 Spec=90.90 |
| [144] | ABIDE | 250 ASD, 218 HC | rs-fMRI | AAL Atlas + CPAC Pipeline | Functional Connectivity + Low-Rank Representation Decomposition (maLRR) | -- | KNN, SVM | Acc= 73.44 Sen= 75.79 Spec= 69.52 |
| [145] | ABIDE | 399 ASD, 472 HC | rs-fMRI | CC200 Atlas + CPAC Pipeline | Feature Extraction (Static FC, Demographic Information, Haralick Texture Features, Kullback-Leibler Divergence) | Feature Selection Algorithms (RFE-CBR, LLCFS, InffS, mRMR, Laplacian Score) | SVM, KNN, LDA, Ensemble Trees | Acc=72.5 Sen=94 Spec=64.7 |
| [146] | ABIDE | 408 ASD, 476 HC | rs-fMRI | CPAC Atlas | 5 Methods for Functional Connectivity Matrix Construction | 6 Feature Extraction/Selection Approaches | 9 Classifiers | -- |
| [147] | Clinical | 30 Pairs of Biological Siblings | rs-fMRI | Social Brain Connectome Atlas | Functional Connectivity | Sparse LR (SLR) | Bootstrapping Approach | Acc=75 Sen= 76.67 Spec= 73.33 |
| [148] | Clinical | 26 ASD, 24 CAS, 18 HC | sMRI | -- | Feature Extraction | Statistical Analysis | SVM | AUC= 73 |
| [149] | Clinical | 15 ASD, 15 HC | Task-fMRI | -- | Functional Connectivity + Effective Connectivity | -- | RCE-SVM | Acc= 95.9 Sen= 96.9 |

| | | | | | | | | |
|-------|----------|-----------------|---------------|----------------------------------|--|--|-----------------------------------|--|
| | | | | | | | | Spec= 94.8 |
| [150] | ABIDE 1 | -- | rs-fMRI | CC200, AAL Atlas + CPAC Pipeline | Graph Extraction + Feature Extraction | PCA | MLP | Different Results |
| [151] | ABIDE | 119 ASD, 116 HC | rs-fMRI | AAL Atlas + DPARSF Pipeline | Resting-State Functional Network Community Pattern Analysis | RFE | LDA | Acc= 74.86 Prec= 76.07 Recall= 71.67 |
| [152] | ABIDE | 42 ASD, 37 HC | rs-fMRI | -- | Functional Connectivity + Joint Symmetrical Non-Negative Matrix Factorization (JSNMF) | -- | SVM | AUC=97.75 |
| [153] | ABIDE | 245 ASD, 272 NC | rs-fMRI | DPARSF Pipeline | Different Features | NAG-FS | SVM | Acc=65.03 |
| [154] | ABIDE 1 | 201 ASD, 251 HC | rs-fMRI | AAL Atlas + CPAC Pipeline | Graph Construction + Graph Signal Processing (GSP) | Fukunaga-Koontz Transform (FKT) | DT | Acc=75 |
| [155] | ABIDE I | 133 ASD, 203 HC | rs-fMRI, sMRI | -- | Functional Connectivity | Statistical Analysis | Sparse LR | Acc=82.14 Sen=79.70 Spec=83.74 |
| | ABIDE II | 60 ASD, 89 HC | | | | | | |
| [156] | ABIDE II | 24 ASD, 35 HC | rs-fMRI | AAL Atlas | large-scale Extended Granger Causality (lsXGC) | Kendall's Tau rank correlation coefficient | SVM | Acc= 79 |
| [297] | Clinical | 15 ASD, 15 HC | fMRI | NA | Functional Connectivity, Effective Connectivity and Fractional anisotropy (FA) From DTI, Behavioral Scores | Recursive Cluster Elimination | SVM | Acc=95.9 |
| [298] | Clinical | 22 ASD, 16 HC | MRI | Cortical Atlas | Thickness and Volume-Based Features | Surface-Based Morphometry | Different Cassifiers(SVM,FT, LMT) | Acc=87 Sen=95 Spe=75 |
| [299] | Clinical | 22 ASD, 22 HC | MRI | NA | GLM, Different Features | RFE-SVM | SVM | Spe=86 Sen=88 |
| [300] | ABIDE | 126 ASD, 126 HC | rs-fMRI | NA | Pearson Correlation Matrix, Connectivity Measures | PSO-SVM | SVM -RFE | Acc=66 Sen=60 Spe=72 |
| [301] | ABIDE | 24 ASD, 24 HC | sMRI | NA | Multivariate Statistical Pattern, Morphological Feature | NA | SVM | Acc = 80 |
| [302] | Clinical | 45 ASD, 30 HC | DTI | EVE | FA (Fractional Anisotropy), MD Mean diffusivity, Anatomical ROI's | Signal-To-Noise (s2n) Ratio Coefficient Filter | SVM | Spe=84 Sen=74 |
| [303] | Clinical | 81 ASD, 50 HC | MRI | NA | Feature Extraction (Voxelwise Tissue Density Maps For GM, WM And ventricles (VN)) | Welch's T-Test | SVM | Acc=73.28 Sen=71.6 Spe=76 |
| [304] | Clinical | 13 ASD, 15 HC | fMRI | NA | Functional ROIs, Functional Connectivity, Seed-Based Connectivity | T-Test | Logistic regression | Acc > 96.3 |
| [305] | Clinical | 23ASD,22 HC | MRI | NA | Orientation Invariant Features of Each ROI's Mean FOD | PCA | SVM | Acc=77 |
| [306] | Clinical | 76 ASD,76 HC | sMRI | NA | Sequences Of The Intensity Values Of The GM Segments | SVM-RFE | SVM | Sen=82 Spe=80 |
| [307] | Clinical | 15 ASD, 15 HC | Task-fMRI | NA | Functional Connectivity, Effective Connectivity | NA | RCE-SVM | Acc= 95.9 Sen= 96.9 Spec= 94.8 |

| | | | | | | | | |
|--------|-----------------|---|-------------|-------------|---|--|--|---|
| [308] | Clinical | 20 ASD, 20 HC | MRI | NA | Morphological Parameters Including Volumetric and Geometric Features | NA | SVM | Sen=90 Spe=80 |
| [309] | Clinical | 10 ASD, 10 HC | DTI | JHU-DTI-MNI | Brain Connectivity Network | Network Regularized SVM-RFE | SVM | Acc=100 |
| [310] | Clinical | 31 Klinefelter syndrome, 8 XYY Syndrome 75 HC | sMRI | NA | Statistical Parametric Mapping (Grey Matter Volume (TGMV) A Volume (TWMV) Measures) | RFE | SVM | NA |
| [311] | Clinical, ABIDE | 79 ASD, 105 HC | MRI | NA | Voxel Locations of VBM Detected Brain Region | T-test | PBL-McRBFN | Acc (Mean)=70 Sen(Mean)=53 Spe(Mean)=72 |
| [312] | Clinical | 82 ASD, 84 HC | sMRI | NA | Inter-Regional Thickness Correlation (IRTC) Using Pearson Correlation Between the Cortical Thicknesses of Each Region. | NA | Support Vector Regression | NA |
| [313] | Clinical | DTI Data: 5 b0 iImages, followed by 30 Diffusion Weighted Images, Child Control dataset | fMRI DTI | Brodmann | Fiber Connectivity Feature, ROIs Extraction, Functional Connectivity Information | NA | mv-EM | Max Percent Error: mv-EM: 8.55 |
| [314] | Clinical | 21 ASD, 21 HC | fMRI | NA | Neural Substrates And Inter-Individual Functional Connectivity | T-test | NA | Acc=74.2±1.9 |
| [315] | BLSA | 17 MCI (mild cognitive impairment) | MRI | NA | Tissue Density Maps, Top-Ranked Features Wavelet Decomposition Level | Wavelet-Based Data Compression | JointMMCC | Different Results |
| [316] | Clinical | 38 ASD, 38 HC | sMRI | NA | Volumetric Variables (GM, WM, CSF, TIV), | SVM-RFE, T-test | SVM | AUC= 80 |
| [317] | Clinical | 13 ASD | MRI | NA | Regional Cortical Thicknesses And Volumes | NA | Three Decision-Tree-Based Models, SVM, logistic Model Tree | Acc > 80 Spe > 34 Sen > 92 |
| [318] | ABIDE | 447 ASD, 517 HC | rs-fMRI | NA | Functional Connectivity From a lattice of ROIs Covering The Gray Matter | NA | leave-one-out | Acc=60 Spe=58 Sen=62 |
| [319] | Clinical | 22 ASD, 16 HC | MRI | NA | Using Surface-based morphometry For Cortical Features (Average thickness, Mean Curvature, Gaussian curvature, Folding index, Curvature index) | NA | SVM, FT, LMT | Acc (SVM)=74 Acc(FT)=76 Acc(LMT)=76 |
| [320] | Clinical | 76 ASD, 76 HC | sMRI | NA | GM Volumes | RFE | SVM | AUC=82 |
| [321] | Clinical | 41 ASD, 40 HC | sMRI | NA | Regional Features | -- | SVM | AUC=81 |
| [3222] | ABIDE | 505 ASD, 530 Neurotypical Subjects | rs-fMRI | NA | Spatial Feature based Detection Method (SFM) (Mean Connectivity Matrices, Discriminative Log-variance Features) | Feature Selection Based on top m Signals | SVM | Acc=95 |
| [323] | Clinical | 41 ASD, 40 HC | sMRI | NA | ROI Features | -- | SVM | AUC=74 |

| | | | | | | | | |
|-------|----------|--|-----------------|----|---|----------------|-----|------------------------|
| [324] | Clinical | 35 ASD, 51 TD, 39 No Known Neuropsychiatric Disorders | fMRI | NA | Individual Difference Measures in BOLD Signals | -- | LR | Sen=63.64 Spe=73.68 |
| [325] | ABIDE | 112 ASD, 128 HC | rs-fMRI | NA | Functional Connectivity Values | F-score Method | SVM | Acc=79.17 |
| [326] | NDAR | 58 ASD, 59 HC | sMRI | NA | Regional and Interregional Morphological Features | T-Test mRMR | SVM | Acc=96.27 AUC=99.52 |
| [327] | ABIDE | 127 ASD, 153 TD | sMRI rs-fMRI | NA | Quantitative Imaging Features (Regional Gray Matter and Cortical Thickness Volumes0 | mRMR | SVM | Acc=70 |

5. Challenges in detecting ASD with MRI neuroimaging modalities and AI techniques

This section introduces the challenges facing in ASD detection from MRI neuroimaging modalities and AI techniques. The challenges mentioned in this section cover dataset limitations, lack of access to multimodal datasets, AI techniques, and suitable hardware resources. They are briefly described below.

- Unavailable MRI neuroimaging datasets with different ASD patient

All datasets available involve two classes of ASD and control fMRI or sMRI modalities. However, there are different types of ASD, and this poses a serious obstacle for researchers in AI wishing to develop systems that can detect different types of disorders. Datasets with different types of ASD can help pave the way for accurate diagnosis of various types of ASD.

- Unavailable multi-modalities datasets for ASD diagnosis

In medical research, specialists have shown that using neuroimaging multimodalities can effectively improve brain disorders diagnosis. Neuroimaging modality fusion is one of the newest methods for diagnosing brain disorders such as ASD [355], SZ [356], and ADHD [357]. Physicians usually use MRI data with other neuroimaging modalities to diagnose brain disorders. To diagnose neurological and mental disorders, fMRI-MEG [358], MRI-PET [359], and EEG-fMRI [360] are the most important multimodalities. Unfortunately, the neuroimaging multimodalities datasets are not available for studies on ASD diagnosis. Such datasets might lead to practical and interesting studies in ASD diagnosis.

- Challenges in AI algorithms in diagnosing ASD

CADS based on ML algorithms are highly time-consuming and complex to design. However, if the appropriate algorithms are selected, it can accurately diagnose ASD. DL methods automatically perform the steps from feature extraction to classification. By using intelligent feature extraction, DL eliminates the need for supervision on features, which may reduce the performance of a CADs based on DL compared to ML. Therefore, when ML methods are combined with DL, promising results can be obtained in CADs for diagnosis of ASD.

- Challenges in hardware's

The lack of access to appropriate hardware resources is another problem encountered by researchers in the field of automated ASD detection. ASD detection datasets that are available publicly, such as ABIDE, have a lot of data; this poses many challenges for the storage and processing of these datasets on ordinary computers. In contrast, research in CAD implementation on cloud servers has not been seriously conducted to eliminate hardware resource problems. As a result, cloud servers are not yet extensively used for data storage and processing. Recently, some DL models called deep compact CNN models been introduced to be implemented on hardware systems with limited resources. Deep compact-size CNN models require fewer hardware sources than other CNN methods [361-362]. Some deep compact-size CNN methods include FBNetV3 [363], MobileNet [364], and TinyNet [365].

6. Discussion

This paper presents and compares the research about automated ASD detection with MRI neuroimaging modalities and AI methods. First, this section comprehensively compares the conducted studies on ASD detection using ML and DL techniques. In subsection one, the number of studies conducted annually in the ASD detection from MRI neuroimaging modalities using different ML and DL techniques are presented. In subsection two, the MRI datasets employed in studies on the automated diagnosis of ASD using ML and DL techniques are compared. In subsection three, the number of MRI studies conducted annually on ASD

detection from MRI neuroimaging modalities are discussed. The employed atlas in ML and DL studies for ASD detection are introduced in subsection four. Section five discusses MRI pipeline techniques in the diagnosis of ASD research using ML and DL methods. Ultimately, different classification algorithms for ML and DL-based diagnosis of ASD are compared.

- **Comparison between the numbers of papers published each year for ML and DL research**

This section presents the number of published papers annually on ASD detection using AI techniques. Studies on the ASD detection from MRI modalities and ML and DL techniques began in 2017. Table (2) represents the papers on ASD detection in MRI neuroimaging modalities using ML methods. In addition, articles in ASD detection in MRI neuroimaging modalities using DL techniques are introduced in Appendix A. Figure (4) illustrates the number of papers published annually on ML and DL techniques for ASD detection.

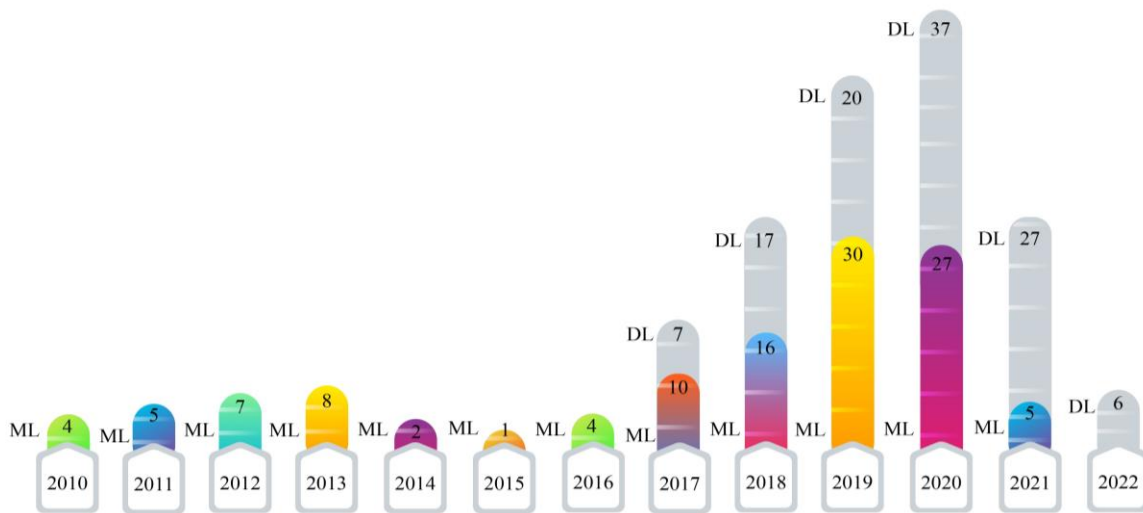


Fig. 4. Shows the number of papers published in ASD detection using ML and DL methods.

As demonstrated in recent years, researchers' interest in using DL architectures has significantly grown compared to ML techniques. According to Fig. (4), DL models are used more in studies on the automated diagnosis of ASD with MRI modalities than ML models. Therefore, implementation of CADs based on DL techniques is promising for developing applied software for ASD detection with MRI neuroimaging modalities in the future. For automated diagnosis of ASD with MRI modalities, various datasets are proposed in ABIDE. Besides, various toolboxes are available for the implementation of different DL models. These reasons are the foundation for many studies on the automated diagnosis of ASD using DL models.

- **Comparison between the numbers of datasets used in the ML and DL research**

As stated in the neuroimaging modalities section, limited datasets are accessible. ABIDE is the most important dataset available in this field, which includes two datasets, ABIDE I and ABIDE II. Figure (5) demonstrates the types of datasets employed in the automated ASD diagnostic research using DL and ML techniques.

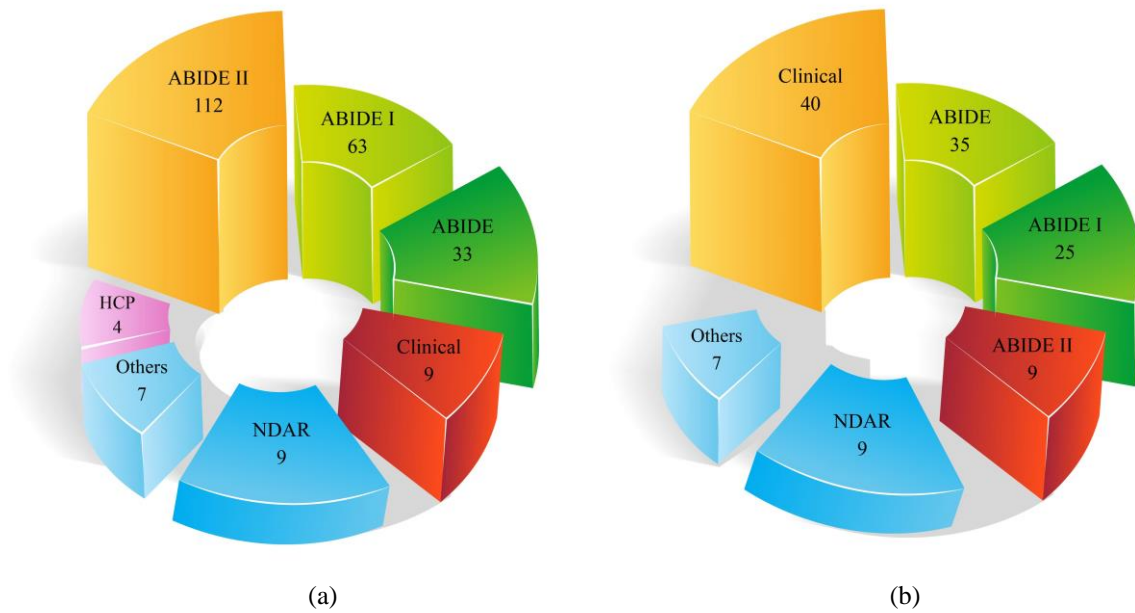


Fig. 5. Number of datasets used for automated ASD detection. a) DL and b) ML methods.

It can be noted from Fig. (5a) and (5b) that a greater number of ABIDE datasets are employed in studies on the automated diagnosis of ASD. The major reason for the wide use of this dataset in various studies on the automated diagnosis of ASD is the availability of many subjects and different MRI modalities.

- **Comparison between the numbers of neuroimaging modalities used in the ML and DL research**

The different structural and functional MRI neuroimaging modalities and ML and DL methods, play an essential role in automated ASD detection. In Table (2) reports studies on the automated ASD detection using ML techniques and different MRI neuroimaging modalities have been presented. Moreover, Table (3) discusses the ASD detection using DL techniques. Figures (6a), and (6b) describes the annual research carried out to detect automated ASD using sMRI and fMRI neuroimaging modalities.

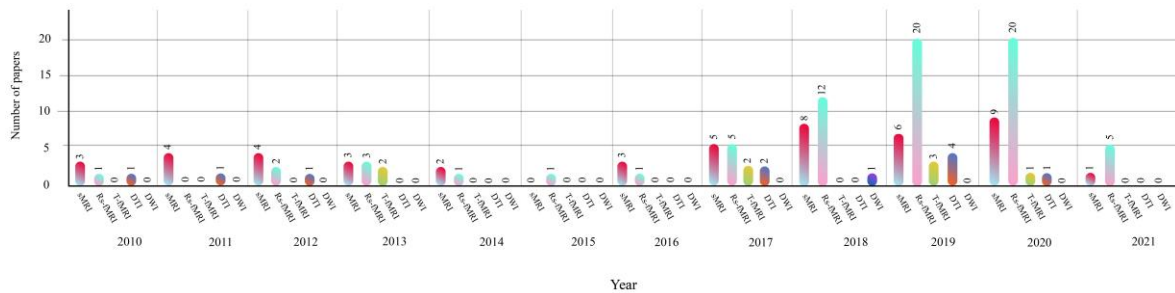


Fig. 6a. Shows the number of MRI neuroimaging modalities used in the CADs based on ML methods.

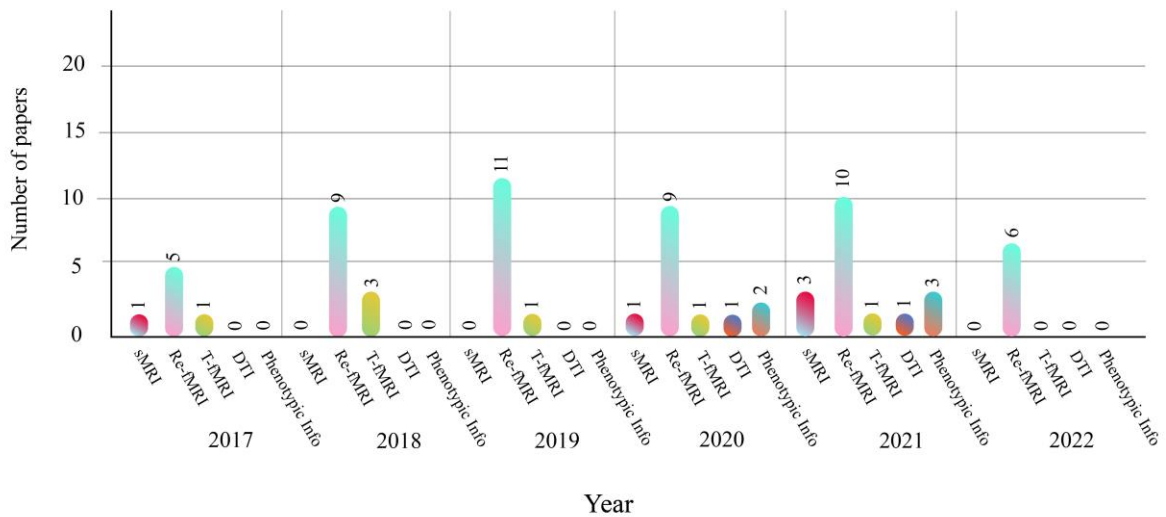


Fig. 6b. Shows the number of MRI neuroimaging modalities used in the CADs based on DL methods.

As shown in Figures (6a) and (6b), the rs-fMRI modalities are most used in studies on ASD detection using ML and DL methods. As mentioned earlier, ASD is a neurological disorder that negatively affects brain function. Accordingly, researchers have used rs-fMRI modalities most widely in studies on ASD detection using AI methods.

- **Comparison between the numbers of Atlases used in the ML and DL research**

In another part of Tables (2) and (3), the types of Atlases for MRI neuroimaging modalities have been provided. Atlases are considered an important preprocessing step discussed in part of this section. The number of atlases and employed in ML and DL research are described in Figure (7).

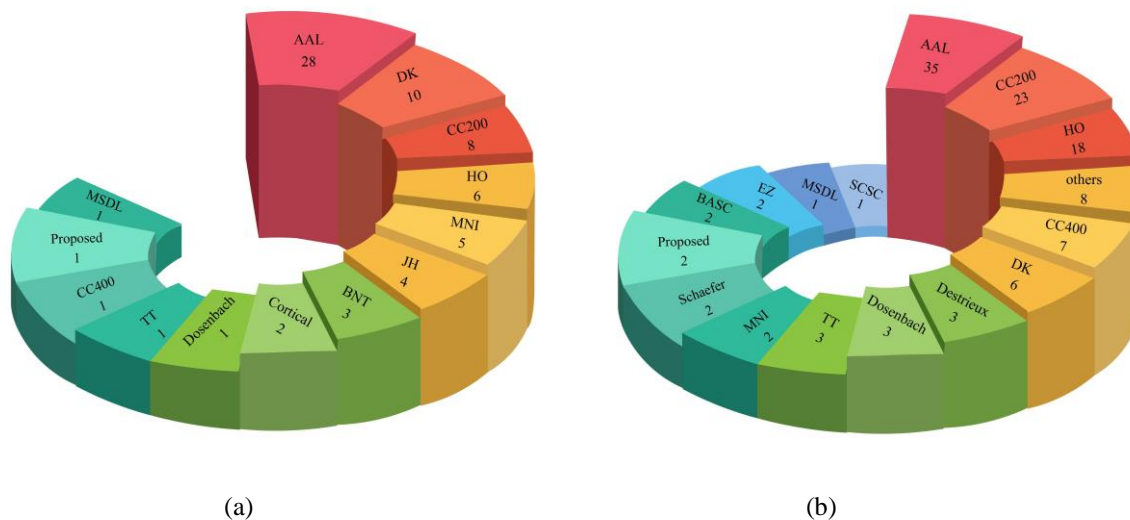


Fig. 7. Number of Atlas used for ASD Detection. a) ML and b) DL methods

As shown in Fig. (7a) and (7b), the AAL atlas is most used in studies for ASD detection in MRI neuroimaging modalities using AI methods.

- **Comparison between the numbers of pipelines used in the ML and DL researches**

Pipelines play a significant role in preprocessing of MRI modalities. The pipelines employed in ASD data preprocessing are presented in Tables (2) and (3). The number of pipelines utilized in DL and ML research is shown in Figure (8). The results of the studies reveal that the CPAC pipeline is the most widely used.

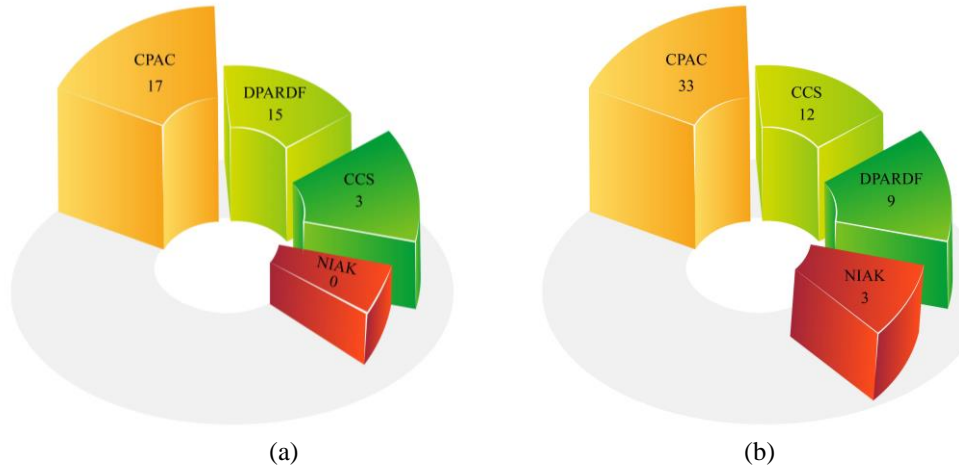


Fig. 8. Number of pipelines used for ASD Detection: a) ML and b) DL methods.

- **Comparison between the numbers of classification methods in the ML and DL research**

Classification is the last step of CADs with ML or DL methods. So far, various classification methods have been proposed in ML and DL, which are presented in Tables (2) and (3). The types of classification algorithms applied in CADs using DL and ML are depicted in Figure (9). As shown in this figures (9a) and (9b), it may be noted that the Softmax method is most used in DL architectures. In addition, compared to other classification methods, SVM is the most widely applied in ML methods.

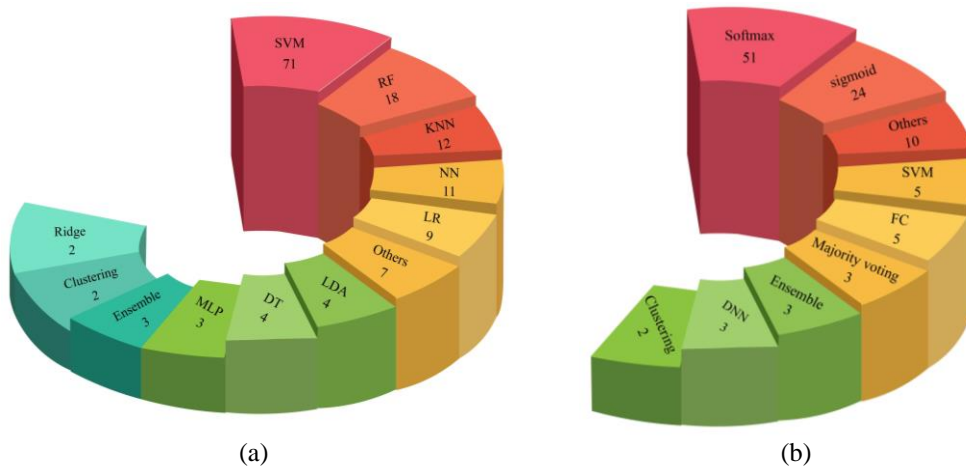


Fig. 9. Number of classifiers used in CADs for ASD detection: a) ML and b) DL methods.

7. Future Works

Lack of access to huge public datasets with various ASD disorders researchers is a big challenge. As mentioned in the introduction, autism has different types [2], and the availability of datasets containing different types of ASD is of paramount importance for researchers. Hence, presenting MRI datasets of different types of autism disorder need to be addressed in future works. These datasets help researchers conduct more studies and compare their studies with other researchers on the automated diagnosis of ASD. As mentioned in previous sections, ABIDE is a free dataset available for researchers and consists of

different cases and MRI modalities of ASD patients. But it does not have a large number of cases of DTI modalities for the diagnosis of ASD. DTI modality is one of the popular methods in ASD detection. Publicly providing more datasets of this type of modality could increase research in the ASD diagnosis field using DTI modality.

Another future work is to provide multimodal datasets, such as fMRI-EEG, for the diagnosis of ASD. In clinical studies [158], it has been indicated that using multimodal neuroimaging, such as fMRI-EEG, plays a pivotal role in diagnosing ASD. Providing datasets with combined modalities paves the way for new studies on the diagnosis of ASD using different AI methods.

Automated diagnosis of ASD with MRI using ML techniques can be the other future work. Various methods have been proposed for feature extraction from MRI data for the diagnosis of ASD, which are summarized in Table (2). According to Table (2), fuzzy-based feature extraction techniques have not been used in the diagnosis of ASD, and they can be introduced in future work. Fuzzy techniques are important in medical applications and allow researchers to develop software close to human logic [159-164]. Hence, providing graph models based on fuzzy theory can be addressed in the future, leading to the accurate diagnosis of ASD with MRI modalities. Connectivity techniques are an essential feature extraction method for structural and functional neuroimaging modalities [165-170]. Proposing new feature extraction methods based on connectivity for structural and functional neuroimaging modalities is also another field for future works. Table (2) also indicates classification algorithms. In this section, fuzzy type 1 and 2 techniques can be used for data classification as future work on the diagnosis of ASD [171-173]. Furthermore, in the future, graph theory-based classification methods can also be used to increase the performance of the CADs for automated diagnosis of ASD [174-175].

In Appendix (A), different studies on the automated diagnosis of ASD using MRI modalities and DL techniques is presented. It may be noted that conducted studies have used standard DL methods to diagnose ASD. In future works, graph theory [176-177], representation learning [178-179], zero-shot learning [180], Q-learning [181], attention learning [182], and advanced models of adversarial networks [183-184] can be used for the automated diagnosis of ASD with MRI modalities.

Feature fusion technique is a new field in diagnosing different diseases, and many studies are being conducted in this field [185-190]. The DL features can be extracted from MRI images for automated ASD detection. Ultimately, ML and DL features can be used to obtain high performance in the automated diagnosis of ASD.

8. Conclusion

ASD is a neurological disorder with unknown symptoms that begins in childhood and cause problems in communication, social relationships, perception processing, and repetitive behaviors. In few studies, physicians have stated that ASD usually occurs due to genetic mutations or the inability of the fetus's brain cells to obey regular growth patterns during the first steps [1-5].

Physicians use different ASD detection methods, among which different neuroimaging modalities are of paramount importance. Among different types of neuroimaging modalities, MRI-based functional and structural modalities are mostly used to diagnose ASD. sMRI and fMRI provide physicians with important information on the structure and function of the brain, respectively. Accurate diagnosis of ASD from sMRI and fMRI is sometimes time-consuming and challenging. Moreover, factors such as tiredness or different noises in MRI modalities may lead to clinicians' wrong diagnosis of ASD.

For this purpose, many studies are being conducted on the automated diagnosis of ASD using AI techniques, aiming to increase the performance of automated diagnosis of ASD. In general, studies on the

automated diagnosis of ASD from MRI modalities using AI cover ML and DL methods. In few papers, researchers have conducted a review study in ASD detection based on DL [6] and ML [191-196] methods with different neuroimaging modalities.

This work is a comprehensive review of studies conducted on ASD detection in different MRI neuroimaging modalities using AI methods. First, AI-based CADs for ASD detection from different MRI neuroimaging modalities was introduced. Then, the steps of the CADs based on ML algorithms for automated ASD detection in MRI neuroimaging modalities were studied. Also, in this section, papers on the automated ASD detection in MRI neuroimaging modalities using ML methods are summarized in Table (2). Previously, some authors of this study previously published a review paper about automatic ASD detection in different neuroimaging modalities using DL techniques [6], which is summarized in Table (3). In another section, the most critical challenges in ASD detection in MRI neuroimaging modalities and AI methods were presented. Also, this section studied the most important challenges in the automated diagnosis of ASD using MRI modalities and AI techniques. The most important challenges in the diagnosis of ASD are the lack of access to public datasets with different MRI modalities, multimodal datasets, such as fMRI-EEG, AI algorithms, and hardware resources.

In the discussion section, first, the number of published annual papers in ASD detection using ML methods and DL techniques were discussed. Then, the number of datasets used in ML and DL studies was presented. In addition, the number of different MRI neuroimaging modalities with ML and DL methods used in annual studies in ML and DL was also indicated. Also, a comparison was made between different atlases used in MRI neuroimaging preprocessing for ASD detection. In another subsection, the number of pipelines in the preprocessing step of the MRI neuroimaging modalities for CADs based on various AI methods is also examined and compared. Finally, the number of classifier algorithms used in ML and DL studies for ASD detection was discussed.

In section 5, the future works for ASD detection in MRI neuroimaging modalities and AI methods were addressed. In this section, future works on MRI datasets for the diagnosis of ASD were first discussed. Then, future works on the diagnosis of ASD using AI techniques were addressed. Besides, future works on the automated diagnosis of ASD with MRI modalities were introduced. The final section also recommended the idea of using feature fusion for the diagnosis of ASD with MRI modalities in future works. Studies on ASD detection using AI techniques indicate that researchers will use the proposed methods in the future. The proposed methods are promising in developing real software for ASD detection using MRI modalities and help clinicians quickly diagnose ASD in the early stage.

Appendix A:

Table 3: Automated diagnosis of ASD with MRI neuroimaging modalities using DL methods.

| Work | Datasets | Neuroimaging Modalities | Image Atlas + Pipeline | Details for Deep Learning Models | | | | |
|-------|--------------------|-------------------------|--------------------------------------|----------------------------------|---|----------------------|------------------------|-----------------|
| | | | | Architecture | Layers | Optimizer | Loss Function | Classifier |
| [197] | Clinical | T-fMRI | MNI152 Atlas | 2CC3D | CNN (6) + Pooling (4) + FC (2) | -- | BCE | MV |
| | | Residual fMRI | | | | | | |
| [198] | Clinical | T-fMRI | AAL Atlas | 2CC3D | CNN (6) + Pooling (4) + FC (3) | -- | -- | Sigmoid |
| [199] | HCP | T-fMRI | -- | 3D-CNN | CNN (2) + LReLU + Pooling (1) + FC (1) | SGD | MNLL | Softmax |
| | | rs-fMRI | | | | | | |
| [200] | Clinical | T-fMRI | AAL Atlas | LSTM | LSTM (1) + Pooling (1) + FC (3) | Adadelata | MSE | Sigmoid |
| [201] | Different Datasets | T-fMRI | AAL Atlas | 2D-CNN | CNN (2) + ReLU + BN (4) + FC (3) | Adam | -- | Softmax |
| | | rs-fMRI | | | | | | |
| | | Phenotypic Info | | | | | | |
| [202] | Clinical | T-fMRI | AAL Atlas | 2CC3D | CNN (6) + Pooling (4) + FC (2) | -- | -- | Sigmoid |
| [202] | ABIDE-I | rs-fMRI | AAL Atlas | 2CC3D | CNN (6) + Pooling (4) + FC (2) | -- | -- | Sigmoid |
| [203] | ABIDE I | rs-fMRI | All Atlases + CPAC Pipeline | 3D-CNN | CNN (2) + ELU + Pooling (2) + FC (2) | SGD | -- | Sigmoid |
| | ABIDE II | | | | | | | |
| [204] | ABIDE I | rs-fMRI | CC-200 and AAL Atlas + CPAC Pipeline | AE | Standard AE with Tanh Activation | -- | MSE | SLP |
| | | | | | | | BCE | |
| [205] | ABIDE I | rs-fMRI | HO Atlas + CPAC Pipeline | G-CNNs | Proposed G-CNN with 3 Layer CNN | Adam | -- | Softmax |
| [206] | ABIDE I | rs-fMRI | AAL Atlas + CCS Pipeline | BrainNet | Element-Wise (1) + E2E (2) + E2N (1) + N2G (1) + FC (3) + Leaky ReLU + Tanh | Adam | Proposed Loss function | Softmax |
| [207] | ABIDE I | rs-fMRI | AAL Atlas | DAE | Standard DAE | -- | Proposed Loss function | -- |
| [208] | ABIDE | rs-fMRI | NA | LeNet-5 | Standard LeNet-5 Architecture | -- | -- | Softmax |
| [209] | ABIDE I | rs-fMRI | AAL Atlas + NIAK Pipeline | SAEs | SAE with LSF Activation | L-BFGS | -- | Softmax |
| [210] | ABIDE I | rs-fMRI | NA | MCNNE | CNN (3) + ReLU + Pooling (3) + FC (1) | Adam | BCE | Binary SR |
| | ABIDE-II | | | | | Adamax | | |
| | ABIDE I + II | | | | | | | |
| [211] | ABIDE | rs-fMRI | All Atlases + CPAC Pipeline | 3D-CNN | CNN (2) + ELU + Pooling (2) + FC (3) | SGD | BCE | Various Methods |
| | | | | | | Adam | MSD | |
| [212] | ABIDE I | rs-fMRI | AAL Atlases + DPARSF Pipeline | VAE | VAE with 3 Layers | Adadelata | Proposed Loss Function | -- |
| [213] | ABIDE I | rs-fMRI | CC200 Atlases + CCS Pipeline | LSTM | LSTM (1) + Pooling (1) + FC (1) | Adadelata | BCE | Sigmoid |
| [214] | ABIDE | rs-fMRI | CC200 Atlases | SAE | SAE (3) + Sigmoid | Proposed Opt. L-BFGS | MSE | Clustering |
| | | Phenotypic Info | | | | | | |
| [215] | ABIDE | rs-fMRI | -- | SAE | LSTM (1) + Pooling (1) + FC (1) | Adadelata | BCE | Sigmoid |
| [216] | ABIDE I | rs-fMRI | AAL Atlases + CCS Pipeline | LSTM | LSTM (2) + Pooling (1) + FC (2) | Adam | BCE | Sigmoid |
| | | | | | | | MSE | |

| | | | | | | | | |
|-------|-------------|-----------------|---|----------------|---|------------------|------------------------|--------------------------|
| [217] | ABIDE I | rs-fMRI | Different Atlas | DANN | 3 MLP (1 Dropout + 4 Dense) + Self-Attention (3) + Fusion (3) + Aggregation + Dense (1) + ReLU, ELU, and Tanh | -- | SE | Sigmoid |
| [218] | ABIDE | rs-fMRI | AAL Atlas + CCS Pipeline | SSAE | 3 SSAE Layers | Gradient Descent | Proposed Loss Function | Softmax Regression |
| [219] | ABIDE I +II | rs-fMRI | Different | 1D-CNN | CNN (1) + Pooling (1) + FC (1) | Adam | -- | Softmax |
| [220] | ABIDE I | rs-fMRI | Different Pipelines | Various Models | CNN (6) + Pooling (4) + BN (2) + FC (2) | Adam | Propose Loss Function | Sigmoid |
| [221] | ABIDE-II | rs-fMRI | NA | 1D-CAE | Encoder (4) + Decoder (4) + CNN (2) + pooling (2) + FC (2) | -- | -- | -- |
| [222] | ABIDE | rs-fMRI | CCS Pipeline | AlexNet | Standard Architecture | -- | CE | Softmax |
| [223] | ABIDE | rs-fMRI | Different Pipelines | ASDDiagNet | Proposed DiagNet | -- | -- | SLP |
| [224] | ABIDE I | rs-fMRI | SCSC Atlas + CPAC Pipeline | Auto-ASD | Proposed Auto-ASD-Network | -- | NLLF | SVM |
| [225] | ABIDE I | rs-fMRI | CC400 Atlas + CPAC Pipeline | 2D-CNN | CNN (7) + Pooling (7) + FC (3) | -- | -- | MLP |
| [226] | ABIDE | rs-fMRI | NA | CNN-AE | Proposed SDAE-CNN with 7 Layes CNN | -- | -- | Softmax |
| [227] | ABIDE I | rs-fMRI | NA | 3D-FCNN | CNN (9) + PReLU + FC (3) | SGD | CE | Softmax |
| [228] | ABIDE I | rs-fMRI | AAL Atlas + DPARSF Pipeline | SSAE | 2 Layers SSAE | -- | -- | Softmax |
| [229] | ABIDE I | rs-fMRI | NA | 3D-CNN | CNN (7) + Pooling (3) + FC (2) + Log-Likelihood Activation | SGD | MNLL | -- |
| [230] | ABIDE I | rs-fMRI | HO Atlas + CPAC Pipeline | GCN | GCN with ReLU and Sigmoid | -- | CE | Softmax |
| | | Phenotypic Info | | AE | SAE with Tanh Activation | | MSE | |
| [231] | ABIDE I | rs-fMRI | CC200 Atlas + CCS Pipeline | LSTM | Proposed Method | Adadelata | BCE | Sigmoid |
| | | Phenotypic Info | | | | | MSE | |
| [232] | ABIDE I | rs-fMRI | CC200 Atlas + CPAC Pipeline | SDAE | Proposed 2-SDAE-MLP Network | -- | MSE | Softmax |
| | | s-MRI | | | | | | |
| | | Phenotypic Info | | | | | | |
| [233] | Clinical | rs-fMRI | NA Atlas | 3D-CNN | CNN (2) + ReLU + Pooling (2) + FC (2) | SGD | BCE | Sigmoid |
| | | Fetal BOLD fMRI | | | | | | |
| [234] | ABIDE I | rs-fMRI | AAL Atlas | DBN | DBN with 5 Hidden Layers | -- | -- | LR |
| | ABIDE-II | s-MRI | | | | | | |
| [235] | IMPAC | rs-fMRI | Different Atlases | Various Models | Dense (5) + LReLU | Adam | BCE | Various Methods |
| | | s-MRI | | | | | | |
| [236] | ABIDE I | rs-fMRI | AAL, CC200, Destrieux Atlas + CPAC Pipeline | SAEs | 5 [AE (3) + MLP (2)] + Softmax | -- | -- | Softmax |
| | | s-MRI | | | | | | |
| [237] | NDAR | rs-fMRI | NA | CNN | CNN (5) + ReLU + Pooling (2) + FC (5) | -- | CE | Softmax |
| | | s-MRI | | | | | | |
| [238] | NDAR | All Modalities | Implement the Proposed Atlas | SAE | 34 [SAE network (2)] | PSVM | L-BFGS | Probabilistic SVM (PSVM) |
| [239] | NDAR | s-MRI | NA | DDUNET | Proposed DDUNET with 11 blocks and ReLU | SGD | CE | -- |
| [240] | ABIDE I | s-MRI | NA | SNCAE | Proposed SNCAE Newtork | -- | -- | Softmax |

| | NDAR/Pitt | | | | | | | |
|-------|-----------------------|-----------------|---|---------------------------|---|-------------------|---------------------------|-------------------------|
| | NDAR/IBIS | | | | | | | |
| [241] | ABIDE 1 | s-MRI | Destrieux | SpAE | SpAE with 2 Networks | -- | MSE | Softmax |
| [242] | HCP | s-MRI | Desikan– Killia (DDK) Atlas | DEA | AE (3) + SELU | Adam | Sum of MSE + 2 CE + CC | -- |
| | ABIDE 1 | | | | | | | |
| [243] | ABIDE | s-MRI | NA | DCNN | CNN (6) + ReLU + Pooling (6) + FC (4) | Adam | BCE | Sigmoid |
| | CombiRx | | | | | | | |
| [244] | ABIDE-II | s-MRI | DKT Atlas | CNN | Proposed FastSurfer CNN Network | Adam | Logistic & Dice Losses | Softmax |
| [245] | ABIDE 1 | s-MRI | Different | 3D-CNN | CNN (3) + ReLU + Pooling (3) + FC (2) | Adadelata | CE | Softmax |
| [246] | Clinical | s-MRI | NA | UNet | DCNN (7) + ReLU + Pooling (2) + BN (6) | SGD | weighted CE | Softmax |
| [247] | ABIDE 1 | rs-fMRI | BN Atlas + CPAC Pipeline | CNN-RNN | CNN (4) + GRU (2) + ReLU + Pooling (2) + FC (5) | Adam | BCE | Sigmoid |
| [248] | Clinical | fNIRS | NA | CNN-LSTM | Proposed 1D-CNN LSTM with ReLU Activation | Adam | CCE | Bagging |
| [249] | Clinical | fNIRS | NA | CGRNN | CNN (3) + ReLU + Pooling (1) + GRU (1) + FC (1) | Adam | BCE | Sigmoid |
| [250] | Different Datasets | s-MRI | Different Atlas | CNN | Variation of the U-net Convolutional Architecture | Adam | Proposed Loss Function | -- |
| [251] | ABIDE 1+II | rs-fMRI | HO Atlas + CPAC Pipeline | 3D-CNN | CNN (2) + ELU + Pooling (2) + FC (2) | SGD | BCE | MV |
| [252] | ABIDE 1 | rs-fMRI | CPAC Pipeline | CNN-RNN | CNN (8) + Conv-BiLSTM (2) + Sigmoid + Pooling (1) + FC (1) | Adam | CE | Softmax |
| | | Phenotypic Info | | | | | | |
| [253] | ABIDE 1 | rs-fMRI | NA | AE | Proposed AE with 7 Layers | -- | -- | DNN |
| | | s-MRI | | | | | | |
| [254] | ABIDE 1 | rs-fMRI | CC200 Atlas + CPAC Pipeline | CapsNet | Standard Architecture | Adam | Proposed Loss Function | K-Means Clustering |
| [255] | ABIDE | rs-fMRI | CCS Pipeline | convGRU-CNN3D | convGRU+ 3D CNN | Adam | CE | -- |
| [256] | ABIDE | rs-fMRI | CC200 Atlas + CPAC Atlas | 1D-CNN | Conv (3) + Pooling (3) + FC (1) | -- | -- | Softmax |
| [257] | ABIDE | rs-fMRI | CC200, AAL, Dosenbach Atlas + CPAC Pipeline | SDA | 3 DAEs (Each 3 Hidden Layers) | -- | -- | Different Classifier |
| [258] | ABIDE 1 | rs-fMRI | AAL Atlas + CPAC Pipeline | Proposed CNN Method | Conv (1) + Max (1) + Res-blocks (4) + Average Pooling (1) + 1 FC + ReLU | Mini-Batch SGD | Softmax CE | 4 FC |
| [259] | ABIDE | MRI | NA | DNN | Different Configurations | -- | -- | -- |
| [260] | ABIDE | rs-fMRI | DPARSF Pipeline | RBM | Proposed Architecture | -- | -- | SVM |
| [261] | ABIDE 1 | rs-fMRI | GCA Atlas | 1D-CNN | Conv (3) + Pooling (1) + FC (2) + ReLU Conv (3) + BN (3) + Pooling (4) + FC (1) + ReLU | -- | CE | Softmax |
| | ABIDE II | | HO Atlas | | | | | |
| | | | DCA Atlas | | | | | |
| [262] | IMPAC | sMRI | Proposed Atlas | 2D-CNN | Conv (3) + Pooling (1) + FC (2) + ReLU Conv (3) + BN (3) + Pooling (4) + FC (1) + ReLU | Proposed Opt | -- | Softmax |
| | | rs-fMRI | | | | | | |
| [263] | ABIDE 1 | MRI | HO, SSA Atlas | 3D-CNN | Conv (3) + Pooling (3) + FC (2) + ReLU | Adadelata | CE | Softmax |
| [264] | ABIDE 1 | rs-fMRI | CC400 Atlas + DPARSF Pipeline | GCN | Proposed Architecture | -- | -- | Majority Voting |
| [265] | ABIDE | fMRI | CC200 Atlas | GAN | Encoder, Generator, Discriminator Networks | Adam | -- | 3-Layer DNN |
| [266] | ABIDE | rs-fMRI | AAL Atlas | PreTrained Arcitectures | Densenet201, GoogleNet, Resnet101, Resnet18 | -- | -- | SVM, KNN |
| [267] | ABIDE 1 | sMRI | NA | ResNet50 | Standard Architecture | Adam | -- | Sigmoid |
| [268] | ABIDE II | rs-fMRI | AAL Atlas | Proposed 3D CNN Method | 3D Convolutional Autoencoders | -- | -- | SVM |

| | | | | | | | | |
|-------|-------------------|---------------|--|--------------------|---|---------|------------------------|------------------------|
| [269] | ABIDE I | rs-fMRI, MRI | Various Atlas | CNN-AE | Hidden Layers (4) | Adam | CE | Softmax |
| [270] | ABIDE I | sMRI | DK Atlas | DenseNet | 4 Dense Blocks | -- | -- | LDA |
| | ABIDE II | | | | | | | |
| [271] | ABIDE I | fMRI, sMRI | NA | 2D-CNN and 3D-CNN | Conv (3) + Pooling (3) + FC (2) | -- | -- | Diferrent Methods |
| [272] | NDAR | Task fMRI | HO Atlas | 2D CNN | Conv (3) + Pooling (3) + FC (2) | SGD | -- | Softmax |
| [273] | ABIDE | rs-fMRI | CC200 Atlas + CCS Pipeline | cGCN | Conv (5) + RNN (Temporal Average Pooling Layer) | Adam | -- | Softmax |
| [274] | ABIDE | rs-fMRI | CC200 Atlas + CPAC Pipeline | 1D-CNN | Conv (3) + Pooling (3) + FC (1) | -- | -- | Softmax |
| [275] | ABIDE I | rs-fMRI | CC400 Atlas + CPAC Pipeline | DNN | Hidden Layers (2) | Adam | BCE | Softmax |
| [276] | ABIDE I | rs-fMRI | AAL Atlas + CPAC Pipeline | FCNN | FC (2) + BN (2) + LeakyReLu | Adam | BCE | Sigmoid |
| [277] | ABIDE I | rs-fMRI | CC200 Atlas + CPAC Pipeline | DCAE | Encoder: 4 CNN Networks [Conv (4) + BN (3) + Pooling (2) + ReLU], Decoder: 4 CNN Networks [Reverse Configuration] | -- | -- | FC Layer + Dense Layer |
| [278] | ABIDE I | rs-fMRI | CC400 Atlas + CPAC Pipeline | 2D-CNN | Conv (2) + EvoNorm-S0 (2) + Tanh + FC Layer (1) | Adam | BCE | Sigmoid |
| [279] | ABIDE I | sMRI | SRI24 Atlas | ResNet | Conv Blocks (5) | Adam | BCE | FC Network |
| [280] | ABIDE I | rs-fMRI | CPAC Pipeline | CNN-AE | AE Network + 1D-Conv (2) + BN (2) + ReLU + Pooling (2) + FC (2) | | | Sigmoid |
| [281] | ABIDE | fMRI | AAL Atlas | FC | Pooling (2) + Conv (3) + FC (1) + ReLU | Adam | -- | Softmax |
| | | | | ALFF Net | Pooling (2) + 3D-Conv (4) + FC (1) + ReLU | | | |
| [282] | ABIDE I | ??? | DK Atlas | CGTS-GAN | Proposed Architecture | -- | -- | -- |
| [283] | ABIDE I | Rs-fMRI | AAL Atlas + DPARSF Pipeline | CNN | NA | -- | -- | Softmax |
| | ABIDE II | | | | | | | |
| [284] | ABIDE I | rs-fMRI | CPAC Pipeline | SAE | Two unsupervised Sparse AEs | -- | -- | Sypervised AE |
| [285] | ABIDE I | rs-fMRI | BASC Pipeline | CNN-RNN | Different Architectures | -- | -- | Sigmoid |
| [286] | ABIDE I | rs-fMRI | MSDL Pipeline | 1D-CNN | Conv (4) + BN (3) + Pooling (3) + FC (2) + ReLU | -- | -- | Sigmoid |
| [287] | ABIDE I | rs-fMRI | CCS Pipeline | Inception-ResNetV2 | InceptionResNetV2 Architecture + Pooling Layers | SGD | -- | Softmax |
| [288] | ABIDE I | rs-fMRI | NA | ResNet-50 | Standard Architecture | -- | -- | Softmax |
| | ABIDE II | | | | | | | |
| [289] | ABIDE I | rs-fMRI | CC200 + CPAC Pipeline | ASD-SAENet | SAE + DNN | Adam | CE | Softmax |
| [290] | ABIDE I | rs-fMRI | BASC, CC200, and AAL Atlas + CPAC Pipeline | DNN | Hidden (2) + ReLU | -- | -- | Sigmoid |
| [291] | ABIDE I | rs-fMRI | CC200 Atlas + CPAC Pipeline | DBN | 3 RBM Layers | RMSProp | CE | Softmax |
| [292] | Different Dataset | sMRI and fMRI | AAL Atlas | 2D-CNN | Conv (1) + FC (3) + BN (3)+ ReLU | Adam | -- | Softmax |
| [293] | ABIDE I | rs-fMRI | AAL Atlas + DPARSF Pipeline | CNNGLasso | Conv Layer + FC Layer | Adam | Proposed Loss Function | Softmax |
| [294] | ABIDE I | sMRI, fMRI | Various Atlas | GCN | p-GCN + s-GCN + ss-GCN Networks | -- | -- | -- |
| | ABIDE II | | | | | | | |
| [295] | KKI | rs-fMRI, DTI | AAL Atlas | MGCN | Proposed Architecture | SGD | | ANN |

| | | | | | | | | |
|-------|----------|---------------------|---------------------|--|---|---------|------------------------|--|
| | HCP | | | | | | Combined Loss Function | |
| [296] | Clinical | rs-fMRI, DTI | AAL Atlas | LSTM-ANN | LSTM (2) + Both the P-ANN and the A-ANN Have 2 Hidden Layers + ReLU | Adam | Proposed Loss Function | Attention-Weighted Average |
| [328] | NDAR | T-fMRI, sMRI | HO | 1D-CNN | CNN (2) + ReLU + Pooling (2) + FC (1) | SGD | -- | Softmax |
| [329] | ABIDE | rs-fMRI | CCS | 3D-CNN | CNN (3) + ReLU + Pooling (3) + FC (1) | Adam | -- | Sigmoid |
| [330] | ABIDE | rs-fMRI | 6 Atlases + CPAC | Multi-Atlas Graph Convolutional Network Method (MAGCN) | GCN Model | -- | Cross Entropy | Stacking Ensemble Learning Method + Ridge Classifier |
| [331] | ABIDE I | rs-fMRI | -- | MHATC | Multi-Head Attention Encoder (MHAE) + Temporal Consolidation Module (TCM) | -- | Cross Entropy | Pooling (1) + FC (1) |
| [332] | ABIDE I | rs-fMRI | CC400 + CPAC | Simplified VAE Unsupervised Pretraining And MLP Supervised Fine-Tuning | Hidden Layers (3) | RMSProp | Cross Entropy | Softmax |
| [333] | NDAR | sMRI, fMRI | Talairach | Deep Fusion Classification Network (DFCN) | 2 Stacked Autoencoder With Non-Negativity Constraint (SNCAE) | -- | -- | Softmax |
| [334] | ABIDE | sMRI | -- | 2D CAM, 3D CAM, 3D Grad-CAM | Proposed Architectures | -- | Cross Entropy | Classification Output Layer |
| [335] | ABIDE | rs-fMRI | HO + CPAC | Invertible Dynamic GCN (ID-GCN) | Three Invertible Blocks (2 Different GCN) | -- | Cross Entropy | Softmax |
| [336] | ABIDE | rs-fMRI | AAL, HO, MODL | Functional Graph Discriminative Network (FGDN) | Functional Graph Construction Layer (1) + Graph Conv Layers (2) + PReLU + FC Layer (1) | Adam | Proposed Loss Function | Sigmoid |
| [337] | ABIDE | rs-fMRI, Phenotypic | CPAC + HO | Combined DFS and GCN Method | Sparse One-To-One Linear Layer + Hidden Layers (3) + Graph Conv Layers + ReLU + Dropout Layer | Adam | Proposed Loss Function | Softmax |
| [338] | ABIDE | rs-fMRI, Phenotypic | -- | Adaptive Multi-Layer Aggregation Graph Convolutional Network (AMA-GCN) | Proposed Architectures | Adam | Fusion Loss | Softmax |
| [339] | ABIDE I | rs-fMRI, Phenotypic | CPAC + HO | DeepGCN | 16 Layers GCN + Dropout + ResNet Units + DropEdge Strategy | -- | -- | Softmax |
| [340] | ABIDE | rs-fMRI | AAL, CC200 + DPARSF | Multi-Scale Graph Representation Learning (MGRL) Framework | Multi-Scale FCNs Construction + FCNs Representation Learning Via Multi-Scale GCNs + Multi-Scale Feature Fusion and Classification | Adam | Cross Entropy | Softmax |
| [341] | ABIDE | rs-fMRI | -- | CNN | CNN (3) + ReLU + Pooling (2) + FC (2) | -- | -- | Softmax |
| [342] | ABIDE I | rs-fMRI | -- | SSAE + MLP | Dense Layers (4) + ReLU + Dense Layers (4) | -- | Cross Entropy | Softmax |
| [343] | ABIDE | rs-fMRI | AAL, CC200 + CPAC | Multi-View Graph Convolutional Neural Network (MVS-GCN) | Graph Structure Learning (GSL) + Multi-Task Graph Embedding Learning for Different Views of Brain Networks (MVL) + View Consistency Regularization (VCR) and the Prior Subnetwork Structure Regularization (SNR). | Adam | Proposed Loss Function | -- |

References

- [1] Ecker, C., Bookheimer, S. Y., & Murphy, D. G. (2015). Neuroimaging in autism spectrum disorder: brain structure and function across the lifespan. *The Lancet Neurology*, *14*(11), 1121-1134.
- [2] Sparks, B. F., Friedman, S. D., Shaw, D. W., Aylward, E. H., Echelard, D., Artru, A. A., ... & Dager, S. R. (2002). Brain structural abnormalities in young children with autism spectrum disorder. *Neurology*, *59*(2), 184-192.
- [3] Brieber, S., Neufang, S., Bruning, N., Kamp-Becker, I., Remschmidt, H., Herpertz-Dahlmann, B., ... & Konrad, K. (2007). Structural brain abnormalities in adolescents with autism spectrum disorder and patients with attention deficit/hyperactivity disorder. *Journal of Child Psychology and Psychiatry*, *48*(12), 1251-1258.
- [4] Hernandez, L. M., Rudie, J. D., Green, S. A., Bookheimer, S., & Dapretto, M. (2015). Neural signatures of autism spectrum disorders: insights into brain network dynamics. *Neuropsychopharmacology*, *40*(1), 171-189.
- [5] Sato, W., Toichi, M., Uono, S., & Kochiyama, T. (2012). Impaired social brain network for processing dynamic facial expressions in autism spectrum disorders. *BMC neuroscience*, *13*(1), 1-17.
- [6] Khodatars, M., Shoeibi, A., Sadeghi, D., Ghaasemi, N., Jafari, M., Moridian, P., ... & Berk, M. (2021). Deep learning for neuroimaging-based diagnosis and rehabilitation of autism spectrum disorder: a review. *Computers in Biology and Medicine*, *139*, 104949.
- [7] Loh, H. W., Ooi, C. P., Barua, P. D., Palmer, E. E., Molinari, F., & Acharya, U. (2022). Automated detection of ADHD: Current trends and future perspective. *Computers in Biology and Medicine*, 105525.
- [8] Noor, M. B. T., Zenia, N. Z., Kaiser, M. S., Mamun, S. A., & Mahmud, M. (2020). Application of deep learning in detecting neurological disorders from magnetic resonance images: a survey on the detection of Alzheimer's disease, Parkinson's disease and schizophrenia. *Brain informatics*, *7*(1), 1-21.
- [9] Gautam, R., & Sharma, M. (2020). Prevalence and diagnosis of neurological disorders using different deep learning techniques: a meta-analysis. *Journal of medical systems*, *44*(2), 1-24.
- [10] Yang, X., Zhang, N., & Schrader, P. (2022). A study of brain networks for autism spectrum disorder classification using resting-state functional connectivity. *Machine Learning with Applications*, *8*, 100290.
- [11] Sadeghi, D., Shoeibi, A., Ghassemi, N., Moridian, P., Khadem, A., Alizadehsani, R., ... & Acharya, U. R. (2022). An overview of artificial intelligence techniques for diagnosis of Schizophrenia based on magnetic resonance imaging modalities: Methods, challenges, and future works. *Computers in Biology and Medicine*, 105554.
- [12] Bakhtyari, M., & Mirzaei, S. (2022). ADHD detection using dynamic connectivity patterns of EEG data and ConvLSTM with attention framework. *Biomedical Signal Processing and Control*, *76*, 103708.
- [13] Shoeibi, A., Ghassemi, N., Khodatars, M., Jafari, M., Moridian, P., Alizadehsani, R., ... & Nahavandi, S. (2021). Applications of epileptic seizures detection in neuroimaging modalities using deep learning techniques: methods, challenges, and future works. *arXiv preprint arXiv:2105.14278*.
- [14] Sahu, L., Sharma, R., Sahu, I., Das, M., Sahu, B., & Kumar, R. (2022). Efficient detection of Parkinson's disease using deep learning techniques over medical data. *Expert Systems*, *39*(3), e12787.
- [15] Highland, D., & Zhou, G. (2022). A review of detection techniques for depression and bipolar disorder. *Smart Health*, 100282.
- [16] Jayanthi, A. K., & Din, Q. M. U. (2022). Early Detection of Autism Spectrum Disorder Using Behavioral Data EEG, MRI and Behavioral Data: A Review. *Assistive Technology Intervention in Healthcare*, 245-267.
- [17] Chen, X., Wang, Z., Zhan, Y., Cheikh, F. A., & Ullah, M. (2022, April). Interpretable learning approaches in structural MRI: 3D-ResNet fused attention for autism spectrum disorder classification. In *Medical Imaging 2022: Computer-Aided Diagnosis* (Vol. 12033, pp. 611-618). SPIE.
- [18] Rakić, M., Cabezas, M., Kushibar, K., Oliver, A., & Llado, X. (2020). Improving the detection of autism spectrum disorder by combining structural and functional MRI information. *NeuroImage: Clinical*, *25*, 102181.
- [19] Maenner, M. J., Shaw, K. A., Bakian, A. V., Bilder, D. A., Durkin, M. S., Esler, A., ... & Cogswell, M. E. (2021). Prevalence and characteristics of autism spectrum disorder among children aged 8 years—autism and developmental disabilities monitoring network, 11 sites, United States, 2018. *MMWR Surveillance Summaries*, *70*(11), 1.
- [20] Kasari, C., & Smith, T. (2013). Interventions in schools for children with autism spectrum disorder: Methods and recommendations. *Autism*, *17*(3), 254-267.

- [21] Matson, M. L., Mahan, S., & Matson, J. L. (2009). Parent training: A review of methods for children with autism spectrum disorders. *Research in Autism Spectrum Disorders*, 3(4), 868-875.
- [22] Volkmar, F. R., Cicchetti, D. V., Bregman, J., & Cohen, D. J. (1992). Three diagnostic systems for autism: DSM-III, DSM-III-R, and ICD-10. *Journal of Autism and Developmental Disorders*, 22(4), 483-492.
- [23] Volkmar, F. R., Cohen, D. J., & Paul, R. (1986). An evaluation of DSM-III criteria for infantile autism. *Journal of the American Academy of Child Psychiatry*, 25(2), 190-197.
- [24] Volkmar, F. R., & McPartland, J. C. (2014). From Kanner to DSM-5: autism as an evolving diagnostic concept. *Annual review of clinical psychology*, 10, 193-212.
- [25] Kim, Y. S., Fombonne, E., Koh, Y. J., Kim, S. J., Cheon, K. A., & Leventhal, B. L. (2014). A comparison of DSM-IV pervasive developmental disorder and DSM-5 autism spectrum disorder prevalence in an epidemiologic sample. *Journal of the American Academy of Child & Adolescent Psychiatry*, 53(5), 500-508.
- [26] Shoeibi, A., Rezaei, M., Ghassemi, N., Namadchian, Z., Zare, A., & Gorriz, J. M. (2022). Automatic Diagnosis of Schizophrenia in EEG Signals Using Functional Connectivity Features and CNN-LSTM Model. In *International Work-Conference on the Interplay Between Natural and Artificial Computation* (pp. 63-73). Springer, Cham.
- [27] Shoeibi, A., Sadeghi, D., Moridian, P., Ghassemi, N., Heras, J., Alizadehsani, R., ... & Gorriz, J. M. (2021). Automatic diagnosis of schizophrenia in EEG signals using CNN-LSTM models. *Frontiers in Neuroinformatics*, 15.
- [28] Esqueda-Elizondo, J. J., Juárez-Ramírez, R., López-Bonilla, O. R., García-Guerrero, E. E., Galindo-Aldana, G. M., Jiménez-Beristáin, L., ... & Inzunza-González, E. (2022). Attention Measurement of an Autism Spectrum Disorder User Using EEG Signals: A Case Study. *Mathematical and Computational Applications*, 27(2), 21.
- [29] Shoeibi, A., Ghassemi, N., Khodatars, M., Moridian, P., Khosravi, A., Zare, A., ... & Acharya, U. R. (2022). Automatic Diagnosis of Schizophrenia and Attention Deficit Hyperactivity Disorder in rs-fMRI Modality using Convolutional Autoencoder Model and Interval Type-2 Fuzzy Regression. *arXiv preprint arXiv:2205.15858*.
- [30] Siewertsen, C. M., French, E. D., & Teramoto, M. (2015). Autism spectrum disorder and pet therapy. *Adv Mind Body Med*, 29(2), 22-25.
- [31] Zürcher, N. R., Bhanot, A., McDougle, C. J., & Hooker, J. M. (2015). A systematic review of molecular imaging (PET and SPECT) in autism spectrum disorder: current state and future research opportunities. *Neuroscience & Biobehavioral Reviews*, 52, 56-73.
- [32] Zhang, F., & Roeyers, H. (2019). Exploring brain functions in autism spectrum disorder: A systematic review on functional near-infrared spectroscopy (fNIRS) studies. *International Journal of Psychophysiology*, 137, 41-53.
- [33] Brambilla, P., Hardan, A., Di Nemi, S. U., Perez, J., Soares, J. C., & Barale, F. (2003). Brain anatomy and development in autism: review of structural MRI studies. *Brain research bulletin*, 61(6), 557-569.
- [34] Ghassemi, N., Shoeibi, A., & Rouhani, M. (2020). Deep neural network with generative adversarial networks pre-training for brain tumor classification based on MR images. *Biomedical Signal Processing and Control*, 57, 101678.
- [35] 5. Hazlett HC, Poe M, Gerig G, Smith RG, Provenzale J, Ross A, et al. Magnetic resonance imaging and head circumference study of brain size in autism: birth through age 2 years. *Arch Gen Psychiatry* (2005) 62:1366–76. doi: 10.1001/archpsyc.62.12.1366
- [36] Nogay, H. S., & Adeli, H. (2020). Machine learning (ML) for the diagnosis of autism spectrum disorder (ASD) using brain imaging. *Reviews in the Neurosciences*, 31(8), 825-841.
- [37] Ahmadi-Dastgerdi, N., Hosseini-Nejad, H., Amiri, H., Shoeibi, A., & Gorriz, J. M. (2021). A Vector Quantization-Based Spike Compression Approach Dedicated to Multichannel Neural Recording Microsystems. *International Journal of Neural Systems*, 2250001-2250001.
- [38] Shoeibi, A., Ghassemi, N., Khodatars, M., Moridian, P., Alizadehsani, R., Zare, A., ... & Gorriz, J. M. (2022). Detection of epileptic seizures on EEG signals using ANFIS classifier, autoencoders and fuzzy entropies. *Biomedical Signal Processing and Control*, 73, 103417.
- [39] Alizadehsani, R., Khosravi, A., Roshanzamir, M., Abdar, M., Sarrafzadegan, N., Shafie, D., ... & Acharya, U. R. (2021). Coronary artery disease detection using artificial intelligence techniques: A survey of trends, geographical differences and diagnostic features 1991–2020. *Computers in Biology and Medicine*, 128, 104095.

- [40] Parikh, M. N., Li, H., & He, L. (2019). Enhancing diagnosis of autism with optimized machine learning models and personal characteristic data. *Frontiers in computational neuroscience*, 13, 9.
- [41] Mohammadpoor, M., Shoeibi, A., & Shojaee, H. (2016). A hierarchical classification method for breast tumor detection. *Iranian Journal of Medical Physics*, 13(4), 261-268.
- [42] Ghassemi, N., Shoeibi, A., Khodatars, M., Heras, J., Rahimi, A., Zare, A., ... & Gorriz, J. M. (2021). Automatic diagnosis of covid-19 from ct images using cyclegan and transfer learning. *arXiv preprint arXiv:2104.11949*.
- [43] Noor, M. B. T., Zenia, N. Z., Kaiser, M. S., Mahmud, M., & Al Mamun, S. (2019, December). Detecting neurodegenerative disease from mri: A brief review on a deep learning perspective. In *International Conference on Brain Informatics* (pp. 115-125). Springer, Cham.
- [44] Altinkaya, E., Polat, K., & Barakli, B. (2020). Detection of alzheimer's disease and dementia states based on deep learning from MRI images: A comprehensive review. *Journal of the Institute of Electronics and Computer*, 1(1), 39-53.
- [45] Yao, A. D., Cheng, D. L., Pan, I., & Kitamura, F. (2020). Deep learning in neuroradiology: a systematic review of current algorithms and approaches for the new wave of imaging technology. *Radiology: Artificial Intelligence*, 2(2), e190026.
- [46] Al-Shoukry, S., Rassem, T. H., & Makbol, N. M. (2020). Alzheimer's diseases detection by using deep learning algorithms: a mini-review. *IEEE Access*, 8, 77131-77141.
- [47] Goodfellow, I., Bengio, Y., & Courville, A. (2016). *Deep learning*. MIT press.
- [48] Soltaninejad, M., Ye, X., Yang, G., Allinson, N., & Lambrou, T. (2014). Brain tumour grading in different MRI protocols using SVM on statistical features.
- [49] Jafarpour, S., Sedghi, Z., & Amirani, M. C. (2012). A robust brain MRI classification with GLCM features. *International Journal of Computer Applications*, 37(12), 1-5.
- [50] Anand, C. S., & Sahambi, J. S. (2010). Wavelet domain non-linear filtering for MRI denoising. *Magnetic Resonance Imaging*, 28(6), 842-861.
- [51] Lee, T. W., & Xue, S. W. (2017). Linking graph features of anatomical architecture to regional brain activity: A multi-modal MRI study. *Neuroscience letters*, 651, 123-127.
- [52] Yeh, C. H., Jones, D. K., Liang, X., Descoteaux, M., & Connelly, A. (2021). Mapping structural connectivity using diffusion MRI: Challenges and opportunities. *Journal of Magnetic Resonance Imaging*, 53(6), 1666-1682.
- [53] Zeng, L. L., Wang, H., Hu, P., Yang, B., Pu, W., Shen, H., ... & Hu, D. (2018). Multi-site diagnostic classification of schizophrenia using discriminant deep learning with functional connectivity MRI. *EBioMedicine*, 30, 74-85.
- [54] Fodor, I. K. (2002). *A survey of dimension reduction techniques* (No. UCRL-ID-148494). Lawrence Livermore National Lab., CA (US).
- [55] Wold, S., Esbensen, K., & Geladi, P. (1987). Principal component analysis. *Chemometrics and intelligent laboratory systems*, 2(1-3), 37-52.
- [56] Yan, K., & Zhang, D. (2015). Feature selection and analysis on correlated gas sensor data with recursive feature elimination. *Sensors and Actuators B: Chemical*, 212, 353-363.
- [57] Zhou, N., & Wang, L. (2007). A modified T-test feature selection method and its application on the HapMap genotype data. *Genomics, proteomics & bioinformatics*, 5(3-4), 242-249.
- [58] Yang, Y., Wu, Q. J., & Wang, Y. (2016). Autoencoder with invertible functions for dimension reduction and image reconstruction. *IEEE Transactions on Systems, Man, and Cybernetics: Systems*, 48(7), 1065-1079.
- [59] Ma, F., Gao, F., Sun, J., Zhou, H., & Hussain, A. (2019). Weakly supervised segmentation of SAR imagery using superpixel and hierarchically adversarial CRF. *Remote Sensing*, 11(5), 512.
- [60] Ye, Z., & Yang, J. (2010). Sliced inverse moment regression using weighted chi-squared tests for dimension reduction. *Journal of Statistical Planning and Inference*, 140(11), 3121-3131.
- [61] Muthukrishnan, R., & Rohini, R. (2016, October). LASSO: A feature selection technique in predictive modeling for machine learning. In *2016 IEEE international conference on advances in computer applications (ICACA)* (pp. 18-20). IEEE.
- [62] Noble, W. S. (2006). What is a support vector machine?. *Nature biotechnology*, 24(12), 1565-1567.

- [63] Suthaharan, S. (2016). Support vector machine. In *Machine learning models and algorithms for big data classification* (pp. 207-235). Springer, Boston, MA.
- [64] Oshiro, T. M., Perez, P. S., & Baranauskas, J. A. (2012, July). How many trees in a random forest?. In *International workshop on machine learning and data mining in pattern recognition* (pp. 154-168). Springer, Berlin, Heidelberg.
- [65] Zhang, Y., Zhou, X., Witt, R. M., Sabatini, B. L., Adjeroh, D., & Wong, S. T. (2007). Dendritic spine detection using curvilinear structure detector and LDA classifier. *Neuroimage*, 36(2), 346-360.
- [66] Liao, Y., & Vemuri, V. R. (2002). Use of k-nearest neighbor classifier for intrusion detection. *Computers & security*, 21(5), 439-448.
- [67] Haweel, R., Dekhil, O., Shalaby, A., Mahmoud, A., Ghazal, M., Khalil, A., ... & El-Baz, A. (2020, April). A Novel Framework for Grading Autism Severity Using Task-Based fMRI. In *2020 IEEE 17th International Symposium on Biomedical Imaging (ISBI)* (pp. 1404-1407). IEEE
- [68] Yang, X., Islam, M. S., & Khaled, A. A. (2019, May). Functional connectivity magnetic resonance imaging classification of autism spectrum disorder using the multisite ABIDE dataset. In *2019 IEEE EMBS International Conference on Biomedical & Health Informatics (BHI)* (pp. 1-4). IEEE.
- [69] Zhang, X., Ding, X., Wu, Z., Xia, J., Ni, H., Xu, X., ... & Li, G. (2020, April). Siamese Verification Framework for Autism Identification During Infancy Using Cortical Path Signature Features. In *2020 IEEE 17th International Symposium on Biomedical Imaging (ISBI)* (pp. 1-4). IEEE
- [70] Bi, X. A., Liu, Y., Sun, Q., Luo, X., Tan, H., Chen, J., & Zeng, N. (2019). The Genetic-Evolutionary Random Support Vector Machine Cluster Analysis in Autism Spectrum Disorder. *IEEE Access*, 7, 30527-30535
- [71] Sartipi, S., Shayesteh, M. G., & Kalbkhani, H. (2018, December). Diagnosing of autism spectrum disorder based on GARCH variance series for rs-fMRI data. In *2018 9th International Symposium on Telecommunications (IST)* (pp. 86-90). IEEE.
- [72] Saad, M., & Islam, S. M. R. (2019, January). Brain Connectivity Network Analysis and Classifications from Diffusion Tensor Imaging. In *2019 International Conference on Robotics, Electrical and Signal Processing Techniques (ICREST)* (pp. 422-427). IEEE.
- [73] Liu, W., Liu, M., Yang, D., Wang, M., & Tao, T. (2020, June). Automatic diagnosis of autism based on functional magnetic resonance imaging and elastic net. In *2020 IEEE 5th Information Technology and Mechatronics Engineering Conference (ITOEC)* (pp. 104-108). IEEE
- [74] Zhuang, J., Dvornek, N. C., Li, X., Yang, D., Ventola, P., & Duncan, J. S. (2018, April). Prediction of pivotal response treatment outcome with task fMRI using random forest and variable selection. In *2018 IEEE 15th International Symposium on Biomedical Imaging (ISBI 2018)* (pp. 97-100). IEEE.
- [75] Zheng, W., Eilamstock, T., Wu, T., Spagna, A., Chen, C., Hu, B., & Fan, J. (2019). Multi-feature based network revealing the structural abnormalities in autism spectrum disorder. *IEEE Transactions on Affective Computing*
- [76] ElNakieb, Y., Soliman, A., Mahmoud, A., Dekhil, O., Shalaby, A., Ghazal, M., ... & El-Baz, A. S. (2019, December). Autism Spectrum Disorder Diagnosis framework using Diffusion Tensor Imaging. In *2019 IEEE International Conference on Imaging Systems and Techniques (IST)* (pp. 1-5). IEEE.
- [77] Ge, F., Chen, H., Zhang, T., Wang, X., Yuan, L., Hu, X., ... & Liu, T. (2018, April). A novel framework for analyzing cortical folding patterns based on sulcal baselines and gyral crestlines. In *2018 IEEE 15th International Symposium on Biomedical Imaging (ISBI 2018)* (pp. 1043-1047). IEEE
- [78] Stevens, E., Dixon, D. R., Novack, M. N., Granpeesheh, D., Smith, T., & Linstead, E. (2019). Identification and analysis of behavioral phenotypes in autism spectrum disorder via unsupervised machine learning. *International journal of medical informatics*, 129, 29-36
- [79] Wang, J., Zhang, L., Wang, Q., Chen, L., Shi, J., Chen, X., ... & Shen, D. (2020). Multi-Class ASD Classification Based on Functional Connectivity and Functional Correlation Tensor via Multi-Source Domain Adaptation and Multi-View Sparse Representation. *IEEE Transactions on Medical Imaging*.
- [80] Dekhil, O., Ali, M., El-Nakieb, Y., Shalaby, A., Soliman, A., Switala, A., ... & Elmaghraby, A. (2019). A personalized autism diagnosis cad system using a fusion of structural mri and resting-state functional mri data. *Frontiers in Psychiatry*, 10

- [81] Abdullah, A. A., Rijal, S., & Dash, S. R. (2019, November). Evaluation on Machine Learning Algorithms for Classification of Autism Spectrum Disorder (ASD). In *Journal of Physics: Conference Series* (Vol. 1372, No. 1, p. 012052). IOP Publishing.
- [82] Demirhan, A. (2018). Performance of machine learning methods in determining the autism spectrum disorder cases. *Mugla Journal of Science and Technology*, 4(1), 79-84.
- [83] Syed, M. A., Yang, Z., Hu, X. P., & Deshpande, G. (2017). Investigating brain connectomic alterations in autism using the reproducibility of independent components derived from resting state functional MRI data. *Frontiers in Neuroscience*, 11, 459.
- [84] Liu, J., Sheng, Y., Lan, W., Guo, R., Wang, Y., & Wang, J. (2020). Improved ASD classification using dynamic functional connectivity and multi-task feature selection. *Pattern Recognition Letters*, 138, 82-87.
- [85] Wang, C., Xiao, Z., & Wu, J. (2019). Functional connectivity-based classification of autism and control using SVM-RFECV on rs-fMRI data. *Physica Medica*, 65, 99-105.
- [86] Xiao, X., Fang, H., Wu, J., Xiao, C., Xiao, T., Qian, L., ... & Ke, X. (2017). Diagnostic model generated by MRI-derived brain features in toddlers with autism spectrum disorder. *Autism Research*, 10(4), 620-630.
- [87] Eill, A., Jahedi, A., Gao, Y., Kohli, J. S., Fong, C. H., Solders, S., ... & Müller, R. A. (2019). Functional connectivities are more informative than anatomical variables in diagnostic classification of autism. *Brain connectivity*, 9(8), 604-612.
- [88] Sarovic, D., Hadjikhani, N., Schneiderman, J., Lundström, S., & Gillberg, C. (2020). Autism classified by magnetic resonance imaging: A pilot study of a potential diagnostic tool. *International Journal of Methods in Psychiatric Research*, e1846.
- [89] Zhao, F., Qiao, L., Shi, F., Yap, P. T., & Shen, D. (2017). Feature fusion via hierarchical supervised local CCA for diagnosis of autism spectrum disorder. *Brain imaging and behavior*, 11(4), 1050-1060.
- [90] Dekhil, O., Hajjdiab, H., Shalaby, A., Ali, M. T., Ayinde, B., Switala, A., ... & El-Baz, A. (2018). Using resting state functional MRI to build a personalized autism diagnosis system. *PLoS one*, 13(10), e0206351.
- [91] Yang, M., Zhong, Q., Chen, L., Huang, F., & Lei, B. (2019, July). Attention Based Semi-Supervised Dictionary Learning for Diagnosis of Autism Spectrum Disorders. In *2019 IEEE International Conference on Multimedia & Expo Workshops (ICMEW)* (pp. 7-12). IEEE
- [92] Jiang, Y., Li, Z., & Zhang, D. (2019, August). Unsupervised Domain Adaptation for Multi-Center Autism Spectrum Disorder Identification. In *2019 IEEE SmartWorld, Ubiquitous Intelligence & Computing, Advanced & Trusted Computing, Scalable Computing & Communications, Cloud & Big Data Computing, Internet of People and Smart City Innovation (SmartWorld/SCALCOM/UIC/ATC/CBDCOM/IOP/SCI)* (pp. 1608-1613). IEEE.
- [93] Madine, M., Rekik, I., & Werghi, N. (2020, October). Diagnosing Autism Using T1-W MRI With Multi-Kernel Learning and Hypergraph Neural Network. In *2020 IEEE International Conference on Image Processing (ICIP)* (pp. 438-442). IEEE.
- [94] Thomas, M., & Chandran, A. (2018, May). Artificial Neural Network for Diagnosing Autism Spectrum Disorder. In *2018 2nd International Conference on Trends in Electronics and Informatics (ICOEI)* (pp. 930-933). IEEE.
- [95] Haweel, R., Dekhil, O., Shalaby, A., Mahmoud, A., Ghazal, M., Khalil, A., ... & El-Baz, A. (2019, October). Functional magnetic resonance imaging based framework for autism diagnosis. In *2019 Fifth International Conference on Advances in Biomedical Engineering (ICABME)* (pp. 1-4). IEEE.
- [96] Huang, F., Elazab, A., OuYang, L., Tan, J., Wang, T., & Lei, B. (2019, April). Sparse Low-rank Constrained Adaptive Structure Learning using Multi-template for Autism Spectrum Disorder Diagnosis. In *2019 IEEE 16th International Symposium on Biomedical Imaging (ISBI 2019)* (pp. 1555-1558). IEEE.
- [97] Benabdallah, F. Z., El Maliani, A. D., Lotfi, D., Jennane, R., & El Hassouni, M. (2018, November). Analysis of under-connectivity in Autism using the minimum spanning tree: application on large multi-site dataset. In *2018 9th International Symposium on Signal, Image, Video and Communications (ISIVC)* (pp. 296-299). IEEE.
- [98] Haweel, R., Dekhil, O., Shalaby, A., Mahmoud, A., Ghazal, M., Keynton, R., ... & El-Baz, A. (2019, December). A Machine Learning Approach for Grading Autism Severity Levels Using Task-based Functional MRI. In *2019 IEEE International Conference on Imaging Systems and Techniques (IST)* (pp. 1-5). IEEE.

- [99] Wang, M., Zhang, D., Huang, J., Yap, P. T., Shen, D., & Liu, M. (2019). Identifying autism spectrum disorder with multi-site fMRI via low-rank domain adaptation. *IEEE Transactions on Medical Imaging*, 39(3), 644-655.
- [100] Alvarez-Jimenez, C., Múnera-Garzón, N., Zuluaga, M. A., Velasco, N. F., & Romero, E. (2020). Autism spectrum disorder characterization in children by capturing local-regional brain changes in MRI. *Medical Physics*, 47(1), 119-131.
- [101] Chaitra, N., Vijaya, P. A., & Deshpande, G. (2020). Diagnostic prediction of autism spectrum disorder using complex network measures in a machine learning framework. *Biomedical Signal Processing and Control*, 62, 102099.
- [102] Fan, G., Chen, Y., Chen, Y., Yang, M., Wang, J., Li, C., ... & Liu, T. (2020). Abnormal Brain Regions in Two-Group Cross-Location Dynamics Model of Autism. *IEEE Access*, 8, 94526-94534.
- [103] Mellema, C. J., Treacher, A., Nguyen, K. P., & Montillo, A. (2020, April). Architectural configurations, atlas granularity and functional connectivity with diagnostic value in Autism Spectrum Disorder. In *2020 IEEE 17th International Symposium on Biomedical Imaging (ISBI)* (pp. 1022-1025). IEEE.
- [104] ElNakieb, Y., Ali, M. T., Dekhil, O., Khalefa, M. E., Soliman, A., Shalaby, A., ... & Keynton, R. (2018, December). Towards Accurate Personalized Autism Diagnosis Using Different Imaging Modalities: sMRI, fMRI, and DTI. In *2018 IEEE International Symposium on Signal Processing and Information Technology (ISSPIT)* (pp. 447-452). IEEE.
- [105] Ke, Q., Zhang, J., Wei, W., Damaševičius, R., & Woźniak, M. (2019). Adaptive independent subspace analysis of brain magnetic resonance imaging data. *IEEE Access*, 7, 12252-12261.
- [106] Mostafa, S., Tang, L., & Wu, F. X. (2019). Diagnosis of autism spectrum disorder based on eigenvalues of brain networks. *IEEE Access*, 7, 128474-128486.
- [107] Bernas, A., Aldenkamp, A. P., & Zinger, S. (2018). Wavelet coherence-based classifier: A resting-state functional MRI study on neurodynamics in adolescents with high-functioning autism. *Computer methods and programs in biomedicine*, 154, 143-151.
- [108] Dekhil, O., Ali, M., Haweel, R., Elnakib, Y., Ghazal, M., Hajjdiab, H., ... & Keynton, R. (2020, March). A Comprehensive Framework for Differentiating Autism Spectrum Disorder from Neurotypicals by Fusing Structural MRI and Resting State Functional MRI. In *Seminars in Pediatric Neurology* (p. 100805). WB Saunders.
- [109] Yassin, W., Nakatani, H., Zhu, Y., Kojima, M., Owada, K., Kuwabara, H., ... & Iwashiro, N. (2020). Machine-learning classification using neuroimaging data in schizophrenia, autism, ultra-high risk and first-episode psychosis. *Translational psychiatry*, 10(1), 1-11.
- [110] Soussia, M., & Rekik, I. (2018). Unsupervised manifold learning using high-order morphological brain networks derived from T1-w MRI for autism diagnosis. *Frontiers in Neuroinformatics*, 12, 70.
- [111] Xiao, X., Fang, H., Wu, J., Xiao, C., Xiao, T., Qian, L., ... & Ke, X. (2017). Diagnostic model generated by MRI-derived brain features in toddlers with autism spectrum disorder. *Autism Research*, 10(4), 620-630.
- [112] Zhao, F., Zhang, H., Rekik, I., An, Z., & Shen, D. (2018). Diagnosis of autism spectrum disorders using multi-level high-order functional networks derived from resting-state functional MRI. *Frontiers in human neuroscience*, 12, 184.
- [113] Fredo, A. J., Jahedi, A., Reiter, M., & Müller, R. A. (2018). Diagnostic classification of autism using resting-state fMRI data and conditional random forest. *Age (years)*, 12(2.76), 6-41.
- [114] Bi, X. A., Wang, Y., Shu, Q., Sun, Q., & Xu, Q. (2018). Classification of autism spectrum disorder using random support vector machine cluster. *Frontiers in genetics*, 9, 18.
- [115] Tejwani, R., Liska, A., You, H., Reinen, J., & Das, P. (2017). Autism classification using brain functional connectivity dynamics and machine learning. *arXiv preprint arXiv:1712.08041*.
- [116] Tang, L., Mostafa, S., Liao, B., & Wu, F. X. (2019). A network clustering-based feature selection strategy for classifying autism spectrum disorder. *BMC Medical Genomics*, 12(7), 153.
- [117] Reiter, M. A., Jahedi, A., Fredo, A. J., Fishman, I., Bailey, B., & Müller, R. A. (2020). Performance of machine learning classification models of autism using resting-state fMRI is contingent on sample heterogeneity. *Neural Computing and Applications*, 1-12.
- [118] Rane, S., Jolly, E., Park, A., Jang, H., & Craddock, C. (2017). Developing predictive imaging biomarkers using whole-brain classifiers: Application to the ABIDE I dataset. *Research Ideas and Outcomes*, 3, e12733.

- [119] Tolan, E., & Isik, Z. (2018, April). Graph theory-based classification of brain connectivity network for autism spectrum disorder. In *International Conference on Bioinformatics and Biomedical Engineering* (pp. 520-530). Springer, Cham.
- [120] ElNakieb, Y., Soliman, A., Mahmoud, A., Ali, M., Dekhil, O., Shalaby, A., ... & Barnes, G. N. (2020). Computer Aided Autism Diagnosis Using Diffusion Tensor Imaging. *IEEE Access*.
- [121] Crimi, A., Doderio, L., Murino, V., & Sona, D. (2017, April). Case-control discrimination through effective brain connectivity. In *2017 IEEE 14th International Symposium on Biomedical Imaging (ISBI 2017)* (pp. 970-973). Ieee.
- [122] Jahedi, A., Nasamran, C. A., Faires, B., Fan, J., & Müller, R. A. (2017). Distributed intrinsic functional connectivity patterns predict diagnostic status in large autism cohort. *Brain connectivity*, 7(8), 515-525.
- [123] Bhaumik, R., Pradhan, A., Das, S., & Bhaumik, D. K. (2018). Predicting autism spectrum disorder using domain-adaptive cross-site evaluation. *Neuroinformatics*, 16(2), 197-205.
- [124] Savva, A. D., Karampasi, A. S., & Matsopoulos, G. K. (2020). Deriving resting-state fMRI biomarkers for classification of autism spectrum disorder. In *Autism 360°* (pp. 101-123). Academic Press.
- [125] Mathur, M., & Lindberg, T. Autism Spectrum Disorder classification using Machine Learning techniques on fMRI.
- [126] Eill, A., Jahedi, A., Gao, Y., Kohli, J. S., Fong, C. H., Solders, S., ... & Müller, R. A. (2019). Functional connectivities are more informative than anatomical variables in diagnostic classification of autism. *Brain connectivity*, 9(8), 604-612.
- [127] Zhuang, J., Dvornek, N. C., Li, X., Ventola, P., & Duncan, J. S. (2018, September). Prediction of Severity and Treatment Outcome for ASD from fMRI. In *International Workshop on PRedictive Intelligence In MEDicine* (pp. 9-17). Springer, Cham.
- [128] Kazeminejad, A., & Sotero, R. C. (2019). Topological properties of resting-state fMRI functional networks improve machine learning-based autism classification. *Frontiers in neuroscience*, 12, 1018.
- [129]
- [130] THOMAS MARTIAL, E. E., Hu, L., & Yuqing, S. O. N. G. (2019). Characterizing and predicting autism spectrum disorder by performing resting-state functional network community pattern analysis. *Frontiers in human neuroscience*, 13, 203.
- [131] Cordova, M., Shada, K., Demeter, D. V., Doyle, O., Miranda-Dominguez, O., Perrone, A., ... & Nigg, J. (2020). Heterogeneity of executive function revealed by a functional random forest approach across ADHD and ASD. *NeuroImage: Clinical*, 102245.
- [132] Sadeghi, M., Khosrowabadi, R., Bakouie, F., Mahdavi, H., Eslahchi, C., & Pouretamad, H. (2017). Screening of autism based on task-free fMRI using graph theoretical approach. *Psychiatry Research: Neuroimaging*, 263, 48-56.
- [133] Zhang, L., Wang, X. H., & Li, L. (2020). Diagnosing autism spectrum disorder using brain entropy: A fast entropy method. *Computer methods and programs in biomedicine*, 190, 105240.
- [134] Shi, C., Zhang, J., & Wu, X. (2020). An fMRI feature selection method based on a minimum spanning tree for identifying patients with autism. *Symmetry*, 12(12), 1995.
- [135] Richards, R., Greimel, E., Kliemann, D., Koerte, I. K., Schulte-Körne, G., Reuter, M., & Wachinger, C. (2020). Increased hippocampal shape asymmetry and volumetric ventricular asymmetry in autism spectrum disorder. *NeuroImage: Clinical*, 26, 102207.
- [136] Payabvash, S., Palacios, E. M., Owen, J. P., Wang, M. B., Tavassoli, T., Gerdes, M., ... & Mukherjee, P. (2019). White matter connectome edge density in children with autism spectrum disorders: potential imaging biomarkers using machine-learning models. *Brain connectivity*, 9(2), 209-220.
- [137] Huang, H., Liu, X., Jin, Y., Lee, S. W., Wee, C. Y., & Shen, D. (2019). Enhancing the representation of functional connectivity networks by fusing multi-view information for autism spectrum disorder diagnosis. *Human brain mapping*, 40(3), 833-854.

- [138] Huang, Z. A., Liu, R., & Tan, K. C. (2020, July). Multi-Task Learning for Efficient Diagnosis of ASD and ADHD using Resting-State fMRI Data. In *2020 International Joint Conference on Neural Networks (IJCNN)* (pp. 1-7). IEEE.
- [139] Jung, M., Tu, Y., Park, J., Jorgenson, K., Lang, C., Song, W., & Kong, J. (2019). Surface-based shared and distinct resting functional connectivity in attention-deficit hyperactivity disorder and autism spectrum disorder. *The British Journal of Psychiatry*, *214*(6), 339-344.
- [140] DSouza, A. M., Abidin, A. Z., & Wismüller, A. (2019, March). Classification of autism spectrum disorder from resting-state fMRI with mutual connectivity analysis. In *Medical Imaging 2019: Biomedical Applications in Molecular, Structural, and Functional Imaging* (Vol. 10953, p. 109531D). International Society for Optics and Photonics.
- [141] Devika, K., & Oruganti, V. R. M. (2021, January). A Machine Learning Approach for Diagnosing Neurological Disorders using Longitudinal Resting-State fMRI. In *2021 11th International Conference on Cloud Computing, Data Science & Engineering (Confluence)* (pp. 494-499). IEEE.
- [142] Ahammed, M. S., Niu, S., Ahmed, M. R., Dong, J., Gao, X., & Chen, Y. (2021, January). Bag-of-Features Model for ASD fMRI Classification using SVM. In *2021 Asia-Pacific Conference on Communications Technology and Computer Science (ACCTCS)* (pp. 52-57). IEEE.
- [143] Yap, S. Y., & Chan, W. H. (2020). Elastic SCAD SVM Cluster for The Selection of Significant Functional Connectivity in Autism Spectrum Disorder Classification. *Academia of Fundamental Computing Research*, *1*(2).
- [144] Wang, M., Zhang, D., Huang, J., Yap, P. T., Shen, D., & Liu, M. (2019). Identifying autism spectrum disorder with multi-site fMRI via low-rank domain adaptation. *IEEE transactions on medical imaging*, *39*(3), 644-655.
- [145] Karampasi, A., Kakkos, I., Miloulis, S. T., Zorzos, I., Dimitrakopoulos, G. N., Gkiatis, K., ... & Matsopoulos, G. (2020, December). A Machine Learning fMRI Approach in the Diagnosis of Autism. In *2020 IEEE International Conference on Big Data (Big Data)* (pp. 3628-3631). IEEE.
- [146] Graña, M., & Silva, M. (2021). Impact of Machine Learning Pipeline Choices in Autism Prediction from Functional Connectivity Data. *International Journal of Neural Systems*, 2150009-2150009.
- [147] Yamagata, B., Itahashi, T., Fujino, J., Ohta, H., Nakamura, M., Kato, N., ... & Aoki, Y. (2019). Machine learning approach to identify a resting-state functional connectivity pattern serving as an endophenotype of autism spectrum disorder. *Brain imaging and behavior*, *13*(6), 1689-1698.
- [148] Conti, E., Retico, A., Palumbo, L., Spera, G., Bosco, P., Biagi, L., ... & Calderoni, S. (2020). Autism Spectrum Disorder and Childhood Apraxia of Speech: Early Language-Related Hallmarks across Structural MRI Study. *Journal of personalized medicine*, *10*(4), 275.
- [149] Deshpande, G., Libero, L., Sreenivasan, K. R., Deshpande, H., & Kana, R. K. (2013). Identification of neural connectivity signatures of autism using machine learning. *Frontiers in human neuroscience*, *7*, 670.
- [150] Kazeminejad, A., & Sotero, R. C. (2020). The importance of anti-correlations in graph theory-based classification of autism spectrum disorder. *Frontiers in neuroscience*, *14*, 676.
- [151] Song, Y., Epalle, T. M., & Lu, H. (2019). Characterizing and predicting autism spectrum disorder by performing resting-state functional network community pattern analysis. *Frontiers in human neuroscience*, *13*, 203.
- [152] Tang, L., Mostafa, S., Liao, B., & Wu, F. X. (2019). A network clustering-based feature selection strategy for classifying autism spectrum disorder. *BMC medical genomics*, *12*(7), 1-10.
- [153] Mhiri, I., & Rekik, I. (2020). Joint functional brain network atlas estimation and feature selection for neurological disorder diagnosis with application to autism. *Medical image analysis*, *60*, 101596.
- [154] Itani, S., & Thanou, D. (2021). Combining anatomical and functional networks for neuropathology identification: A case study on autism spectrum disorder. *Medical image analysis*, *69*, 101986.
- [155] Zhan, Y., Wei, J., Liang, J., Xu, X., He, R., Robbins, T. W., & Wang, Z. (2021). Diagnostic classification for human autism and obsessive-compulsive disorder based on machine learning from a primate genetic model. *American Journal of Psychiatry*, *178*(1), 65-76.
- [156] Wismüller, A., Foxe, J. J., Geha, P., & Saboksayr, S. S. (2020, March). Large-scale Extended Granger Causality (lsXGC) for classification of Autism Spectrum Disorder from resting-state functional MRI. In *Medical Imaging 2020: Computer-Aided Diagnosis* (Vol. 11314, p. 113141Y). International Society for Optics and Photonics.

- [157] Mash, L. E., Keehn, B., Linke, A. C., Liu, T. T., Helm, J. L., Haist, F., ... & Müller, R. A. (2020). Atypical relationships between spontaneous EEG and fMRI activity in autism. *Brain connectivity*, 10(1), 18-28.
- [158] Cociu, B. A., Das, S., Billeci, L., Jamal, W., Maharatna, K., Calderoni, S., ... & Muratori, F. (2017). Multimodal functional and structural brain connectivity analysis in autism: a preliminary integrated approach with EEG, fMRI, and DTI. *IEEE Transactions on Cognitive and Developmental Systems*, 10(2), 213-226.
- [159] Javed, U., Riaz, M. M., Ghafoor, A., & Cheema, T. A. (2013). MRI brain classification using texture features, fuzzy weighting and support vector machine. *Progress In Electromagnetics Research B*, 53, 73-88.
- [160] Chanussot, J., Mauris, G., & Lambert, P. (1999). Fuzzy fusion techniques for linear features detection in multitemporal SAR images. *IEEE Transactions on Geoscience and Remote Sensing*, 37(3), 1292-1305.
- [161] Ullah, H., Ullah, B., Wu, L., Abdalla, F. Y., Ren, G., & Zhao, Y. (2020). Multi-modality medical images fusion based on local-features fuzzy sets and novel sum-modified-Laplacian in non-subsampled shearlet transform domain. *Biomedical Signal Processing and Control*, 57, 101724.
- [162] Davidson, V. J., Ryks, J., & Chu, T. (2001). Fuzzy models to predict consumer ratings for biscuits based on digital image features. *IEEE Transactions on Fuzzy Systems*, 9(1), 62-67.
- [163] Meena, D., & Agilandeewari, L. (2020). Invariant features-based fuzzy inference system for animal detection and recognition using thermal images. *International Journal of Fuzzy Systems*, 22(6), 1868-1879.
- [164] Jiang, Q., Jin, X., Lee, S. J., & Yao, S. (2017). A novel multi-focus image fusion method based on stationary wavelet transform and local features of fuzzy sets. *IEEE Access*, 5, 20286-20302.
- [165] Park, H. J., Friston, K. J., Pae, C., Park, B., & Razi, A. (2018). Dynamic effective connectivity in resting state fMRI. *NeuroImage*, 180, 594-608.
- [166] Zarghami, T. S., & Friston, K. J. (2020). Dynamic effective connectivity. *Neuroimage*, 207, 116453.
- [167] Bhattacharya, S., Ho, M. H. R., & Purkayastha, S. (2006). A Bayesian approach to modeling dynamic effective connectivity with fMRI data. *Neuroimage*, 30(3), 794-812.
- [168] Rowe, J. B., Hughes, L. E., Barker, R. A., & Owen, A. M. (2010). Dynamic causal modelling of effective connectivity from fMRI: are results reproducible and sensitive to Parkinson's disease and its treatment?. *Neuroimage*, 52(3), 1015-1026.
- [169] Gilson, M., Deco, G., Friston, K. J., Hagmann, P., Mantini, D., Betti, V., ... & Corbetta, M. (2018). Effective connectivity inferred from fMRI transition dynamics during movie viewing points to a balanced reconfiguration of cortical interactions. *Neuroimage*, 180, 534-546.
- [170] Smith, J. F., Pillai, A. S., Chen, K., & Horwitz, B. (2012). Effective connectivity modeling for fMRI: six issues and possible solutions using linear dynamic systems. *Frontiers in systems neuroscience*, 5, 104.
- [171] Melin, P., & Castillo, O. (2014). A review on type-2 fuzzy logic applications in clustering, classification and pattern recognition. *Applied soft computing*, 21, 568-577.
- [172] Melin, P., & Castillo, O. (2013). A review on the applications of type-2 fuzzy logic in classification and pattern recognition. *Expert Systems with Applications*, 40(13), 5413-5423.
- [173] de Aguiar, E. P., Fernando, M. D. A., Vellasco, M. M., & Ribeiro, M. V. (2017). Set-membership type-1 fuzzy logic system applied to fault classification in a switch machine. *IEEE Transactions on Intelligent Transportation Systems*, 18(10), 2703-2712.
- [174] Cai, H., Zheng, V. W., & Chang, K. C. C. (2018). A comprehensive survey of graph embedding: Problems, techniques, and applications. *IEEE Transactions on Knowledge and Data Engineering*, 30(9), 1616-1637.
- [175] Wu, Z., Pan, S., Chen, F., Long, G., Zhang, C., & Philip, S. Y. (2020). A comprehensive survey on graph neural networks. *IEEE transactions on neural networks and learning systems*, 32(1), 4-24.
- [176] Zhang, Z., Cui, P., & Zhu, W. (2020). Deep learning on graphs: A survey. *IEEE Transactions on Knowledge and Data Engineering*.
- [177] Ma, X., Wu, J., Xue, S., Yang, J., Zhou, C., Sheng, Q. Z., ... & Akoglu, L. (2021). A comprehensive survey on graph anomaly detection with deep learning. *IEEE Transactions on Knowledge and Data Engineering*.
- [178] Zhang, D., Yin, J., Zhu, X., & Zhang, C. (2018). Network representation learning: A survey. *IEEE transactions on Big Data*, 6(1), 3-28.

- [179] Hamilton, W. L., Ying, R., & Leskovec, J. (2017). Representation learning on graphs: Methods and applications. *arXiv preprint arXiv:1709.05584*.
- [180] Wang, W., Zheng, V. W., Yu, H., & Miao, C. (2019). A survey of zero-shot learning: Settings, methods, and applications. *ACM Transactions on Intelligent Systems and Technology (TIST)*, 10(2), 1-37.
- [181] Jang, B., Kim, M., Harerimana, G., & Kim, J. W. (2019). Q-learning algorithms: A comprehensive classification and applications. *IEEE Access*, 7, 133653-133667.
- [182] Li, R., Xian, K., Shen, C., Cao, Z., Lu, H., & Hang, L. (2018, December). Deep attention-based classification network for robust depth prediction. In *Asian Conference on Computer Vision* (pp. 663-678). Springer, Cham.
- [183] Creswell, A., White, T., Dumoulin, V., Arulkumaran, K., Sengupta, B., & Bharath, A. A. (2018). Generative adversarial networks: An overview. *IEEE Signal Processing Magazine*, 35(1), 53-65.
- [184] Liu, M. Y., & Tuzel, O. (2016). Coupled generative adversarial networks. *Advances in neural information processing systems*, 29, 469-477.
- [185] Fan, Z., Sun, L., Ding, X., Huang, Y., Cai, C., & Paisley, J. (2018). A segmentation-aware deep fusion network for compressed sensing mri. In *Proceedings of the European Conference on Computer Vision (ECCV)* (pp. 55-70).
- [186] Antropova, N., Huynh, B. Q., & Giger, M. L. (2017). A deep feature fusion methodology for breast cancer diagnosis demonstrated on three imaging modality datasets. *Medical physics*, 44(10), 5162-5171.
- [187] Amemiya, S., Takao, H., Kato, S., Yamashita, H., Sakamoto, N., & Abe, O. (2021). Feature-fusion improves MRI single-shot deep learning detection of small brain metastases. *Journal of Neuroimaging*.
- [188] Liu, X., Wang, J., Sun, H., Chandra, S. S., Crozier, S., & Liu, F. (2021). On the regularization of feature fusion and mapping for fast MR multi-contrast imaging via iterative networks. *Magnetic resonance imaging*, 77, 159-168.
- [189] Hermessi, H., Mourali, O., & Zagrouba, E. (2019). Deep feature learning for soft tissue sarcoma classification in MR images via transfer learning. *Expert Systems with Applications*, 120, 116-127.
- [190] Wang, S. H., Du, J., Xu, H., Yang, D., Ye, Y., Chen, Y., ... & Yang, Z. H. (2021). Automatic discrimination of different sequences and phases of liver MRI using a dense feature fusion neural network: a preliminary study. *Abdominal Radiology*, 1-12.
- [191] de Belen, R. A. J., Bednarz, T., Sowmya, A., & Del Favero, D. (2020). Computer vision in autism spectrum disorder research: a systematic review of published studies from 2009 to 2019. *Translational psychiatry*, 10(1), 1-20.
- [192] Kollias, K. F., Syriopoulou-Delli, C. K., Sarigiannidis, P., & Fragulis, G. F. (2021). The Contribution of Machine Learning and Eye-Tracking Technology in Autism Spectrum Disorder Research: A Systematic Review. *Electronics*, 10(23), 2982.
- [193] Brihadiswaran, G., Haputhanthri, D., Gunathilaka, S., Meedeniya, D., & Jayarathna, S. (2019). EEG-based processing and classification methodologies for autism spectrum disorder: A review. *Journal of Computer Science*, 15(8).
- [194] Hosseinzadeh, M., Koohpayehzadeh, J., Bali, A. O., Rad, F. A., Souri, A., Mazaherinezhad, A., ... & Bohlouli, M. (2021). A review on diagnostic autism spectrum disorder approaches based on the Internet of Things and Machine Learning. *The Journal of Supercomputing*, 77(3), 2590-2608.
- [195] Song, D. Y., Topriceanu, C. C., Ilie-Ablachim, D. C., Kinali, M., & Bisdas, S. (2021). Machine learning with neuroimaging data to identify autism spectrum disorder: a systematic review and meta-analysis. *Neuroradiology*, 63(12), 2057-2072.
- [196] Tawhid, M. N. A., Siuly, S., Wang, H., Whittaker, F., Wang, K., & Zhang, Y. (2021). A spectrogram image based intelligent technique for automatic detection of autism spectrum disorder from EEG. *Plos one*, 16(6), e0253094.
- [197] X. Li, N. C. Dvornek, X. Papademetris, J. Zhuang, L. H. Staib, P. Ventola, and J. S. Duncan, "2-channel convolutional 3d deep neural network (2cc3d) for fmri analysis: Asd classification and feature learning," in 2018 IEEE 15th International Symposium on Biomedical Imaging (ISBI 2018). IEEE, 2018, pp. 1252-1255.
- [198] X. Li, N. C. Dvornek, Y. Zhou, J. Zhuang, P. Ventola, and J. S. Duncan, "Efficient interpretation of deep learning models using graph structure and cooperative game theory: Application to asd biomarker discovery," in International Conference on Information Processing in Medical Imaging. Springer, 2019, pp. 718-730

- [199] Zhao, Y., Dong, Q., Zhang, S., Zhang, W., Chen, H., Jiang, X., ... & Liu, T. (2017). Automatic recognition of fMRI-derived functional networks using 3-D convolutional neural networks. *IEEE Transactions on Biomedical Engineering*, 65(9), 1975-1984.
- [200] Dvornek, N. C., Yang, D., Ventola, P., & Duncan, J. S. (2018, September). Learning generalizable recurrent neural networks from small task-fMRI datasets. In *International Conference on Medical Image Computing and Computer-Assisted Intervention* (pp. 329-337). Springer, Cham.
- [201] Leming, M., Górriz, J. M., & Suckling, J. (2020). Ensemble deep learning on large, mixed-site fMRI datasets in autism and other tasks. *International journal of neural systems*, 30(07), 2050012.
- [202] Li, X., Dvornek, N. C., Zhuang, J., Ventola, P., & Duncan, J. S. (2018, September). Brain biomarker interpretation in ASD using deep learning and fMRI. In *International Conference on Medical Image Computing and Computer-Assisted Intervention* (pp. 206-214). Springer, Cham.
- [203] Khosla, M., Jamison, K., Kuceyeski, A., & Sabuncu, M. R. (2018). 3D convolutional neural networks for classification of functional connectomes. In *Deep Learning in Medical Image Analysis and Multimodal Learning for Clinical Decision Support* (pp. 137-145). Springer, Cham.
- [204] Eslami, T., Mirjalili, V., Fong, A., Laird, A. R., & Saeed, F. (2019). ASD-DiagNet: a hybrid learning approach for detection of autism spectrum disorder using fMRI data. *Frontiers in neuroinformatics*, 13, 70.
- [205] Anirudh, R., & Thiagarajan, J. J. (2019, May). Bootstrapping graph convolutional neural networks for autism spectrum disorder classification. In *ICASSP 2019-2019 IEEE International Conference on Acoustics, Speech and Signal Processing (ICASSP)* (pp. 3197-3201). IEEE.
- [206] Brown, C. J., Kawahara, J., & Hamarneh, G. (2018, April). Connectome priors in deep neural networks to predict autism. In *2018 IEEE 15th International Symposium on Biomedical Imaging (ISBI 2018)* (pp. 110-113). IEEE.
- [207] Liao, D., & Lu, H. (2018, March). Classify autism and control based on deep learning and community structure on resting-state fMRI. In *2018 Tenth International Conference on Advanced Computational Intelligence (ICACI)* (pp. 289-294). IEEE.
- [208] Yang, X., Sarraf, S., & Zhang, N. (2018). Deep learning-based framework for Autism functional MRI image classification. *Journal of the Arkansas Academy of Science*, 72(1), 47-52.
- [209] Guo, X., Dominick, K. C., Minai, A. A., Li, H., Erickson, C. A., & Lu, L. J. (2017). Diagnosing autism spectrum disorder from brain resting-state functional connectivity patterns using a deep neural network with a novel feature selection method. *Frontiers in neuroscience*, 11, 460.
- [210] Aghdam, M. A., Sharifi, A., & Pedram, M. M. (2019). Diagnosis of autism spectrum disorders in young children based on resting-state functional magnetic resonance imaging data using convolutional neural networks. *Journal of digital imaging*, 32(6), 899-918.
- [211] Khosla, M., Jamison, K., Kuceyeski, A., & Sabuncu, M. R. (2019). Ensemble learning with 3D convolutional neural networks for functional connectome-based prediction. *NeuroImage*, 199, 651-662.
- [212] Choi, H. (2017). Functional connectivity patterns of autism spectrum disorder identified by deep feature learning. *arXiv preprint arXiv:1707.07932*.
- [213] Dvornek, N. C., Ventola, P., Pelphrey, K. A., & Duncan, J. S. (2017, September). Identifying autism from resting-state fMRI using long short-term memory networks. In *International Workshop on Machine Learning in Medical Imaging* (pp. 362-370). Springer, Cham.
- [214] Lu, H., Liu, S., Wei, H., & Tu, J. (2020). Multi-kernel fuzzy clustering based on auto-encoder for fMRI functional network. *Expert Systems with Applications*, 159, 113513.
- [215] Xiao, Z., Wang, C., Jia, N., & Wu, J. (2018). SAE-based classification of school-aged children with autism spectrum disorders using functional magnetic resonance imaging. *Multimedia Tools and Applications*, 77(17), 22809-22820.
- [216] Dvornek, N. C., Li, X., Zhuang, J., & Duncan, J. S. (2019, October). Jointly discriminative and generative recurrent neural networks for learning from fMRI. In *International Workshop on Machine Learning in Medical Imaging* (pp. 382-390). Springer, Cham.

- [217] Niu, K., Guo, J., Pan, Y., Gao, X., Peng, X., Li, N., & Li, H. (2020). Multichannel deep attention neural networks for the classification of autism spectrum disorder using neuroimaging and personal characteristic data. *Complexity*, 2020.
- [218] Li, H., Parikh, N. A., & He, L. (2018). A novel transfer learning approach to enhance deep neural network classification of brain functional connectomes. *Frontiers in neuroscience*, 12, 491.
- [219] El Gazzar, A., Cerliani, L., van Wingen, G., & Thomas, R. M. (2019, July). Simple 1-D convolutional networks for resting-state fMRI based classification in autism. In *2019 International Joint Conference on Neural Networks (IJCNN)* (pp. 1-6). IEEE.
- [220] Ahmed, M. R., Zhang, Y., Liu, Y., & Liao, H. (2020). Single volume image generator and deep learning-based ASD classification. *IEEE Journal of Biomedical and Health Informatics*, 24(11), 3044-3054.
- [221] Zhao, Y., Dai, H., Zhang, W., Ge, F., & Liu, T. (2019, April). Two-stage spatial temporal deep learning framework for functional brain network modeling. In *2019 IEEE 16th International Symposium on Biomedical Imaging (ISBI 2019)* (pp. 1576-1580). IEEE.
- [222] Pugazhenthii, B., Senapathy, G. S., & Pavithra, M. (2019, March). Identification of Autism in MR Brain Images Using Deep Learning Networks. In *2019 International Conference on Smart Structures and Systems (ICSSS)* (pp. 1-7). IEEE.
- [223] Eslami, T., Raiker, J. S., & Saeed, F. (2021). Explainable and scalable machine learning algorithms for detection of autism spectrum disorder using fMRI data. In *Neural Engineering Techniques for Autism Spectrum Disorder* (pp. 39-54). Academic Press.
- [224] Eslami, T., & Saeed, F. (2019, September). Auto-ASD-network: a technique based on deep learning and support vector machines for diagnosing autism spectrum disorder using fMRI data. In *Proceedings of the 10th ACM International Conference on Bioinformatics, Computational Biology and Health Informatics* (pp. 646-651).
- [225] Sherkatghanad, Z., Akhondzadeh, M., Salari, S., Zomorodi-Moghadam, M., Abdar, M., Acharya, U. R., ... & Salari, V. (2020). Automated detection of autism spectrum disorder using a convolutional neural network. *Frontiers in neuroscience*, 13, 1325.
- [226] Sairam, K., Naren, J., Vithya, G., & Srivathsan, S. (2019). Computer Aided System for Autism Spectrum Disorder Using Deep Learning Methods. *International Journal of Psychosocial Rehabilitation*, 23(01).
- [227] Dolz, J., Desrosiers, C., & Ayed, I. B. (2018). 3D fully convolutional networks for subcortical segmentation in MRI: A large-scale study. *NeuroImage*, 170, 456-470.
- [228] Wang, C., Xiao, Z., Wang, B., & Wu, J. (2019). Identification of autism based on SVM-RFE and stacked sparse auto-encoder. *IEEE Access*, 7, 118030-118036.
- [229] Zhao, Y., Ge, F., Zhang, S., & Liu, T. (2018, September). 3D deep convolutional neural network revealed the value of brain network overlap in differentiating autism spectrum disorder from healthy controls. In *International Conference on Medical Image Computing and Computer-Assisted Intervention* (pp. 172-180). Springer, Cham.
- [230] Parisot, S., Ktena, S. I., Ferrante, E., Lee, M., Guerrero, R., Glocker, B., & Rueckert, D. (2018). Disease prediction using graph convolutional networks: application to autism spectrum disorder and Alzheimer's disease. *Medical image analysis*, 48, 117-130.
- [231] Dvornek, N. C., Ventola, P., & Duncan, J. S. (2018, April). Combining phenotypic and resting-state fMRI data for autism classification with recurrent neural networks. In *2018 IEEE 15th International Symposium on Biomedical Imaging (ISBI 2018)* (pp. 725-728). IEEE.
- [232] Heinsfeld, A. S., Franco, A. R., Craddock, R. C., Buchweitz, A., & Meneguzzi, F. (2018). Identification of autism spectrum disorder using deep learning and the ABIDE dataset. *NeuroImage: Clinical*, 17, 16-23.
- [233] Li, X., Hect, J., Thomason, M., & Zhu, D. (2020, April). Interpreting age effects of human fetal brain from spontaneous fMRI using deep 3D convolutional neural networks. In *2020 IEEE 17th International Symposium on Biomedical Imaging (ISBI)* (pp. 1424-1427). IEEE.
- [234] Aghdam, M. A., Sharifi, A., & Pedram, M. M. (2018). Combination of rs-fMRI and sMRI data to discriminate autism spectrum disorders in young children using deep belief network. *Journal of digital imaging*, 31(6), 895-903.
- [235] Mellema, C., Treacher, A., Nguyen, K., & Montillo, A. (2019, April). Multiple deep learning architectures achieve superior performance diagnosing autism spectrum disorder using features previously extracted from structural

- and functional mri. In *2019 IEEE 16th International Symposium on Biomedical Imaging (ISBI 2019)* (pp. 1891-1895). IEEE.
- [236] Rakić, M., Cabezas, M., Kushibar, K., Oliver, A., & Lladó, X. (2020). Improving the detection of autism spectrum disorder by combining structural and functional MRI information. *NeuroImage: Clinical*, *25*, 102181.
- [237] Li, G., Liu, M., Sun, Q., Shen, D., & Wang, L. (2018, September). Early diagnosis of autism disease by multi-channel CNNs. In *International Workshop on Machine Learning in Medical Imaging* (pp. 303-309). Springer, Cham.
- [238] Dekhil, O., Hajjdiab, H., Shalaby, A., Ali, M. T., Ayinde, B., Switala, A., ... & El-Baz, A. (2018). Using resting state functional mri to build a personalized autism diagnosis system. *PloS one*, *13*(10), e0206351.
- [239] Li, G., Chen, M. H., Li, G., Wu, D., Sun, Q., Shen, D., & Wang, L. (2019, April). A preliminary volumetric MRI study of amygdala and hippocampal subfields in autism during infancy. In *2019 IEEE 16th International Symposium on Biomedical Imaging (ISBI 2019)* (pp. 1052-1056). IEEE.
- [240] Ismail, M., Barnes, G., Nitzken, M., Switala, A., Shalaby, A., Hosseini-Asl, E., ... & El-Baz, A. (2017, September). A new deep-learning approach for early detection of shape variations in autism using structural MRI. In *2017 IEEE International Conference on Image Processing (ICIP)* (pp. 1057-1061). IEEE.
- [241] Kong, Y., Gao, J., Xu, Y., Pan, Y., Wang, J., & Liu, J. (2019). Classification of autism spectrum disorder by combining brain connectivity and deep neural network classifier. *Neurocomputing*, *324*, 63-68.
- [242] Pinaya, W. H., Mechelli, A., & Sato, J. R. (2019). Using deep autoencoders to identify abnormal brain structural patterns in neuropsychiatric disorders: A large-scale multi-sample study. *Human brain mapping*, *40*(3), 944-954.
- [243] Sujit, S. J., Coronado, I., Kamali, A., Narayana, P. A., & Gabr, R. E. (2019). Automated image quality evaluation of structural brain MRI using an ensemble of deep learning networks. *Journal of Magnetic Resonance Imaging*, *50*(4), 1260-1267.
- [244] Henschel, L., Conjeti, S., Estrada, S., Diers, K., Fischl, B., & Reuter, M. (2020). Fastsurfer-a fast and accurate deep learning based neuroimaging pipeline. *NeuroImage*, *219*, 117012.
- [245] Shahamat, H., & Abadeh, M. S. (2020). Brain MRI analysis using a deep learning based evolutionary approach. *Neural Networks*, *126*, 218-234.
- [246] Iglesias, J. E., Lerma-Usabiaga, G., Garcia-Peraza-Herrera, L. C., Martinez, S., & Paz-Alonso, P. M. (2017, September). Retrospective head motion estimation in structural brain MRI with 3D CNNs. In *International Conference on Medical Image Computing and Computer-Assisted Intervention* (pp. 314-322). Springer, Cham.
- [247] Byeon, K., Kwon, J., Hong, J., & Park, H. (2020, February). Artificial neural network inspired by neuroimaging connectivity: application in autism spectrum disorder. In *2020 IEEE International Conference on Big Data and Smart Computing (BigComp)* (pp. 575-578). IEEE.
- [248] Xu, L., Liu, Y., Yu, J., Li, X., Yu, X., Cheng, H., & Li, J. (2020). Characterizing autism spectrum disorder by deep learning spontaneous brain activity from functional near-infrared spectroscopy. *Journal of neuroscience methods*, *331*, 108538.
- [249] Xu, L., Geng, X., He, X., Li, J., & Yu, J. (2019). Prediction in autism by deep learning short-time spontaneous hemodynamic fluctuations. *Frontiers in neuroscience*, *13*, 1120.
- [250] Thyreau, B., & Taki, Y. (2020). Learning a cortical parcellation of the brain robust to the MRI segmentation with convolutional neural networks. *Medical image analysis*, *61*, 101639.
- [251] Thomas, R. M., Gallo, S., Cerliani, L., Zhutovsky, P., El-Gazzar, A., & van Wingen, G. (2020). Classifying autism spectrum disorder using the temporal statistics of resting-state functional MRI data with 3D convolutional neural networks. *Frontiers in psychiatry*, *11*, 440.
- [252] El-Gazzar, A., Quaak, M., Cerliani, L., Bloem, P., van Wingen, G., & Thomas, R. M. (2019). A hybrid 3dcnn and 3dc-1stm based model for 4d spatio-temporal fMRI data: an abide autism classification study. In *OR 2.0 Context-Aware Operating Theaters and Machine Learning in Clinical Neuroimaging* (pp. 95-102). Springer, Cham.
- [253] Mostafa, S., Yin, W., & Wu, F. X. (2019, November). Autoencoder based methods for diagnosis of autism spectrum disorder. In *International Conference on Computational Advances in Bio and Medical Sciences* (pp. 39-51). Springer, Cham.

- [254] Jiao, Z., Li, H., & Fan, Y. (2020, April). Improving Diagnosis of Autism Spectrum Disorder and Disentangling its Heterogeneous Functional Connectivity Patterns Using Capsule Networks. In *2020 IEEE 17th International Symposium on Biomedical Imaging (ISBI)* (pp. 1331-1334). IEEE.
- [255] Bengs, M., Gessert, N., & Schlaefer, A. (2020). 4d spatio-temporal deep learning with 4d fmri data for autism spectrum disorder classification. *arXiv preprint arXiv:2004.10165*.
- [256] Gupta, D., Vij, I., & Gupta, M. Autism Detection using r-fMRI: Subspace Approximation and CNN Based Approach.
- [257] Wang, Y., Wang, J., Wu, F. X., Hayrat, R., & Liu, J. (2020). AIMAFE: autism spectrum disorder identification with multi-atlas deep feature representation and ensemble learning. *Journal of Neuroscience Methods*, 108840.
- [258] Tang, M., Kumar, P., Chen, H., & Shrivastava, A. (2020). Deep multimodal learning for the diagnosis of autism spectrum disorder. *Journal of Imaging*, 6(6), 47.
- [259] Ke, F., Choi, S., Kang, Y. H., Cheon, K. A., & Lee, S. W. (2020). Exploring the structural and strategic bases of autism spectrum disorders with deep learning. *IEEE Access*, 8, 153341-153352.
- [260] Ahmed, M. R., Ahammed, M. S., Niu, S., & Zhang, Y. (2020, March). Deep learning approached features for asd classification using svm. In *2020 IEEE International Conference on Artificial Intelligence and Information Systems (ICAIS)* (pp. 287-290). IEEE.
- [261] Ronicko, J. F. A., Thomas, J., Thangavel, P., Koneru, V., Langs, G., & Dauwels, J. (2020). Diagnostic classification of autism using resting-state fMRI data improves with full correlation functional brain connectivity compared to partial correlation. *Journal of Neuroscience Methods*, 345, 108884.
- [262] Zhang, M., Zhao, X., Zhang, W., Chaddad, A., Evans, A., & Poline, J. B. (2020, September). Deep discriminative learning for autism spectrum disorder classification. In *International Conference on Database and Expert Systems Applications* (pp. 435-443). Springer, Cham.
- [263] Shahamat, H., & Abadeh, M. S. (2020). Brain MRI analysis using a deep learning based evolutionary approach. *Neural Networks*, 126, 218-234.
- [264] Felouat, H., & Oukid-Khouas, S. (2020, November). Graph Convolutional Networks and Functional Connectivity for Identification of Autism Spectrum Disorder. In *2020 Second International Conference on Embedded & Distributed Systems (EDiS)* (pp. 27-32). IEEE.
- [265] Geng, X., Yao, Q., Jiang, K., & Zhu, Y. (2020, November). Deep Neural Generative Adversarial Model based on VAE+ GAN for Disorder Diagnosis. In *2020 International Conference on Internet of Things and Intelligent Applications (ITIA)* (pp. 1-7). IEEE.
- [266] Al-Hiyali, M. I., Yahya, N., Faye, I., Khan, Z., & Laboratoire, K. A. (2021, March). Classification of BOLD FMRI Signals using Wavelet Transform and Transfer Learning for Detection of Autism Spectrum Disorder. In *2020 IEEE-EMBS Conference on Biomedical Engineering and Sciences (IECBES)* (pp. 94-98). IEEE.
- [267] Tummala, S. (2021, April). Deep Learning Framework using Siamese Neural Network for Diagnosis of Autism from Brain Magnetic Resonance Imaging. In *2021 6th International Conference for Convergence in Technology (I2CT)* (pp. 1-5). IEEE.
- [268] Pominova, M., Kondrateva, E., Sharaev, M., Bernstein, A., & Burnaev, E. (2021, January). Fader networks for domain adaptation on fMRI: ABIDE-II study. In *Thirteenth International Conference on Machine Vision* (Vol. 11605, p. 116051Z). International Society for Optics and Photonics.
- [269] Yin, W., Mostafa, S., & Wu, F. X. (2021). Diagnosis of Autism Spectrum Disorder Based on Functional Brain Networks with Deep Learning. *Journal of Computational Biology*, 28(2), 146-165.
- [270] Hiremath, Y., Ismail, M., Verma, R., Antunes, J., & Tiwari, P. (2020, March). Combining deep and hand-crafted MRI features for identifying sex-specific differences in autism spectrum disorder versus controls. In *Medical Imaging 2020: Computer-Aided Diagnosis* (Vol. 11314, p. 113141W). International Society for Optics and Photonics.
- [271] Du, Y., Li, B., Hou, Y., & Calhoun, V. D. (2020, September). A deep learning fusion model for brain disorder classification: Application to distinguishing schizophrenia and autism spectrum disorder. In *Proceedings of the 11th ACM International Conference on Bioinformatics, Computational Biology and Health Informatics* (pp. 1-7).

- [272] Haweel, R., Shalaby, A., Mahmoud, A., Seada, N., Ghoniemy, S., Ghazal, M., ... & El-Baz, A. (2021). A robust DWT–CNN-based CAD system for early diagnosis of autism using task-based fMRI. *Medical Physics*, 48(5), 2315-2326.
- [273] Wang, L., Li, K., & Hu, X. P. (2021). Graph convolutional network for fMRI analysis based on connectivity neighborhood. *Network Neuroscience*, 5(1), 83-95.
- [274] Gupta, D., Vij, I., & Gupta, M. Autism Detection using r-fMRI: Subspace Approximation and CNN Based Approach.
- [275] Yang, X., Schrader, P. T., & Zhang, N. (2020). A deep neural network study of the ABIDE repository on autism spectrum classification. *Int. J. Adv. Computer Sci. Appl*, 11, 1-6.
- [276] Hu, J., Cao, L., Li, T., Liao, B., Dong, S., & Li, P. (2020). Interpretable Learning Approaches in Resting-State Functional Connectivity Analysis: The Case of Autism Spectrum Disorder. *Computational and Mathematical Methods in Medicine*, 2020.
- [277] Mahmoud, A. M., Karamti, H., & Alrowais, F. (2020). A Two Consequent Multi-layers Deep Discriminative Approach for Classifying fMRI Images. *International Journal on Artificial Intelligence Tools*, 29(06), 2030001.
- [278] Shrivastava, S., Mishra, U., Singh, N., Chandra, A., & Verma, S. (2020, July). Control or autism-classification using convolutional neural networks on functional mri. In *2020 11th International Conference on Computing, Communication and Networking Technologies (ICCCNT)* (pp. 1-6). IEEE.
- [279] Gao, J., Chen, M., Li, Y., Gao, Y., Li, Y., Cai, S., & Wang, J. (2021). Multisite Autism Spectrum Disorder Classification Using Convolutional Neural Network Classifier and Individual Morphological Brain Networks. *Frontiers in Neuroscience*, 14, 1473.
- [280] Sewani, H., & Kashef, R. (2020). An autoencoder-based deep learning classifier for efficient diagnosis of autism. *Children*, 7(10), 182.
- [281] You, Y., Liu, H., Zhang, S., & Shao, L. (2020). Classification of Autism Based on fMRI Data with Feature-Fused Convolutional Neural Network. In *Cyberspace Data and Intelligence, and Cyber-Living, Syndrome, and Health* (pp. 77-88). Springer, Singapore.
- [282] Ji, J., Xing, X., Yao, Y., Li, J., & Zhang, X. (2021). Convolutional kernels with an element-wise weighting mechanism for identifying abnormal brain connectivity patterns. *Pattern Recognition*, 109, 107570.
- [283] Sserwadda, A., & Rekik, I. (2021). Topology-guided cyclic brain connectivity generation using geometric deep learning. *Journal of Neuroscience Methods*, 353, 108988.
- [284] Mahmoud, A. M., Karamti, H., & Alrowais, F. M. (2020). An Effective Sparse Autoencoders based Deep Learning Framework for fMRI Scans Classification. In *ICEIS (1)* (pp. 540-547).
- [285] Bayram, M. A., İlyas, Ö. Z. E. R., & Temurtaş, F. (2021). Deep Learning Methods for Autism Spectrum Disorder Diagnosis Based on fMRI Images. *Sakarya University Journal of Computer and Information Sciences*, 4(1), 142-155.
- [286] Mozhdefarabhaksh, A., Chitsazian, S., Chakrabarti, P., Rao, K. J., Kateb, B., & Nami, M. (2021). A Convolutional Neural Network Model to Differentiate Attention Deficit Hyperactivity Disorder and Autism Spectrum Disorder Based on the Resting State fMRI Data.
- [287] Dominic, N., Cenggoro, T. W., Budiarto, A., & Pardamean, B. (2021). Transfer learning using inception-ResNet-v2 model to the augmented neuroimages data for autism spectrum disorder classification. *Commun. Math. Biol. Neurosci.*, 2021, Article-ID.
- [288] Husna, R. N. S., Syafeeza, A. R., Hamid, N. A., Wong, Y. C., & Raihan, R. A. (2021). FUNCTIONAL MAGNETIC RESONANCE IMAGING FOR AUTISM SPECTRUM DISORDER DETECTION USING DEEP LEARNING. *Jurnal Teknologi*, 83(3), 45-52.
- [289] Almuqhim, F., & Saeed, F. (2021). ASD-SAENet: A Sparse Autoencoder, and Deep-Neural Network Model for Detecting Autism Spectrum Disorder (ASD) Using fMRI Data. *Frontiers in Computational Neuroscience*, 15, 27.
- [290] Subah, F. Z., Deb, K., Dhar, P. K., & Koshiba, T. (2021). A Deep Learning Approach to Predict Autism Spectrum Disorder Using Multisite Resting-State fMRI. *Applied Sciences*, 11(8), 3636.
- [291] Huang, Z. A., Zhu, Z., Yau, C. H., & Tan, K. C. (2020). Identifying autism spectrum disorder from resting-state fMRI using deep belief network. *IEEE Transactions on Neural Networks and Learning Systems*.

- [292] Leming, M. J., Baron-Cohen, S., & Suckling, J. (2021). Single-participant structural similarity matrices lead to greater accuracy in classification of participants than function in autism in MRI. *Molecular Autism*, 12(1), 1-15.
- [293] Ji, J., & Yao, Y. (2020). Convolutional Neural Network with Graphical Lasso to Extract Sparse Topological Features for Brain Disease Classification. *IEEE/ACM transactions on computational biology and bioinformatics*.
- [294] Arya, D., Olij, R., Gupta, D. K., El Gazzar, A., Wingen, G., Worrying, M., & Thomas, R. M. (2020, September). Fusing Structural and Functional MRIs using Graph Convolutional Networks for Autism Classification. In *Medical Imaging with Deep Learning* (pp. 44-61). PMLR.
- [295] Dsouza, N. S., Nebel, M. B., Crocetti, D., Robinson, J., Mostofsky, S., & Venkataraman, A. (2021, February). M-GCN: A Multimodal Graph Convolutional Network to Integrate Functional and Structural Connectomics Data to Predict Multidimensional Phenotypic Characterizations. In *Medical Imaging with Deep Learning*.
- [296] D'Souza, N. S., Nebel, M. B., Crocetti, D., Wymbs, N., Robinson, J., Mostofsky, S., & Venkataraman, A. (2020, October). A Deep-Generative Hybrid Model to Integrate Multimodal and Dynamic Connectivity for Predicting Spectrum-Level Deficits in Autism. In *International Conference on Medical Image Computing and Computer-Assisted Intervention* (pp. 437-447). Springer, Cham.
- [297] Deshpande, G., Libero, L., Sreenivasan, K. R., Deshpande, H., & Kana, R. K. (2013). Identification of neural connectivity signatures of autism using machine learning. *Frontiers in human neuroscience*, 670.
- [298] Jiao, Y., Chen, R., Ke, X., Chu, K., Lu, Z., & Herskovits, E. H. (2010). Predictive models of autism spectrum disorder based on brain regional cortical thickness. *Neuroimage*, 50(2), 589-599.
- [299] Ecker, C., Rocha-Rego, V., Johnston, P., Mourao-Miranda, J., Marquand, A., Daly, E. M., ... & MRC AIMS Consortium. (2010). Investigating the predictive value of whole-brain structural MR scans in autism: a pattern classification approach. *Neuroimage*, 49(1), 44-56.
- [300] Chen, C. P., Keown, C. L., & Müller, R. A. (2013). Towards Understanding autism Risk Factors: a Classification of Brain Images with Support Vector Machines. *Int. J. Semantic Comput.*, 7(2), 205.
- [301] Uddin, L. Q., Menon, V., Young, C. B., Ryali, S., Chen, T., Khouzam, A., ... & Hardan, A. Y. (2011). Multivariate searchlight classification of structural magnetic resonance imaging in children and adolescents with autism. *Biological psychiatry*, 70(9), 833-841.
- [302] Ingalhalikar, M., Parker, D., Bloy, L., Roberts, T. P., and Verma, R. (2011). Diffusion based abnormality markers of pathology: toward learned diagnostic prediction of ASD. *Neuroimage* 57, 918–927. doi: 10.1016/j.neuroimage.2011.05.023
- [303] Varol, E., Gaonkar, B., Erus, G., Schultz, R., & Davatzikos, C. (2012, May). Feature ranking based nested support vector machine ensemble for medical image classification. In *2012 9Th IEEE international symposium on biomedical imaging (ISBI)* (pp. 146-149). IEEE.
- [304] Murdaugh, D. L., Shinkareva, S. V., Deshpande, H. R., Wang, J., Pennick, M. R., & Kana, R. K. (2012). Differential deactivation during mentalizing and classification of autism based on default mode network connectivity. *PLoS one*, 7(11), e50064.
- [305] Bloy, L., Ingalhalikar, M., Eavani, H., Roberts, T. P., Schultz, R. T., & Verma, R. (2011, September). HARDI based pattern classifiers for the identification of white matter pathologies. In *International Conference on Medical Image Computing and Computer-Assisted Intervention* (pp. 234-241). Springer, Berlin, Heidelberg.
- [306] Giuliano, A., Calderoni, S., Muratori, F., Biagi, L., Tosetti, M., & Retico, A. (2013, March). Multivariate analysis of structural MRI data to detect gender-related brain abnormalities in children with autism spectrum disorder. European Congress of Radiology-ECR 2013.
- [307] Deshpande, G., Libero, L., Sreenivasan, K. R., Deshpande, H., & Kana, R. K. (2013). Identification of neural connectivity signatures of autism using machine learning. *Frontiers in human neuroscience*, 7, 670.
- [308] Ecker, C., Marquand, A., Mourão-Miranda, J., Johnston, P., Daly, E. M., Brammer, M. J., ... & Murphy, D. G. (2010). Describing the brain in autism in five dimensions—magnetic resonance imaging-assisted diagnosis of autism spectrum disorder using a multiparameter classification approach. *Journal of Neuroscience*, 30(32), 10612-10623.

- [309] Li, H., Xue, Z., Ellmore, T. M., Frye, R. E., & Wong, S. T. (2012, May). Identification of faulty DTI-based subnetworks in autism using network regularized SVM. In *2012 9th IEEE International Symposium on Biomedical Imaging (ISBI)* (pp. 550-553). IEEE.
- [310] Bryant, D. M., Hoeft, F., Lai, S., Lackey, J., Roeltgen, D., Ross, J., & Reiss, A. L. (2012). Sex chromosomes and the brain: a study of neuroanatomy in XYY syndrome. *Developmental Medicine & Child Neurology*, *54*(12), 1149-1156.
- [311] Vigneshwaran, S., Mahanand, B. S., Suresh, S., & Savitha, R. (2013, August). Autism spectrum disorder detection using projection based learning meta-cognitive RBF network. In *The 2013 International Joint Conference on Neural Networks (IJCNN)* (pp. 1-8). IEEE.
- [312]. Sato, J. R., Hoexter, M. Q., de Magalhães Oliveira Jr, P. P., Brammer, M. J., Murphy, D., Ecker, C., & MRC AIMS Consortium. (2013). Inter-regional cortical thickness correlations are associated with autistic symptoms: a machine-learning approach. *Journal of psychiatric research*, *47*(4), 453-459.
- [313] An, M., Ho, H. P., Staib, L., Pelphrey, K., & Duncan, J. (2010, November). Multimodal MRI analysis of brain subnetworks in autism using multi-view EM. In *2010 Conference Record of the Forty Fourth Asilomar Conference on Signals, Systems and Computers* (pp. 786-789). IEEE.
- [314] Sadato, N., & Tanabe, H. C. (2012, July). Neural substrates and inter-individual functional connectivity during mutual gaze and joint attention using dual functional MRI. In *2012 ICME International Conference on Complex Medical Engineering (CME)* (pp. 527-530). IEEE.
- [315] Filipovych, R., Resnick, S. M., & Davatzikos, C. (2012). JointMMCC: joint maximum-margin classification and clustering of imaging data. *IEEE transactions on medical imaging*, *31*(5), 1124-1140.
- [316] Calderoni, S., Retico, A., Biagi, L., Tancredi, R., Muratori, F., & Tosetti, M. (2012). Female children with autism spectrum disorder: an insight from mass-univariate and pattern classification analyses. *Neuroimage*, *59*(2), 1013-1022.
- [317] Jiao, Y., Chen, R., Ke, X., Cheng, L., Chu, K., Lu, Z., & Herskovits, E. H. (2011). Predictive models for subtypes of autism spectrum disorder based on single-nucleotide polymorphisms and magnetic resonance imaging. *Advances in medical sciences*, *56*(2), 334-342.
- [318] Nielsen, J. A., Zielinski, B. A., Fletcher, P. T., Alexander, A. L., Lange, N., Bigler, E. D., ... & Anderson, J. S. (2013). Multisite functional connectivity MRI classification of autism: ABIDE results. *Frontiers in human neuroscience*, *7*, 599.
- [319] Jiao, Y., & Lu, Z. (2011, July). Predictive models for autism spectrum disorder based on multiple cortical features. In *2011 Eighth International Conference on Fuzzy Systems and Knowledge Discovery (FSKD)* (Vol. 3, pp. 1611-1615). IEEE.
- [320] Retico, A., Giuliano, A., Tancredi, R., Cosenza, A., Apicella, F., Narzisi, A., ... & Calderoni, S. (2016). The effect of gender on the neuroanatomy of children with autism spectrum disorders: a support vector machine case-control study. *Molecular autism*, *7*(1), 1-20.
- [321] Retico, A., Gori, I., Giuliano, A., Muratori, F., & Calderoni, S. (2016). One-class support vector machines identify the language and default mode regions as common patterns of structural alterations in young children with autism spectrum disorders. *Frontiers in neuroscience*, *10*, 306.
- [322] Subbaraju, V., Suresh, M. B., Sundaram, S., & Narasimhan, S. (2017). Identifying differences in brain activities and an accurate detection of autism spectrum disorder using resting state functional-magnetic resonance imaging: A spatial filtering approach. *Medical image analysis*, *35*, 375-389.
- [323] Gori, I., Giuliano, A., Oliva, P., Tosetti, M., Muratori, F., Calderoni, S., & Retico, A. (2016, February). Processing Magnetic Resonance Image Features with One-class Support Vector Machines-Investigation of the Autism Spectrum Disorder Heterogeneity. In *International Conference on Bioimaging* (Vol. 3, pp. 111-117). SciTePress.
- [324] Lu, J. T., Kishida, K. T., De Asis-Cruz, J., Lohrenz, T., Treadwell-Deering, D., Beauchamp, M., & Montague, P. R. (2015). Single-stimulus functional MRI produces a neural individual difference measure for autism spectrum disorder. *Clinical Psychological Science*, *3*(3), 422-432.

- [325] Chen, H., Duan, X., Liu, F., Lu, F., Ma, X., Zhang, Y., ... & Chen, H. (2016). Multivariate classification of autism spectrum disorder using frequency-specific resting-state functional connectivity—a multi-center study. *Progress in Neuro-Psychopharmacology and Biological Psychiatry*, *64*, 1-9.
- [326] Wee, C. Y., Wang, L., Shi, F., Yap, P. T., & Shen, D. (2014). Diagnosis of autism spectrum disorders using regional and interregional morphological features. *Human brain mapping*, *35*(7), 3414-3430.
- [327] Zhou, Y., Yu, F., & Duong, T. (2014). Multiparametric MRI characterization and prediction in autism spectrum disorder using graph theory and machine learning. *PloS one*, *9*(6), e90405.
- [328] Haweel, R., Shalaby, A., Mahmoud, A., Ghazal, M., Seada, N., Ghoniemy, S., ... & El-Baz, A. (2021, April). A Novel Dwt-Based Discriminant Features Extraction From Task-Based Fmri: An Asd Diagnosis Study Using Cnn. In *2021 IEEE 18th International Symposium on Biomedical Imaging (ISBI)* (pp. 196-199). IEEE.
- [329] Jönemo, J., Abramian, D., & Eklund, A. (2021). Evaluation of augmentation methods in classifying autism spectrum disorders from fMRI data with 3D convolutional neural networks. *arXiv preprint arXiv:2110.10489*.
- [330] Wang, Y., Liu, J., Xiang, Y., Wang, J., Chen, Q., & Chong, J. (2022). MAGE: automatic diagnosis of autism spectrum disorders using multi-atlas graph convolutional networks and ensemble learning. *Neurocomputing*, *469*, 346-353.
- [331] Jha, R. R., Bhardwaj, A., Garg, D., Bhavsar, A., & Nigam, A. (2021). MHATC: Autism Spectrum Disorder identification utilizing multi-head attention encoder along with temporal consolidation modules. *arXiv preprint arXiv:2201.00404*.
- [332] Zhang, F., Wei, Y., Liu, J., Wang, Y., Xi, W., & Pan, Y. (2022). Identification of Autism spectrum disorder based on a novel feature selection method and Variational Autoencoder. *arXiv preprint arXiv:2204.03654*.
- [333] Dekhil, O., Ismail, M., Shalaby, A., Switala, A., Elmaghraby, A., Keynton, R., ... & El-Baz, A. (2017, April). A novel CAD system for autism diagnosis using structural and functional MRI. In *2017 IEEE 14th International Symposium on Biomedical Imaging (ISBI 2017)* (pp. 995-998). IEEE.
- [334] Yang, R., Ke, F., Liu, H., Zhou, M., & Cao, H. M. (2021). Exploring sMRI Biomarkers for Diagnosis of Autism Spectrum Disorders Based on Multi Class Activation Mapping Models. *IEEE Access*, *9*, 124122-124131.
- [335] Chen, Y., Liu, A., Fu, X., Wen, J., & Chen, X. (2021). An Invertible Dynamic Graph Convolutional Network for Multi-Center ASD Classification. *Frontiers in Neuroscience*, *15*.
- [336] Li, J., Wang, F., Pan, J., & Wen, Z. (2021). Identification of Autism Spectrum Disorder With Functional Graph Discriminative Network. *Frontiers in Neuroscience*, 1282.
- [337] Shao, L., Fu, C., You, Y., & Fu, D. (2021). Classification of ASD based on fMRI data with deep learning. *Cognitive Neurodynamics*, *15*(6), 961-974.
- [338] Chen, H., Zhuang, F., Xiao, L., Ma, L., Liu, H., Zhang, R., ... & He, Q. (2021). AMA-GCN: Adaptive Multi-layer Aggregation Graph Convolutional Network for Disease Prediction. *arXiv preprint arXiv:2106.08732*.
- [339] Cao, M., Yang, M., Qin, C., Zhu, X., Chen, Y., Wang, J., & Liu, T. (2021). Using DeepGCN to identify the autism spectrum disorder from multi-site resting-state data. *Biomedical Signal Processing and Control*, *70*, 103015.
- [340] Chu, Y., Wang, G., Cao, L., Qiao, L., & Liu, M. (2022). Multi-Scale Graph Representation Learning for Autism Identification With Functional MRI. *Frontiers in Neuroinformatics*, *15*, 802305.
- [341] https://papers.ssrn.com/sol3/papers.cfm?abstract_id=4057056
- [342] Yin, W., Li, L., & Wu, F. X. (2022). A semi-supervised autoencoder for autism disease diagnosis. *Neurocomputing*, *483*, 140-147.
- [343] Wen, G., Cao, P., Bao, H., Yang, W., Zheng, T., & Zaiane, O. (2022). MVS-GCN: A prior brain structure learning-guided multi-view graph convolution network for autism spectrum disorder diagnosis. *Computers in Biology and Medicine*, 105239.
- [344] Pagnozzi, A. M., Conti, E., Calderoni, S., Fripp, J., & Rose, S. E. (2018). A systematic review of structural MRI biomarkers in autism spectrum disorder: A machine learning perspective. *International Journal of Developmental Neuroscience*, *71*, 68-82.
- [345] Nogay, H. S., & Adeli, H. (2020). Machine learning (ML) for the diagnosis of autism spectrum disorder (ASD) using brain imaging. *Reviews in the Neurosciences*, *31*(8), 825-841.

- [346] Rahman, M., Usman, O. L., Muniyandi, R. C., Sahran, S., Mohamed, S., & Razak, R. A. (2020). A Review of machine learning methods of feature selection and classification for autism spectrum disorder. *Brain sciences*, *10*(12), 949.
- [347] Eslami, T., Almuqhim, F., Raiker, J. S., & Saeed, F. (2021). Machine learning methods for diagnosing autism spectrum disorder and attention-deficit/hyperactivity disorder using functional and structural MRI: A survey. *Frontiers in neuroinformatics*, *14*, 62.
- [348] <https://archive.ics.uci.edu/ml/datasets.php>
- [349] <https://ndar.nih.gov>
- [350] <https://www.autismspeaks.org/agre>
- [351] <https://www.nimhgenetics.org>
- [352] <https://www.ncbi.nlm.nih.gov/geo>
- [353] <https://www.sfari.org/resource/simons-simplex-collection>
- [354] <https://www.sfari.org/funded-project/simons-variation-in-individualsproject-simons-vip>
- [355] Jones, C. R., Pickles, A., Falcato, M., Marsden, A. J., Happé, F., Scott, S. K., ... & Charman, T. (2011). A multimodal approach to emotion recognition ability in autism spectrum disorders. *Journal of Child Psychology and Psychiatry*, *52*(3), 275-285.
- [356] Bora, E., Fornito, A., Radua, J., Walterfang, M., Seal, M., Wood, S. J., ... & Pantelis, C. (2011). Neuroanatomical abnormalities in schizophrenia: a multimodal voxelwise meta-analysis and meta-regression analysis. *Schizophrenia research*, *127*(1-3), 46-57.
- [357] Sibley, M. H., Arnold, L. E., Swanson, J. M., Hechtman, L. T., Kennedy, T. M., Owens, E., ... & MTA Cooperative Group. (2021). Variable patterns of remission from ADHD in the multimodal treatment study of ADHD. *American Journal of Psychiatry*, appi-ajp.
- [358] Kober, H., Grummich, P., & Vieth, J. (1993). Precise fusion of MEG and MRI tomography using a surface fit.
- [359] Loeffelbein, D. J., Souvatzoglou, M., Wankerl, V., Martinez-Möller, A., Dinges, J., Schwaiger, M., & Beer, A. J. (2012). PET-MRI fusion in head-and-neck oncology: current status and implications for hybrid PET/MRI. *Journal of Oral and Maxillofacial Surgery*, *70*(2), 473-483.
- [360] Valdes-Sosa, P. A., Sanchez-Bornot, J. M., Sotero, R. C., Iturria-Medina, Y., Aleman-Gomez, Y., Bosch-Bayard, J., ... & Ozaki, T. (2009). Model driven EEG/fMRI fusion of brain oscillations. *Human brain mapping*, *30*(9), 2701-2721.
- [361] Wong, A., Famuori, M., Shafiee, M. J., Li, F., Chwyl, B., & Chung, J. (2019, December). Yolo nano: a highly compact you only look once convolutional neural network for object detection. In *2019 Fifth Workshop on Energy Efficient Machine Learning and Cognitive Computing-NeurIPS Edition (EMC2-NIPS)* (pp. 22-25). IEEE.
- [362] Tian, Y., Gelernter, J., Wang, X., Chen, W., Gao, J., Zhang, Y., & Li, X. (2018). Lane marking detection via deep convolutional neural network. *Neurocomputing*, *280*, 46-55.
- [363] Srinivas, S. V. K., Nair, H., & Vidyasagar, V. (2019). Hardware aware neural network architectures using FbNet. *arXiv preprint arXiv:1906.07214*.
- [364] Michele, A., Colin, V., & Santika, D. D. (2019). Mobilenet convolutional neural networks and support vector machines for palmprint recognition. *Procedia Computer Science*, *157*, 110-117.
- [365] Wu, W., Wu, A., & Zheng, W. S. (2018, October). Light person re-identification by multi-cue tiny net. In *2018 25th IEEE International Conference on Image Processing (ICIP)* (pp. 1643-1647). IEEE.
- [366] Usha, R., & Perumal, K. (2019). SVM classification of brain images from MRI scans using morphological transformation and GLCM texture features. *International journal of computational systems engineering*, *5*(1), 18-23.
- [367] Gupta, N., Bhatele, P., & Khanna, P. (2019). Glioma detection on brain MRIs using texture and morphological features with ensemble learning. *Biomedical Signal Processing and Control*, *47*, 115-125.
- [368] Georgiadis, P., Cavouras, D., Kalatzis, I., Daskalakis, A., Kagadis, G. C., Sifaki, K., ... & Solomou, E. (2008). Improving brain tumor characterization on MRI by probabilistic neural networks and non-linear transformation of textural features. *Computer methods and programs in biomedicine*, *89*(1), 24-32.
- [369] Saritha, M., Joseph, K. P., & Mathew, A. T. (2013). Classification of MRI brain images using combined wavelet entropy based spider web plots and probabilistic neural network. *Pattern Recognition Letters*, *34*(16), 2151-2156.